University of Alberta

The Timing and petrogenesis of the Creighton pluton, Ontario: an example of felsic magmatism associated with Matachewan Igneous Events?

By

Mark David Smith

A thesis submitted to the Faculty of Graduate Studies and Research in partial fulfilment of the requirements for the degree of Master of Science

Department of Earth and Atmospheric Sciences

Edmonton, Alberta

Spring 2002

National Library of Canada

Acquisitions and Bibliographic Services

395 Wellington Street
Ottawa ON K1A 0N4
Canada

Bibliothèque nationale du Canada

Acquisitions et services bibliographiques

395, rue Wellington
Ottawa ON K1A 0N4
Canada

Your file Votre référence

Our file Notre référence

The author has granted a non-exclusive licence allowing the National Library of Canada to reproduce, loan, distribute or sell copies of this thesis in microform, paper or electronic formats.

L'auteur a accordé une licence non exclusive permettant à la Bibliothèque nationale du Canada de reproduire, prêter, distribuer ou vendre des copies de cette thèse sous la forme de microfiche/film, de reproduction sur papier ou sur format électronique.

The author retains ownership of the copyright in this thesis. Neither the thesis nor substantial extracts from it may be printed or otherwise reproduced without the author's permission.

L'auteur conserve la propriété du droit d'auteur qui protège cette thèse. Ni la thèse ni des extraits substantiels de celle-ci ne doivent être imprimés ou autrement reproduits sans son autorisation.

0-612-69761-4

Canada

University of Alberta

Library Release Form

Name of Author: Mark David Smith

Title of Thesis: The Timing and petrogenesis of the Creighton pluton, Ontario: an example of felsic magmatism associated with Matachewan Igneous Events?

Degree: Master of Science

Year this Degree Granted: 2002

Permission is hereby granted to the University of Alberta Library to reproduce single copies of this thesis and to lend or sell such copies for private, scholarly or scientific research purposes only.

The author reserves all other publication and other rights in association with the copyright in the thesis, and except as herein before provided, neither the thesis nor any substantial portion thereof may be printed or otherwise reproduced in any material form whatever without the author's prior written permission.

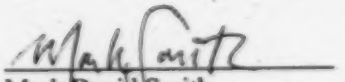

Mark David Smith
#203 10616- 84 Ave NW
Edmonton, AB
T6E 2H6

Date: 10/04/2002

University of Alberta

Faculty of Graduate Studies and Research

The undersigned certify that they have read, and recommend to the Faculty of Graduate Studies and Research for acceptance, a thesis entitled *"The Timing and petrogenesis of the Creighton pluton, Ontario: an example of felsic magmatism associated with Matachewan Igneous Events?"* submitted by **Mark David Smith** in partial fulfilment of the requirements for the degree of Master of Science.

Dr. Larry Heaman

Dr. Tom Chacko

Dr. Robert Creaser

Dr. Al Meldrum

Date: 10/04/2002

DEDICATION

In the memory of:

Reverend Dr. R. R. Smith

&

Chico Conejito

ABSTRACT

The Creighton Pluton is located in the southern Superior Province of Ontario and intrudes the lowermost volcanic strata of the Paleoproterozoic Huronian Supergroup. The granitoid pluton is actually composed of two temporally separate intrusions (dated at 2415 ± 5 Ma and 2376.3 ± 2.3 Ma), each of which has distinctive mineralogy, chemistry and isotopic signatures. Overall, the intrusions have ε_{Nd} values of –2 and similar rare-earth element pattern (LREE enrichment, negative Eu, flat HREE). These characteristics conform to other plutonic and volcanic rocks in the region. I propose that the Creighton Pluton was derived by partial melting of two sources, a mafic granulitic crust that formed by the underplating of Matachewan Igneous Events related mafic magmas and older pre-existing lower crust.

ACKNOWLEDGEMENTS

As with most of the work done on this thesis, these acknowledgements are being completed seconds before the final deadline. The first person that I would like to thank is my supervisor Dr. Larry Heaman for allowing me to research some very interesting material and for having patience when things went wrong or I got lost in the isotopic wasteland. Thanks also go out to Drs. Robert Creaser and Tom Chacko for being on my committee and helping me understand what was going on in my thesis. Dr. Al Meldrum from physics (although he is an ex-geologist) is thanked for serving on my committee and throwing me off guard with the first, easy question.

I would also like to thank members of the Radiogenic Isotope Facility (as it is called now) past and present for assisting in mineral separation and laboratory work: Laura Raynor, Stacey Hagen, Kim Toope, Barb Boehm, Al Berggren, Olga Levner and likely others that I have forgotten. Others staff in the department who helped along the way: Dr. Robert Luth, Don and Mark down in the thin section lab, George Braybrook for help on the SEM, Lang Shi for guidance on the Microprobe, Randy Pakan at the Digital Image Facility and Dr. Dave Selby for kicking the soccer ball at my head in the warm-up too many times. Support (and tasty beverages) also came from many fellow graduate students: French, Frank, Paul Glombick, Jenny U, Rajeev, Trevor and likely many others.

I would like to thank a number of people out east in Ontario: Dr. Bob Bowins and the staff at the Geosciences Laboratories in Sudbury, Ontario for processing and analyzing my geochemical samples, Gary Beakhouse of the Ontario Geological Survey for the tour of the Sudbury area and helping me get started on my fieldwork and Jack Parker and Lindsay Hall of the Ontario Geological Survey for providing me with a diverting summer of fieldwork in 2001 when I probably should have been finishing my thesis.

Closer to home in Edmonton, my parents deserve credit for supporting their son and bailing him out when he needed it. The class of 2002, for making teaching two field schools very entertaining and many friends around town (Kanna, Paul V, and Harnaik) for being there. Thank you to Chico, Oreo, Toffee and Squeaker for companionship and making life less stressful. And finally, my eternally thanks and love to Chelsea Hermus for dealing with me during this ordeal.

And as a final word: I never thought that I could learn so much about Pennsylvanian geology by studying rocks from Ontario at the University of Alberta.

TABLE OF CONTENTS

CHAPTER 1: Introduction 1

CHAPTER 2: Geological Background 4
Introduction 4
Archean rocks 8
Huronian Supergroup 8
Gabbro-anorthosite Intrusions 12
Mafic dikes 13
Ca. 2.45 Ga Matachewan Igneous Events 14
Street Township intrusions 15
Sudbury Structure 15

CHAPTER 3: Field Observations and Petrography 17
Introduction 17
Field observations 18
Petrography 21
Discussion 25

CHAPTER 4: Geochemistry 27
Introduction 27
Major- and trace-element chemistry 30
Rare-earth-element chemistry 34
Discussion 36

CHAPTER 5: U-Pb Geochronology 38
Introduction 38
LH98-63 41
MS99-50 46
Discussion 51

CHAPTER 6: Tracer Isotopes 55
Introduction 55
Rb-Sr 59
Sm-Nd 60
Common Pb-feldspar 62
Discussion 62

CHAPTER 7: Tectono-magmatic setting 69
Introduction 69
Field relations 70
Mineralogy 70

Geochemistry 71
Isotopes 78
Discussion 84

CHAPTER 8: Matachewan Igneous Events 87
Introduction 87
Granitoid comparison 87
Ca. 2.45 Ga magmatism 94

CHAPTER 9: Conclusions 99

References 101

Appendix A: Sample locations 109

Appendix B: Major-, trace- and rare-earth element chemistry 111

Appendix C: Mineral separation flow chart 116

Appendix D: Analytical Techniques – U-Pb Geochronology 117

Appendix E: Anaylytical Techniques – Rb-Sr, Sm-Nd and common Pb 119

Appendix F: Isotopic data for the Murray pluton 122

Appendix G: Mafic Dike 123

LIST OF TABLES

Table 2.1: Table of Paleoproterozoic U-Pb data from the south central Superior Province. 7

Table 4.1: Table showing the range and average geochemistry of the Type 1 and Type 2 granitoids of the Creighton pluton. 29

Table 5.1: Complete U-Pb data from Creighton pluton. 39
Table 5.2: Complete zircon fraction descriptions from the Creighton pluton. 40

Table 6.1: Summary of Rb-Sr whole rock and apatite data from the Creighton pluton. 56
Table 6.2: Summary of Sm-Nd whole rock data from the Creighton pluton. 57
Table 6.3: Summary of common Pb-feldspar data from the Creighton pluton. 58

Table 8.1: Comparison of average geochemistry from Creighton pluton Type 1 and Type 2, Murray pluton and Street Township granites. 88

LIST OF FIGURES

Figure 2.1: Simplified regional geology map of central Superior Province with ca. 2.45 Ga magmatism. 5

Figure 2.2: Summary diagram of Paleoproterozoic U-Pb ages from the south central Superior Province along an east-west axis. 6

Figure 2.3: Generalized stratigraphic column of the Huronian Super-group adapted. 10

Figure 3.1: Photographs showing Sudbury Impact related brecciation texture in the Creighton pluton. 19

Figure 3.2: Photographs showing felsic microgranular enclaves from the Creighton pluton. 20

Figure 3.3: IUGS granitoid rock classification diagram showing plotted CIPW norms calculated for the Creighton pluton. 23

Figure 3.4: Backscatter electron images showing mineralogy and texture of the Creighton pluton (sample MS99-50). 24

Figure 4.1: Simplified geological map of the Creighton pluton area showing distribution of rock types and sample locations for geochemistry, U-Pb geochronology and tracer isotopes. 28

Figure 4.2: Major element oxide (wt %) Harker diagrams for the Creighton pluton. 31

Figure 4.3: Selected trace element (ppm) Harker diagrams for the Creighton pluton. 32

Figure 4.4: ASI (alumina-saturation index) diagrams, AFM ternary diagram and comparative multi-elemental diagrams for the Creighton pluton. 33

Figure 4.5: Chondrite normalized rare-earth element diagrams for the Creighton pluton. 35

Figure 4.6: Primitive mantle and MORB normalized multi-element spidergrams for the Creighton pluton. 37

Figure 5.1: Photograph of Type 1 sample LH98-63 and U-Pb concordia diagram showing results. 42

Figure 5.2: Backscatter electron images of zircons from LH98-63. 43

Figure 5.3: Secondary electron images of shocked zircons from the Creighton pluton (sample LH98-63) displaying PDF (planar deformation features). 44

Figure 5.4: Photographs of zircon fractions from LH98-63. Magnification is x100. 45

Figure 5.5: Photograph of Type 2 sample MS99-50 and U-Pb concordia diagram showing results. 47

Figure 5.6: Backscatter electron images of zircons from MS99-50. 48
Figure 5.7: Photographs of zircon fractions from MS99-50. Magnification is x100. 50
Figure 5.8: U-Pb concordia diagram showing results from all zircon analyses for the Creighton pluton. 52
Figure 5.9: U-Pb concordia diagrams showing results from samples LH98-63 and MS99-50. 53

Figure 6.1: ε_{Nd} vs. time (Ma) diagram of Creighton pluton samples with respect to CHUR (CHondritic Uniform Reservoir) and Depleted Mantle (DM). 61
Figure 6.2: Rb/Sr vs. initial $^{87}Sr/^{86}Sr$ ratio and Rb-Sr isochron diagram of four Type 1 granitoid samples from the Creighton pluton. 64
Figure 6.3: Pb isochrons for the two U-Pb ages of the Creighton pluton plotted with corresponding potassium feldspar residues and leachates. 66
Figure 6.4: Pb isochron diagrams from the Creighton pluton. 67
Figure 6.5: Pb evolution curve ($\mu = 9.74$) plotted with k-feldspar residues from Creighton pluton. 68

Figure 7.1: Granitoid tectonic discrimination diagrams. 72
Figure 7.2: Various A-type granite tectonic discrimination diagrams. 76
Figure 7.3: Multi-element profile diagrams comparing the Creighton pluton granitoids and the C-type Ardery Charnockites. 77
Figure 7.4: $^{207}Pb/^{204}Pb$ vs. $^{206}Pb/^{204}Pb$ diagram of the Creighton pluton k-feldspar residues and potential source materials. 79
Figure 7.5: ε_{Nd} vs. time (Ma) diagram of Creighton pluton samples and potential source material with respect to CHUR (CHondritic Uniform Reservoir) and Depleted Mantle. 81
Figure 7.6: Multi-element spidergrams comparing average Creighton pluton Type 1 and Type 2 granitoids to average Hearst-Matachewan dike. 83

Figure 8.1: Multi-element spidergrams of the Creighton pluton, Murray pluton and Street Township granites. 90
Figure 8.2: Comparative geochemical and tectonic discrimination diagrams showing similarities and contrasts between Creighton pluton, Murray pluton and Street Township granites 91
Figure 8.3: Primitive mantle normalized multi-element spidergram of average values for all Paleoproterozoic MIE linked magmatism. 96

CHAPTER 1: INTRODUCTION

Although a considerable amount of Paleoproterozoic mafic magmatism is located within the southern Superior craton, it is only recent studies that have recognized its importance in the breakup and rifting of an Archean supercontinent (Heaman, 1997; Vogel et al., 1998). Collectively, the Hearst-Matachewan dike swarms, Huronian flood basalts and a number of gabbro-anorthosite plutons are defined as Matachewan Igneous Events (MIE) (Heaman, 1997) and are constrained by precise U-Pb geochronology to an interval of 50 m.y. between 2490 and 2440 Ma (Krogh et al., 1984; Prevec, 1993; Heaman, 1997). Despite its importance as possibly being one of the first Large Igneous Provinces in Earth's history, the nature of this magmatism and mechanism of rifting has remained enigmatic. There is controversy pertaining to the mechanism of rifting (active vs. passive), the origin of the magma's enriched geochemical signatures in the Huronian-aged volcanic rocks and the genetic link between felsic and mafic magmatism. Although there is a general consensus on the enriched nature of the source region for Matachewan magmatism, a wide range of interpretations has been invoked to explain the origin of this signature. These include AFC (assimilation-fractional crystallization) processes, an inherited Archean subduction signature or a compositionally distinct Archean-Paleoproterozoic mantle (Nelson et al., 1990; Boily and Ludden, 1991; Jolly et al., 1992; Smith et al., 1992; Tomlinson, 1996; Vogel et al., 1998).

The Creighton pluton is one of a number of Paleoproterozoic felsic igneous bodies that may be temporally and genetically linked to the Matachewan Igneous Events. These bodies include the nearby 2477 ± 9 Ma Murray pluton (Krogh et al., 1996), the 2450 +25/-10 Ma Copper Cliff rhyolite (Krogh et al., 1984) and two (2460 Ma and 2475 Ma) Street Township granites located in the Grenville Province (Corfu and Easton, 2001). The Creighton pluton is located near the southern margin of the 1850 Ma Sudbury Nickel Irruptive and intrudes the lowermost volcanic strata of the Proterozoic Huronian Supergroup.

Previous geochronological studies that have attempted to establish the emplacement age of the Creighton pluton have yielded a Rb-Sr isochron age of 2165 Ma (no age uncertainty reported) (Stockwell, 1982) and a U-Pb zircon age of 2333 +33/-22 Ma (lower intercept at 195 Ma) (Frarey et al., 1982). However, recent U-Pb zircon ages for other similar granitic bodies noted above (Krogh et al., 1996; Corfu and Easton, 2001) indicate that most of the Proterozoic granite bodies in this region are 2450 – 2477 Ma. Therefore, previous age determinations for the Creighton pluton are suspect, raising questions about the genetic relationship between this intrusion and other lithologically similar plutons in the area. Moreover, there have been no studies that have focussed on the issue of identifying the tectonic setting and source of the parental magma of these plutons.

The Creighton pluton is the largest Paleoproterozoic granitic intrusion in the southern Superior Province but has not been extensively studied. The purpose of this study is to integrate petrography, geochemistry, U-Pb geochronology and Sr-, Nd-, Pb-isotope tracer studies to constrain the timing and examine the petrogenesis of the

Creighton pluton. The pluton will be compared to other temporally related granitic bodies in an attempt to unravel the evolution of felsic magmatism potentially associated with the mafic Matachewan Igneous Events. The significance of this study is that it will be the first to address the petrogenesis of felsic plutonism that may be linked to the 2.45 Ga Matachewan Igneous Events (Bennett et al., 1991; Heaman, 1997).

CHAPTER 2: GEOLOGICAL BACKGROUND

Introduction

The Southern Province of the Canadian Shield is primarily composed of the Paleoproterozoic Huronian Supergroup (Figure 2.1). These supracrustal rocks outcrop along the northern shore of Lake Huron, bounded to the north by K-rich Archean granites and to the east by the ca. 1.0 Ga Grenville Front, an area of intense deformation and metamorphism. A major feature in the vicinity of the present field area is the elliptical Sudbury Structure which is important due to its unique impact origin and economic significance (e.g. Dietz, 1964).

A considerable amount of Paleoproterozoic mafic magmatism occurred in the south-central Superior craton and is collectively designated as Matachewan Igneous Events (MIE) (Heaman, 1997) (Figure 2.1). MIE are constrained to an interval from ca. 2.49 Ga to 2.45 Ga and include the Matachewan-Hearst dike swarms, Huronian flood basalts and a series of gabbro-anorthosite intrusions (Krogh et al., 1984; Heaman, 1997). The Creighton pluton, together with the Murray pluton, Street Township granites and the Copper Cliff rhyolite may represent a felsic component of this magmatic event. A compilation of data for ca. 2.45 Ga MIE magmatism in the Superior Province is presented in Figure 2.2 and Table 2.1. Recent studies on this mafic magmatic event (Heaman,

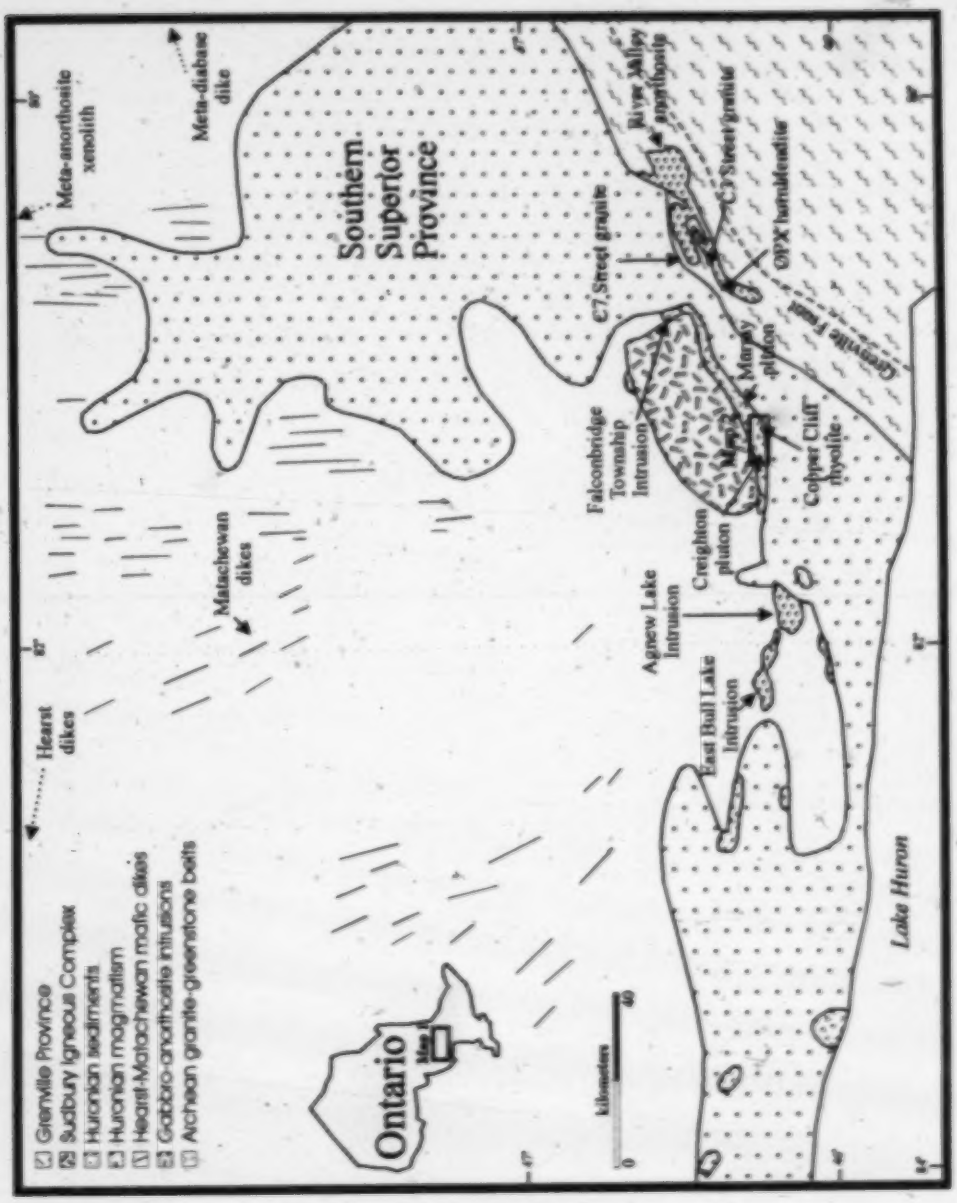

Figure 2.1: Simplified regional geology map of central Superior Province with ca. 2.45 Ga magmatism adapted from Vogel et al. (1998).

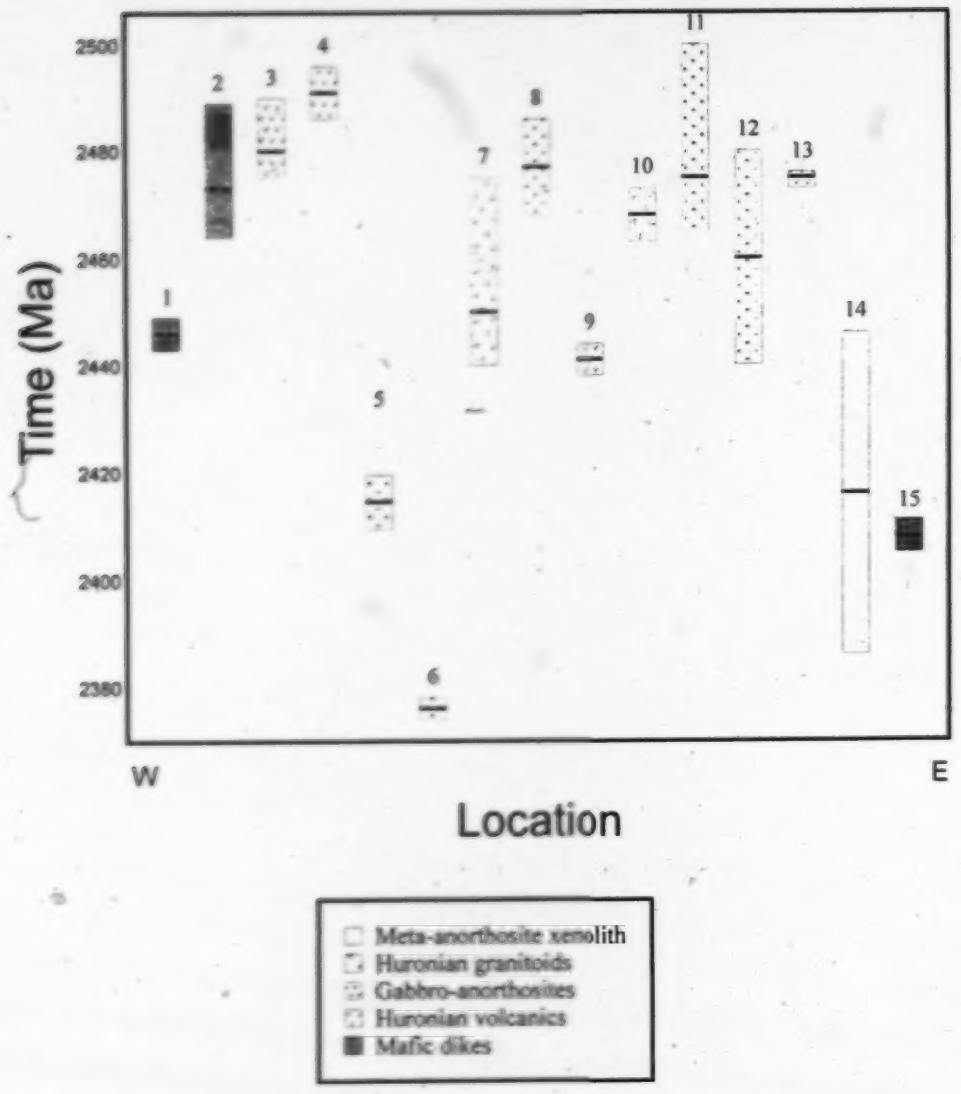

Figure 2.2: Summary diagram of Paleoproterozoic U-Pb ages from the south central Superior Province along an east-west axis. Numbers correspond with igneous bodies and U-Pb ages in Table 2.1.

Table 2.1: Table of Paleoproterozoic U-Pb data from the south central Superior Province.

#	Magmatic Intrusion (W-E)	Age (Ma)	Err (+Ma)	Err (-Ma)	References
1	Hearst dikes	2446	2.9	2.6	Heaman, 1997
2	Matachewan dikes	2473	16	9	Heaman, 1997
3	East Bull Lake Intrusion	2480	10	5	Krogh et al., 1984
4	Agnew Lake Intrusion	2491	5	5	Krogh et al., 1984
5	Creighton pluton (T1)	2415	5	5	This study
6	Creighton pluton (T2)	2376	2.3	2.3	This study
7	Copper Cliff rhyolite	2450	25	10	Krogh et al., 1984
8	Murray pluton	2477	9	9	Krogh et al., 1996
9	Falconbridge Township	2441	3	3	Prevec, 1993
10	OPX hornblendite	2468	5	5	Corfu & Easton, 2001
11	C3 Street granite	2475	25	10	Corfu & Easton, 2001
12	C7 Street granite	2460	20	20	Corfu & Easton, 2001
13	River Valley anorthosite	2475	1	2	Heaman, pers. comm.
14	Meta-anorthosite xenolith	2416	30	30	Moser & Heaman, 1997
15	Meta-diabase dike	2408	3	3	Krogh, 1994

1997) have recognized the global scale of the event and its potential importance in the recognition of the breakup of large continental masses.

Archean rocks

Located to the north of the southern Superior Province is a large volume of felsic plutonic magmatism associated with high-grade gneisses and mafic suites exposed in east-west trending greenstone belts. This includes the 2711 Ma Levack Gneiss (Krogh et al., 1984) and the "Algoman" granites: the Birch Lake Batholith, the 2665 Ma Ramsay-Algoman granite complex (Heather and van Breeman, 1994), the 2642 ± 1 Ma Cartier Batholith (Meldrum et al., 1997) and a number of 2616 Ma plutons (Gariepy and Allegre, 1985). These intrusives are primarily granodiorite to monzogranite (quartz monzonite) in composition that are intensely deformed in areas and show signs of hydrothermal alteration (Meldrum et al., 1997). These igneous bodies represent a 100 Ma period of felsic plutonic activity (Card et al., 1984; Gariepy and Allegre, 1985) that resulted from widespread crustal anatexis common to the Archean (Meldrum et al., 1997).

Huronian Supergroup

The Huronian Supergroup is a 12-km-thick stratigraphic succession of Paleoproterozoic metavolcanics and metasediments. It is primarily located along the northern shore of Lake Huron in the Southern Province and forms a 450 km arcuate east-west trending fold belt (Bennett et al., 1991). The Supergroup lies unconformably on

Archean basement and is thought to have formed in an extensional regime, possibly representing the rifting of an Archean craton (Bennett et al., 1991; Roscoe and Card, 1993). The Supergroup is regionally deformed and metamorphosed by the ca. 1.85 Ga Penokean Orogeny (Card, 1978) and shows the effects of other geological events such as the 1850 Ma Sudbury Impact Event (Krogh et al., 1996) and 1.7 Ga Na and K metasomatism (e.g. Schandl et al, 1994; Fedo et al., 1997). Recently it has also been proposed that these events were preceded by the 2.4 – 2.2 Ga Blezardian orogeny in the Lake Huron area (Riller et al., 1999) but the existence of this tectonic event has been called into question (Young et al., 2001).

The Paleoproterozoic Huronian Supergroup is comprised of four main sedimentary packages (Figure 2.3). In ascending stratigraphic order, they are the Elliot Lake, Hough Lake, Quirke Lake and Cobalt Groups. Volcanics occur only in the lowermost Elliot Lake Group including the felsic plutonism of the Murray and Creighton plutons. The upper three groups generally consist of cyclical repetitions of conglomerates, pelitic rocks and sandstones (Card, 1978). Detailed descriptions of the upper sedimentary sequences can be found in Card (1978) and Bennett et al. (1991).

In the western region of the Southern Province, the Livingstone Creek Formation underlies the Elliot Lake Group volcanics. It consists primarily of arenites and wackes with some polymictic conglomerate (Bennett et al., 1991). In the eastern region around Sudbury, the volcanics of the Elliot Lake Group are subdivided into 3 formations, the Elsie Mountain, Stobie and Copper Cliff Formations (Card, 1978). A fourth formation located at the base of the Huronian sequence in the Massey area is called the Salmay Lake -

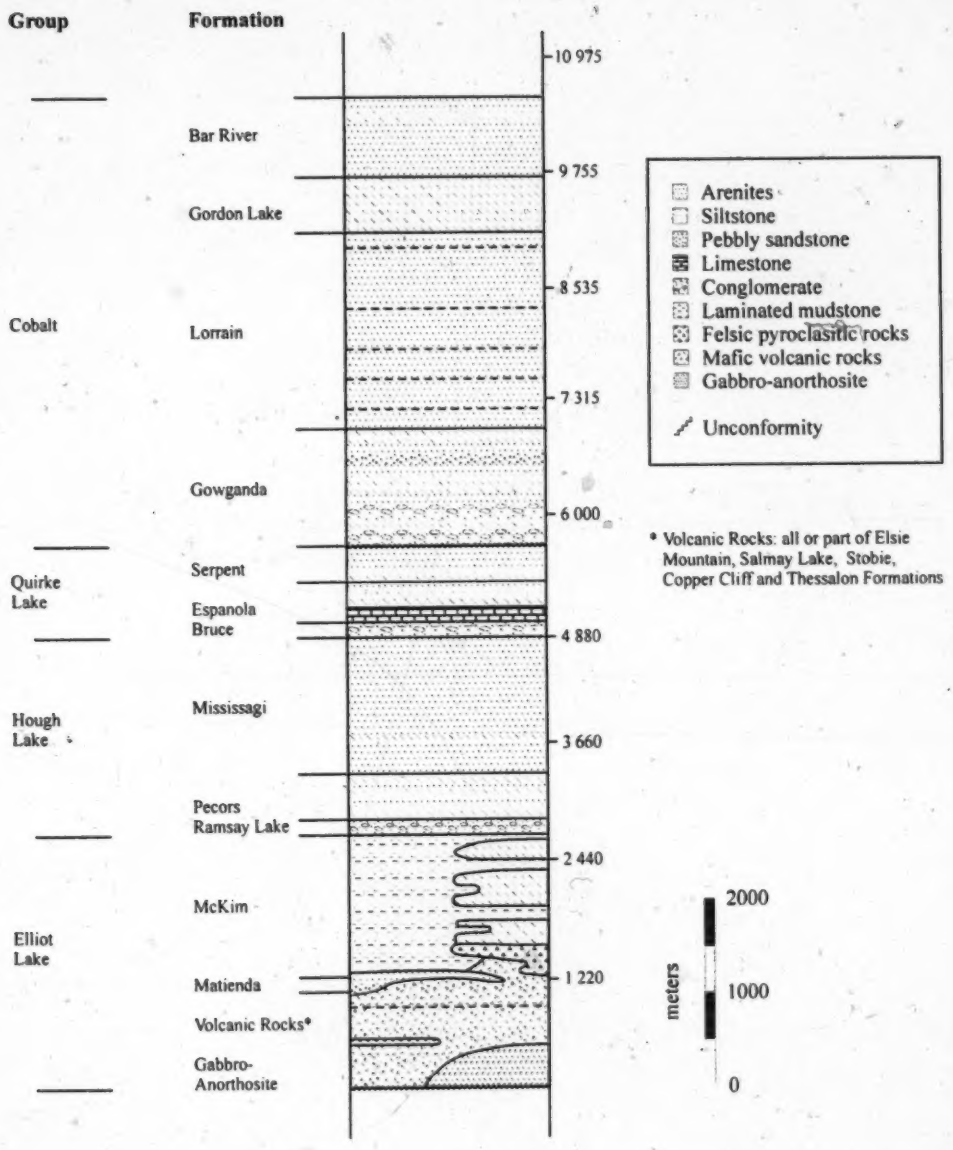

Figure 2.3: Generalised stratigraphic column of the Huronian Supergroup adapted from Bennett et al. (1991).

Formation (Robertson, 1970). In the western portion of the Penokean Fold Belt, the bimodal Thessalon volcanics are correlated with the basal Elliot Lake Group volcanics.

The Elsie Mountain formation is dominated by massive and foliated basalt flows with subsidiary metasediments (Card, 1978). The Stobie Formation has both felsic and mafic volcanics with a higher proportion of metasediments and is characterized by the cyclical repetitions of the mafic volcanics and intercalated sediments (Card, 1978). The Copper Cliff Formation is primarily composed of felsic rhyolite with minor pyroclastic rocks and metasediments (Card, 1978). The rhyolite has a U-Pb zircon age of 2450 +25/-10 Ma but may be as old as 2475 Ma depending on the regression treatment (Krogh et al., 1984). The Salmay Lake Formation consists of basaltic to andesitic flows and is lithologically similar to the rocks of the Elsie Mountain Formation (Card, 1978). The Elliot Lake Group volcanics are associated with a number of east-west regional faults that may have initiated sedimentary deposition and controlled volcanic emplacement (Card, 1978). The Elliot Lake Group is capped by the sedimentary successions of the Matinenda and McKim Formations.

The Murray and Creighton plutons are two local, NE trending granitic bodies that intrude the metavolcanic package of the Elliot Lake Group in the Sudbury region. The two bodies have been thought to be coeval based on proximity and similarities in petrography and chemistry. Both plutons have been the focus of studies because of ambiguous field relations with the Sudbury Nickel Irruptive (Lewis, 1951; Gibbins and McNutt, 1975). The ambiguities were resolved by the application of radiometric dating. The Murray pluton is precisely dated by an U-Pb zircon age of 2477 ± 9 Ma with a lower intercept age of 1850 Ma interpreted to reflect Pb-loss related to the nearby Sudbury

Impact Event (Krogh et al., 1996). Prior to the present study, the most recent age obtained for the Creighton pluton is an U-Pb zircon age of 2333 +33/-22 Ma (Frarey et al., 1982). The Creighton pluton has been proposed to be associated with the 2.4 – 2.2 Ga Blezardian orogeny (Riller et al., 1999). However, the zircon analyses are very discordant and the accuracy of this age determination is in question.

Regional metamorphism by the 1.85 Ga Penokean Orogeny is expressed by the sub-greenschist to lower greenschist grade assemblages in the Huronian rocks (Card, 1978). The sediments of the Huronian Supergroup have also been affected by regional Na + K metasomatism at ca. 1.7 Ga (Schandl et al., 1994; Fedo et al., 1997)

Gabbro-anorthosite Intrusions

Temporally associated with the volcanics of the Huronian Supergroup are a series of 2.49 – 2.44 Ga Paleoproterozoic layered mafic intrusions collectively identified as the East Bull Lake Suite (Bennett et al., 1991; Vogel et al., 1998). This suite includes the 2480 +10/-5 Ma East Bull Lake Intrusion (Krogh et al., 1984), the 2491 ± 5 Ma Agnew Lake Intrusion (Krogh et al., 1984), the 2475 +1/-2 Ma River Valley anorthosite (Heaman, personal communication), the 2441 ± 3 Ma ($^{207}Pb/^{206}Pb$ age from one fraction) Falconbridge Township intrusion (Prevec, 1993) and intrusives located in the Drury, May and Wisner townships. The intrusives are all located in the Southern Province with the exception of the River Valley anorthosite that is located immediately south of the Grenville Front. The intrusions are grouped together based on similarities in morphology, stratigraphic correlations (for example, between Agnew Lake and East Bull

Lake) and high precision U-Pb geochronology. These ages either indicate an extended period of mafic magmatism or possibly two (or more) temporally distinct events at ca. 2.48 Ga and ca. 2.44 Ga associated with the major dike swarms (see below).

The mafic intrusions generally consist of layered gabbronorite with associated anothositic and syenitic rocks. Some of the intrusions are interpreted to have intruded as subvolcanic sills and in a series of magma pulses (Peck et al., 1995; Vogel et al., 1998; Vogel et al., 1999). The intrusions are thought to be overlain by the volcanics of the Elliot Lake Group but in many areas the contacts are obscured by pseudotachylite associated with Sudbury breccias (Chubb et al., 1994). Economically, the bodies are of importance because of the associated PGE-Cu-Ni mineralization (e.g. Peck et al., 1995).

Mafic dikes

The 2473 +16/-9 Ma Matachewan and 2446 ± 3 Ma Hearst dike swarms (Heaman, 1997) are located in the south-central region of the Superior Craton extending over an area of 250 000 km^2 (Halls and Bates, 1990). They are dominantly Fe-rich quartz tholeiites with a median width of 20 m and have undergone lower greenschist-grade metamorphism (Halls, 1991). The Matachewan dike swarm is located east of the Kapuskasing Structural Zone. It trends N-S and is characterized by a porphyritic texture with abundant calcic plagioclase megacrysts (Heaman, 1997). The Hearst dikes are NW-SE trending intrusives located west of the Kapuskasing Structural Zone and are distinctly non-porphyritic (Heaman, 1997). All the dikes exhibit both normal- and reverse- polarity magnetization with a greater abundance of the reverse polarity dikes (Halls and Palmer,

1990; Halls, 1991). The dike swarms are interpreted as cogenetic based on similar geochemical signatures (Nelson et al, 1990) and may be feeders to the Huronian mafic magmatism (Heaman, 1997).

Ca. 2.45 Matachewan Igneous Events

Bennett et al. (1991) proposed that the Huronian Supergroup formed in an evolving rift – passive margin setting. The early stages of rifting were passive as recorded by the deposition of the sedimentary Livingstone Creek Formation. Subsequent active rifting was initiated by the onset of volcanism represented by the Elliot Lake Group flood basalts, gabbro-anorthosite intrusions and the major dike swarms. The upper Elliot Lake Group (some volcanics and sediments) represents a late-stage rift or early passive margin stage and the sedimentary Hough Lake, Quirke Lake and Cobalt Groups represent an extended passive margin stage. Deposition of the entire package was completed prior to the intrusion of the 2.2 Ga Nippissing diabase sills. The package was subsequently deformed and metamorphosed by the ca. 1.85 Ga Penokean Orogeny.

The Paleoproterozoic dike swarms, mafic intrusions and Huronian flood basalts that comprise the MIE are thought to represent a large continental igneous province initiated by the rifting of an Archean granite-greenstone terrane (Heaman, 1997; Vogel et al., 1998). This rifting and mafic magmatism could have been a consequence of a mantle plume activity (Heaman, 1997).

Street Township intrusions

Recent geochemical and U-Pb geochronological studies (Easton, 1998; Corfu and Easton, 2001) east of the Grenville Front have also identified Huronian-aged magmatism. The felsic bodies have similarities in major- and rare-earth-element geochemistry to the Murray and Creighton plutons and the Paleoproterozoic felsic volcanics of the region (Easton, 1998). A 2468 ± 5 Ma age was obtained for an orthopyroxene hornblendite, interpreted as metamorphosed Huronian age volcanics (Corfu and Easton, 2001). The granitoid gneiss yielded an age of 2475 +25/-10 Ma and a metamorphosed foliated monzogranite an age of 2460 ± 20 Ma (Corfu and Easton, 2001). The ca. 2.45 Ga ages and similar geochemical signatures provide additional evidence for the preservation of Huronian-age magmatism east of the Grenville Front other than the River Valley anorthosite.

Sudbury Structure

The Sudbury Structure, located between the Archean gneisses and granites to the north and the Paleoproterozoic rocks to the south has continued to be the focus of many studies because of the enigmatic features of its origin and its economic significance. The 60 by 30 km layered elliptical structure comprises three parts, the Sudbury Igneous Complex, the concentric turbidite sediments of the Sudbury basin and the brecciated basement rocks in the surrounding region. The base of the igneous complex is host to a

series of Ni-Cu-PGE deposits making the area the most productive nickel camp and one of the largest mining districts in the world.

The uniqueness of the Sudbury Structure has led to many interpretations regarding its origin and its geological history. Currently, three differing hypotheses have been proposed for the formation of the Sudbury Igneous Complex. The first is a meteorite impact model (Dietz, 1964; Grieve et al., 1991), the second is explosive volcanism (Muir, 1984) and the third is an integrated model of impact induced magmatism (Naldrett, 1984). Although the emplacement mechanisms remain controversial, the impact origin first postulated by Dietz (1964) and substantiated by subsequent authors (e.g. Grieve et al., 1991) is generally accepted. A U-Pb zircon age of 1850 ±1 Ma has been established for the age of the irruptive from the average of numerous dates from the norite (Krogh et al., 1982; Krogh et al., 1984). This age is further corroborated by the U-Pb baddelyite age of 1850.5 ± 3.0 Ma for the granophyre unit (Krogh et al., 1984) and a series of ages ranging from 1848.1 to 1849.8 Ma reported from a number of different phases (Corfu and Lightfoot, 1996). The precision of these age-dates limits the magmatic episode of the igneous complex to a few million years. The shock metamorphism effect of the ca. 1850 Sudbury impact event is widespread in the surrounding units and is represented in geological structures such as shatter cones, "Sudbury breccias" and PDFs (planar deformation features) that occur in zircon crystals from the Murray pluton.

CHAPTER 3: FIELD OBSERVATIONS & PETROGRAPHY

Introduction

The Creighton pluton is a small (20 km x 3 km), NE trending granitic body that is located in Graham, Waters and Snider townships near the city of Sudbury, Ontario (Figure 4.1). It lies along the southern flank of the Sudbury Structure and intrudes the metasediments and metavolcanics of the Paleoproterozoic Elliot Lake Group, specifically the Elsie Mountain, Stobie and Copper Cliff Formations (Figure 4.1). The pluton is intruded by the 1850 Ma Sudbury Nickel Irruptive and olivine diabase dikes of the 1235 Ma Sudbury Swarm (Krogh et al., 1987). Previous work on the Creighton pluton has included a number of mapping and structural projects (Card, 1978; Dutch, 1976, 1979) and geochronology studies (Fairbairn et al., 1965; Stockwell, 1982; Frarey et al., 1982). Fieldwork and systematic sampling on the Creighton pluton was conducted during June 1999. Thirty-one samples were collected to form a representative suite including two felsic microgranular enclaves and three Sudbury Impact related breccias. Five samples from the Murray pluton and two samples from the Copper Cliff rhyolite were also acquired.

Field observations

The Creighton pluton is a composite quartz-two feldspar granitoid intrusive with minor mafic interstitial minerals. There is very little variation in the basic mineralogy despite a wide variety of textural phases in the pluton. The dominant phase in the pluton is a pink to grey medium-grained porphyritic granite. Phenocrysts of potassic feldspar are commonly 1 – 2.5 cm in size, are contained in a groundmass of 2 – 4 mm crystals. Other textures include coarse- to medium-grained granites that are pink to grey in colour. Foliation is present in many areas but is more pronounced in regions with an abundance of mafic minerals. Contacts between individual textural types are gradational in nature with no obvious correlation between composition and type of texture.

Brecciation related to the 1850 Ma Sudbury Impact Event is common within the Creighton granite and generally forms irregular-shaped bodies. These bodies contain round granitic fragments in a dark coloured fine-grained granitoid matrix (Figure 3.1).

Contacts with the Huronian Supergroup are sharp when not brecciated. There is little evidence for contact metamorphism, but the Creighton pluton contains abundant inclusions of metasediments and metavolcanics ranging from centimetre scale up to 8 km in size. Small, ovoid microgranular enclaves with 1 – 2 cm potassium feldspar phenocrysts are uncommon but present in the pluton (Figure 3.2).

Previous mapping and structural studies (Card, 1978; Dutch, 1976, 1979) have identified a number of foliations in the granitic intrusion. The first is a strong pre-Sudbury Impact brecciation event foliation that is defined by the parallel alignment of quartz and feldspar grains on the macro scale (Dutch, 1979). This foliation is interpreted

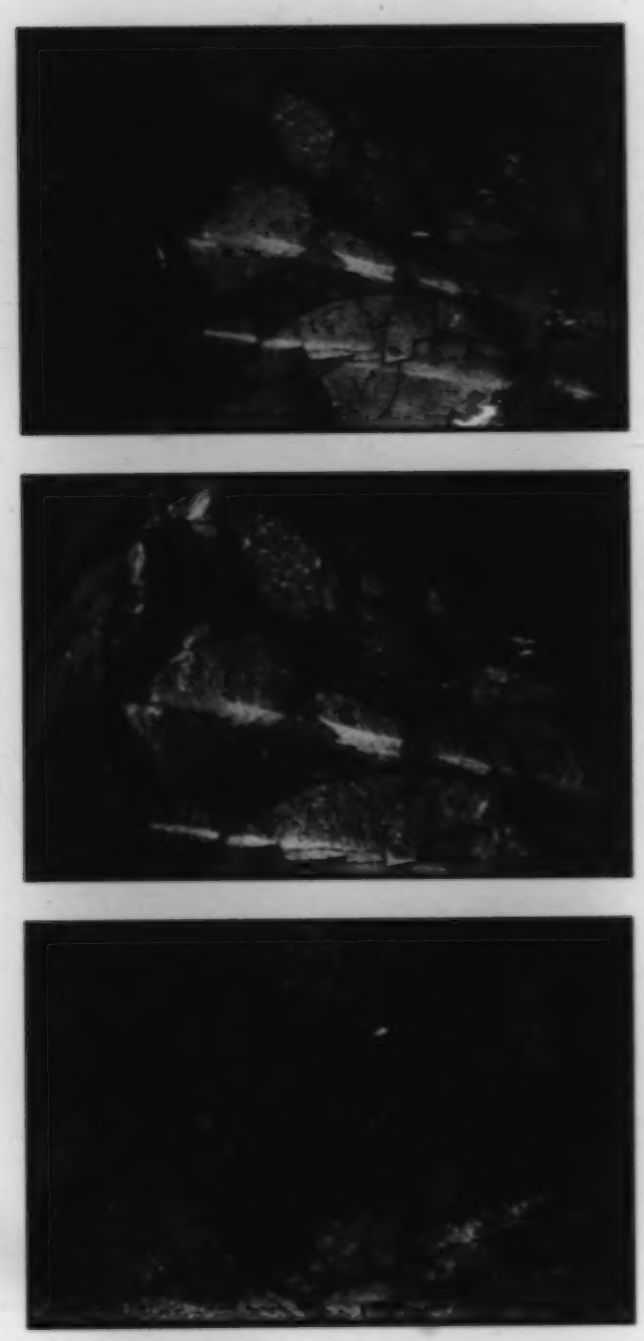

Figure 3.1: Photographs showing Sudbury Impact related brecciation texture in the Creighton pluton.

(a)

(b)

Figure 3.2: Photographs showing felsic microgranular enclaves from the Creighton pluton. **(a)** Enclave sample MS99-57. **(b)** Enclave in outcrop.

to be a syn-intrusive deformation feature primarily based on the observation that it is roughly parallel to the intrusive contact (Dutch, 1979). In the eastern portion of the pluton this foliation forms a complete loop suggesting that the Creighton is made up of two structurally independent deep granitoid bodies (Dutch, 1979). The completely closed form of the foliation event is difficult to explain solely based on a regional metamorphic event. The second foliation is a pervasive, post-breccia, ENE trending cataclastic fabric that formed as a result of regional metamorphism during the Penokean Orogeny (Dutch, 1979). The Creighton pluton has undergone the effects of regional deformation and has been elongated and deformed parallel to the major structural trends in the region

Modelling of geophysical gravity data (Bouguer anomaly) by Popelar (1972 cf. Dutch, 1979) indicates estimated pluton depths of 4 km in the western and 2.5 km in the eastern portion of the pluton. This information is interpreted to represent two separate intrusive centres and corresponds well with the existing structural data.

Petrography

Both modal mineralogy and major-element chemistry can be used to properly identify plutonic igneous rocks with no genetic context. Modal analyses of the Creighton pluton plot within the fields of monzogranite to granodiorite using the IUGS classification (Streckeisen, 1976). On the CIPW normative equivalent to the IUGS classification diagram (Streckeisen and LeMaitre, 1979), the Creighton pluton is dominantly monzogranite with a few of the samples classified as granite or granodiorite

(Figure 3.3). The microgranular enclaves tend to contain more mafic minerals and plot in the granodiorite field. The estimated modal and normative chemical classification schemes are in agreement and are consistent with previous determinations by Card (1968) and Dutch (1976, 1979). There are a number of samples that contain a greater proportion of mafic minerals but appear indistinguishable using these classification schemes.

The Creighton pluton is dominated by holocrystalline quartz-plagioclase-potassic feldspar framework and potassic feldspar phenocrysts (Figure 3.4). In most of the samples these three minerals comprised nearly 90% of the modal mineralogy except near the centre of the intrusion where this decreases to approximately 80%. Grains are dominated by an anhedral to subhedral shape with some of the minor constituents having an euhedral form. Quartz is the most abundant mineral showing typical undulose extinction and uniaxial character. A poikilitic texture with euhedral epidote inclusions is common in the larger plagioclase grains. Microprobe analyses on a JEOL Microprobe and microscope determination indicate plagioclase composition of An_{15}–An_{30} (oligoclase) with these regions encompassed by thin zones of secondary albitization. Microcline twinning is common in the potassic feldspar crystals whereas lamellar twins are rare in plagioclase.

Minor constituents include interstitial biotite, hornblende, epidote and zircon with rare allanite, apatite, chlorite, ilmenite, muscovite and titanite. Biotite is the dominant mafic mineral and can comprise up to ~20% of the total mineralogy. It is more prevalent along contacts and in the central portion of the pluton where it commonly occurs as foliated clots with other mafic minerals. Both the enclaves and the breccias tend to have higher proportions of the minor constituents. A poikilitic texture is common often with

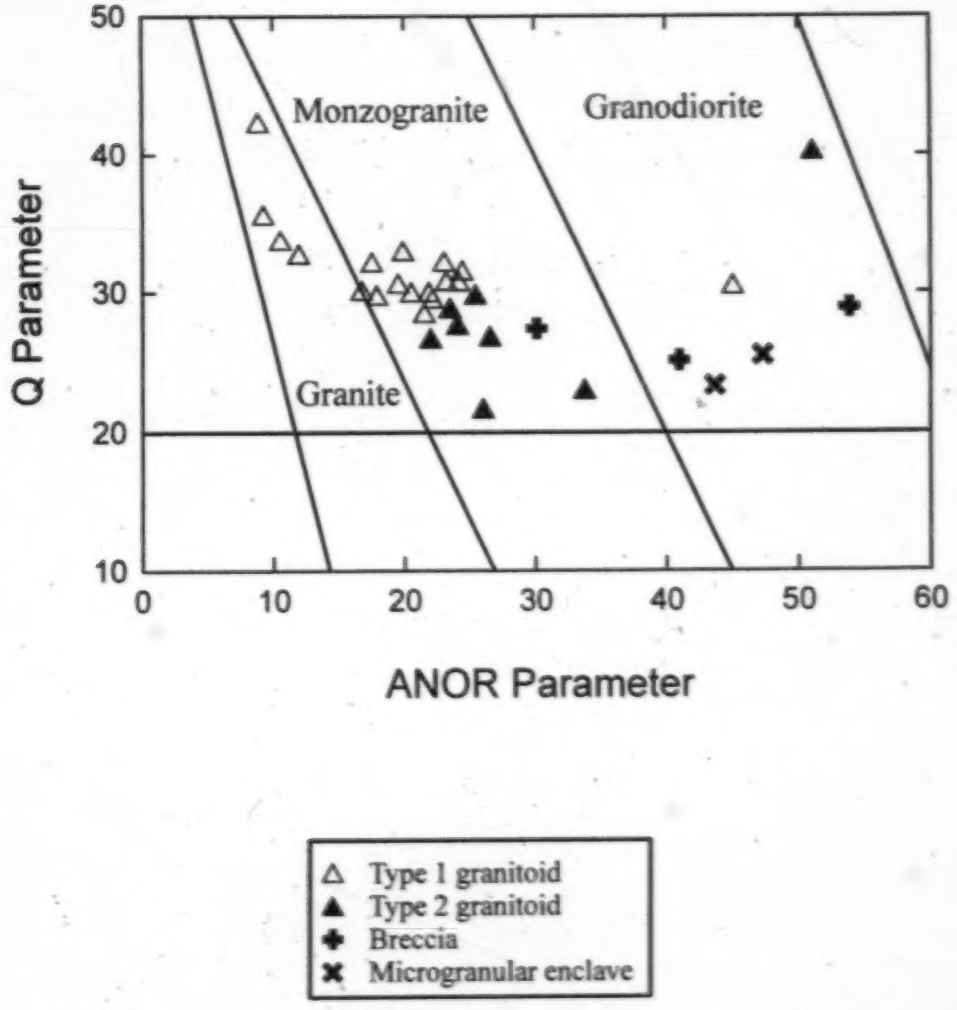

Figure 3.3: IUGS granitoid rock classification diagram (Streckeisen and LeMaitre, 1979) showing plotted CIPW norms calculated for the Creighton pluton. ANOR parameter = [An/(An + Or)] * 100; Q parameter = [Q/Q + Ab+ Or + An)] * 100.

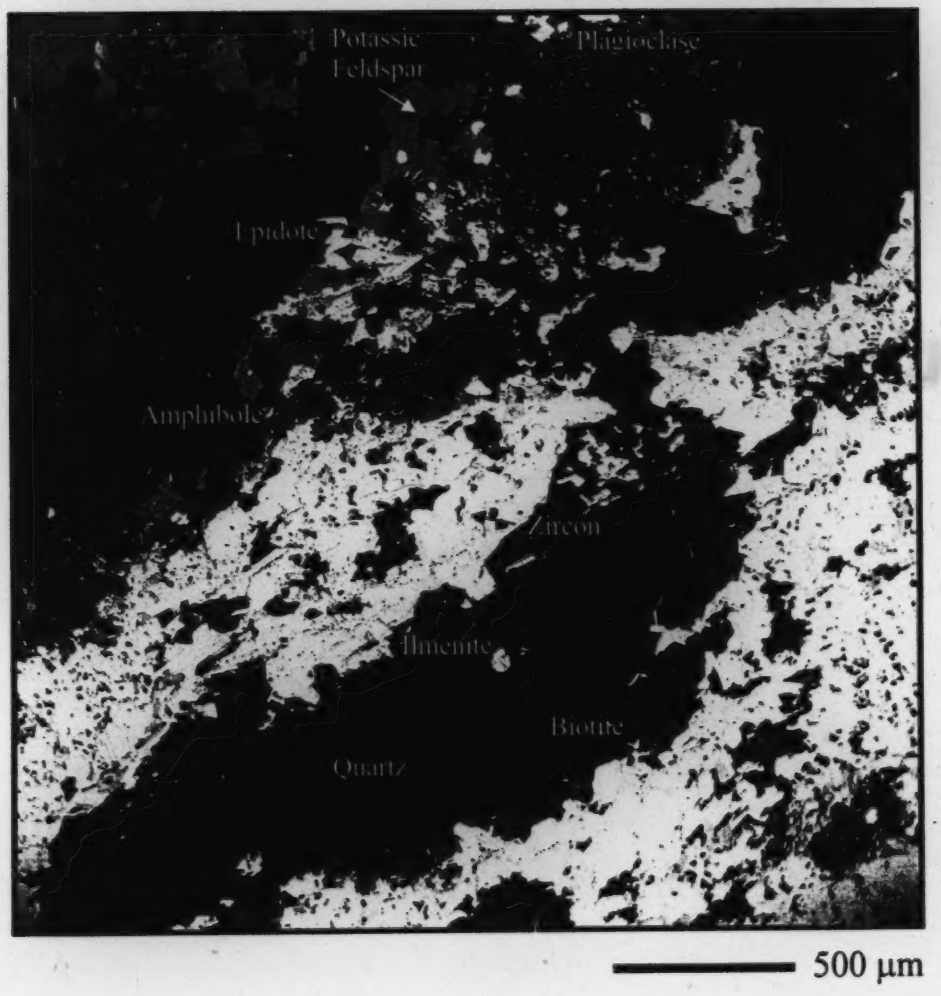

Figure 3.4: Backscatter electron images showing mineralogy and texture of the Creighton pluton (sample MS99-50).

anhedral crystals of epidote, allanite or titanite comprising the poikoblasts. Primary muscovite is extremely rare and occurs only in the most silicic sample (MS99-31). The influence of later metamorphic or hydrothermal events is displayed by obvious replacement textures and secondary mineral growth. Many of the larger crystals of quartz or feldspar show recrystallization to smaller domains from metamorphic or deformation events (Dutch, 1976; 1979). Relict amphibole grains are present having altered to biotite or chlorite. Epidote, titanite and albitization of the plagioclase are secondary in nature, possibly the result of hydrothermal fluids from the 1850 Ma Sudbury Impact event (Ames et al., 1998). Hydrothermal fluids may also explain the relative high abundance of epidote (>10%) found in the microcrystalline Sudbury Breccia samples.

Discussion

Although all the granite samples from the Creighton pluton contain similar modal and chemical abundance of quartz-plagioclase-potassic feldspar, there appear to be two broad lithological types based on the quantitative proportions of these framework minerals. The Type 1 granites are predominantly classified as granite to monzogranite and comprise most of the Creighton pluton. The Type 2 granitoids are generally located near the centre of the pluton, are strictly monzogranites and are recognisable in the field by more abundant mafic (and accessory) minerals (Figure 4.1). These samples have higher contents of biotite, zircon, epidote and titanite when compared to the Type 1 samples. Green calcic amphibole grains can only be identified in the Type 2 granitoids whereas they are absent in the Type 1 grouping. The microgranular enclaves are

petrographically similar to the Type 2 granitoids containing calcic amphibole, abundant biotite and other accessory minerals. These two groupings correspond well with the previous structural and geophysical data that indicate that the Creighton pluton is composed of two distinct intrusive centres. This petrographic grouping of the granite samples will be further explored using the major- and trace-element and isotopic compositions to determine if there is a genetic basis to these mineralogical groupings.

CHAPTER 4: GEOCHEMISTRY

Introduction

Thirty-one samples from the Creighton pluton were analyzed for major, trace and rare-earth element compositions at the Geoscience Laboratories in Sudbury, Ontario (Figure 4.1). Within this sample set, two were microgranular enclaves, three were hydrothermally altered Sudbury Impact related breccias, with the remaining samples being granitoids. Samples weighed approximately 5 kg; their locations can be found in Appendix A. Major elements were determined by X-ray fluorescence (XRF) and the concentration of the trace and rare-earth elements by Inductively Coupled Plasma Mass Spectrometry (ICP-MS). Sample preparation, quality control and analytical procedures are outlined in Dressler et al. (1992). Complete XRF and ICP-MS elemental abundances are located in Appendix B. The primary objectives of the geochemical study are to identify separate geochemical phases, constrain the tectonic setting and gain insight into the crystallisation history and potential sources of the Creighton pluton. As discussed above, the samples investigated from the Creighton pluton have no apparent distinctive textural features but can be subdivided into two types according to certain mineralogical and chemical differences. A summary of the range of values and averages for the two-granitoid types is given in Table 4.1.

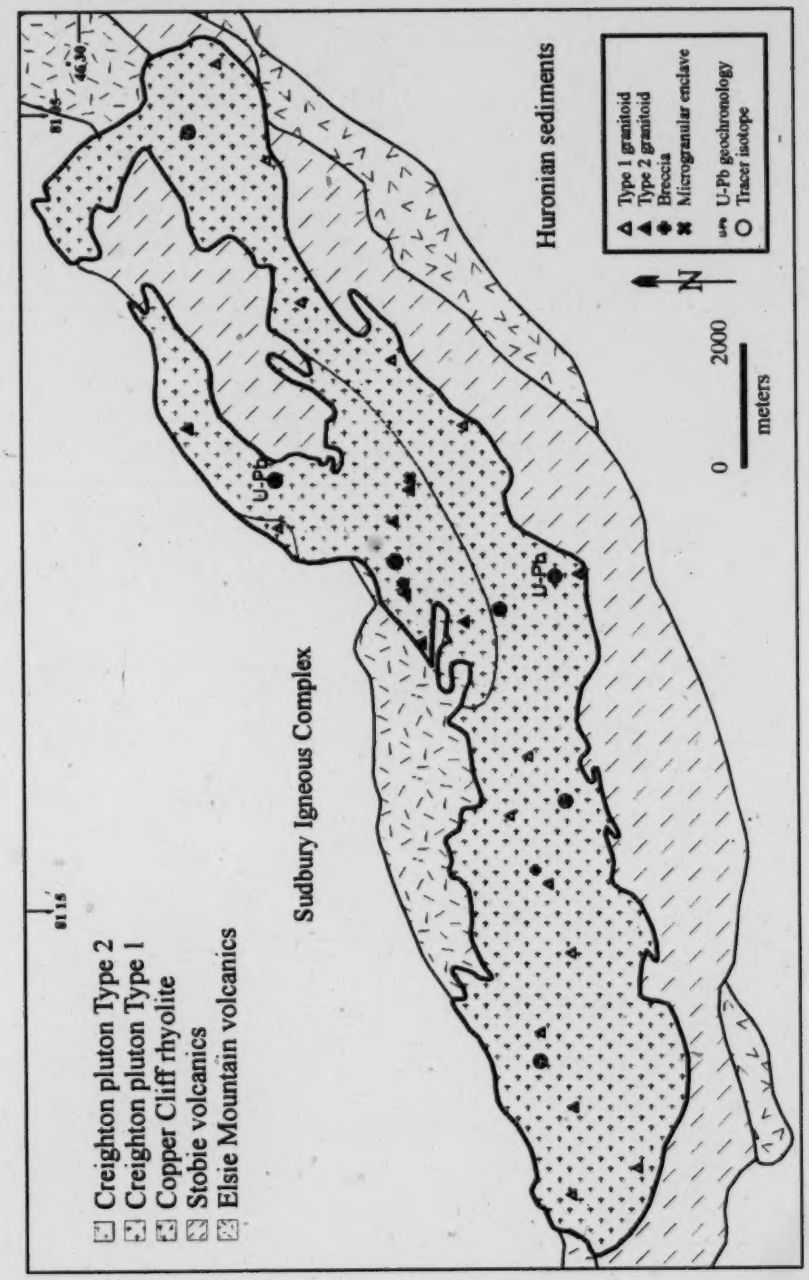

Figure 4.1: Simplified geological map of the Creighton pluton area modified from Dressler (1984) showing distribution of rock types and sample locations for geochemistry, U-Pb geochronology and tracer isotopes.

	Type 1 Granitoid		Type 2 Granitoid	
	Range	Average	Range	Average
SiO_2	67.73 - 79.41	72.59	63.69 - 71.81	68.47
Al_2O_3	11.06 - 13.98	13.12	13.62 - 15.04	13.99
MnO	0.01 - 0.07	0.04	0.05 - 0.12	0.07
MgO	0.13 - 0.81	0.58	0.76 - 1.24	0.93
FeO*	1.01 - 3.53	2.52	3.67 - 7.52	4.91
TiO_2	0.09 - 0.40	0.31	0.42 - 0.93	0.66
CaO	0.58 - 2.48	1.58	2.09 - 3.59	2.59
Na_2O	2.65 - 4.61	3.05	2.56 - 3.35	3.06
K_2O	2.24 - 5.80	4.94	1.93 - 5.50	4.55
P_2O_5	0.01 - 0.11	0.07	0.09 - 0.26	0.16
Mg#	18.5 - 33.8	28.5	21.2 - 31.8	25.7
Ba	437 - 767	654	545 - 1777	1197
Nb	16.4 - 42.8	28.1	24.9 - 49.4	34.3
Rb	146.6 - 400.0	289.7	128.7 - 400.0	218.7
Sc	2.6 - 8.5	6.5	5.8 - 19.0	11.8
Sr	18.2 - 219.3	103.0	144.1 - 237.6	184.8
Th	32.5 - 76.1	44.1	20.4 - 47.3	29.1
U	4.6 - 11.0	7.1	2.2 - 5.2	3.8
Y	45.5 - 106.7	78.3	42.6 - 152.8	101.8
Zn	22 - 80	45	60 - 109	79
Zr	130.7 - 320.1	231.8	316.7 - 440.0	363.1
La	29.94 - 88.51	72.87	79.36 - 126.68	105.02
Ce	72.01 - 203.88	165.16	177.21 - 250.00	231.03
Eu	0.37 - 1.45	1.09	1.52 - 2.86	2.28
Gd	4.66 - 11.00	8.80	8.54 - 21.18	14.03
Yb	3.75 - 10.42	6.91	3.44 - 12.88	7.61
Eu/Eu*	0.20 - 0.44	0.36	0.34 - 0.75	0.51
$(La/Yb)_n$	5.62 - 9.45	7.69	7.06 - 23.46	10.08
$(Gd/Yb)_n$	0.87 - 1.45	1.06	1.36 - 2.05	1.36

Table 4.1: Table showing the range and average geochemistry of the Type 1 (n=18) and Type 2 (n=8) granitoids of the Creighton pluton.

Major- and trace-element chemistry

The Creighton pluton is a potassic ($Na_2O/K_2O < 1$) granitic body that shows continuous linear trends with SiO_2 (Figure 4.2). It consists of a wide compositional range of SiO_2 values from 63% to 79% with no clear cut-off boundary between the two defined granitoid types. Major element trends with increasing SiO_2 are typified by decreasing Al_2O_3, CaO, MgO, MnO, FeO* (total Fe), TiO_2 and P_2O_5 whereas K_2O increases. Na_2O compositions are relatively constant regardless of the silica content. The Creighton pluton has high values of K_2O, CaO, Na_2O+K_2O, and an average Mg# (=100*Mg/(Mg+Fe*) of 27.6. Although all granitoid samples (both Type 1 and 2) show continuous linear trends with no clear slope differences, there are some discrepancies in the major element chemistry. Type 2 granitoids (solid triangles) tend to be less fractionated with higher values of Al_2O_3, CaO, MgO, FeO*, TiO_2, P_2O_5 and (FeO* + MgO + TiO_2). These granites are strictly metaluminous when classified by the alumina-saturation index (ASI = molar $Al_2O_3/(CaO + Na_2O + K_2O)$ (Figure 4.4a) and plot slightly in the tholeiitic field on an AFM ternary diagram (Irvine and Baragar, 1971) (Figure 4.4b). Conversely, the Type 1 granitoids (open triangles) are metaluminous to weakly peraluminous and show a calc-alkaline affinity. Overall, the ASI index becomes more peraluminous as the SiO_2 content increases.

Both types of granitoids exhibit similar trace-element patterns on Harker Diagrams (Figure 4.3). With increasing SiO_2, Ba, Ce, Ga, Hf, Sc, Sr, Yb, Zn and Zr decrease whereas Th increases. Other elements such as Nb and Y show slight decreases.

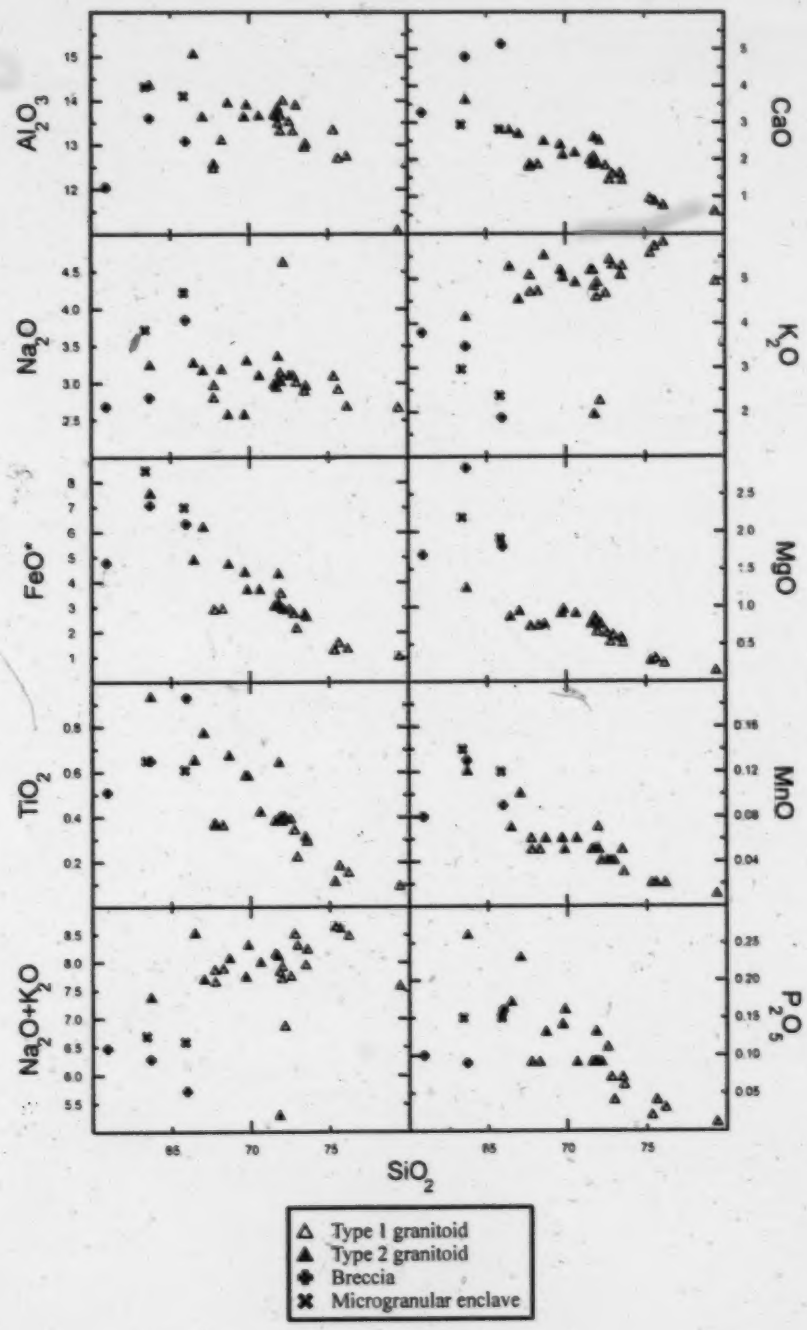

Figure 4.2: Major element oxide (wt %) Harker diagrams for the Creighton pluton.

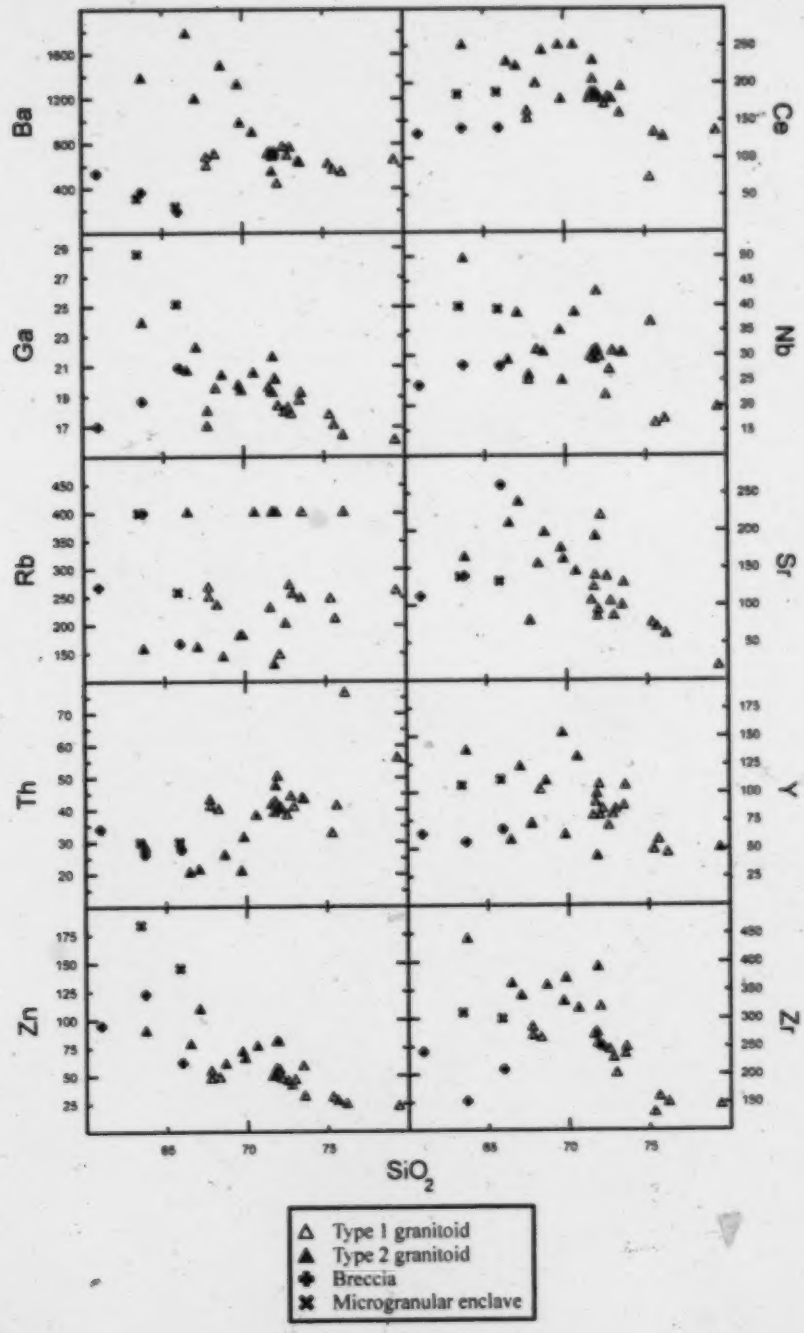

Figure 4.3: Selected trace element (ppm) Harker diagrams for the Creighton pluton.

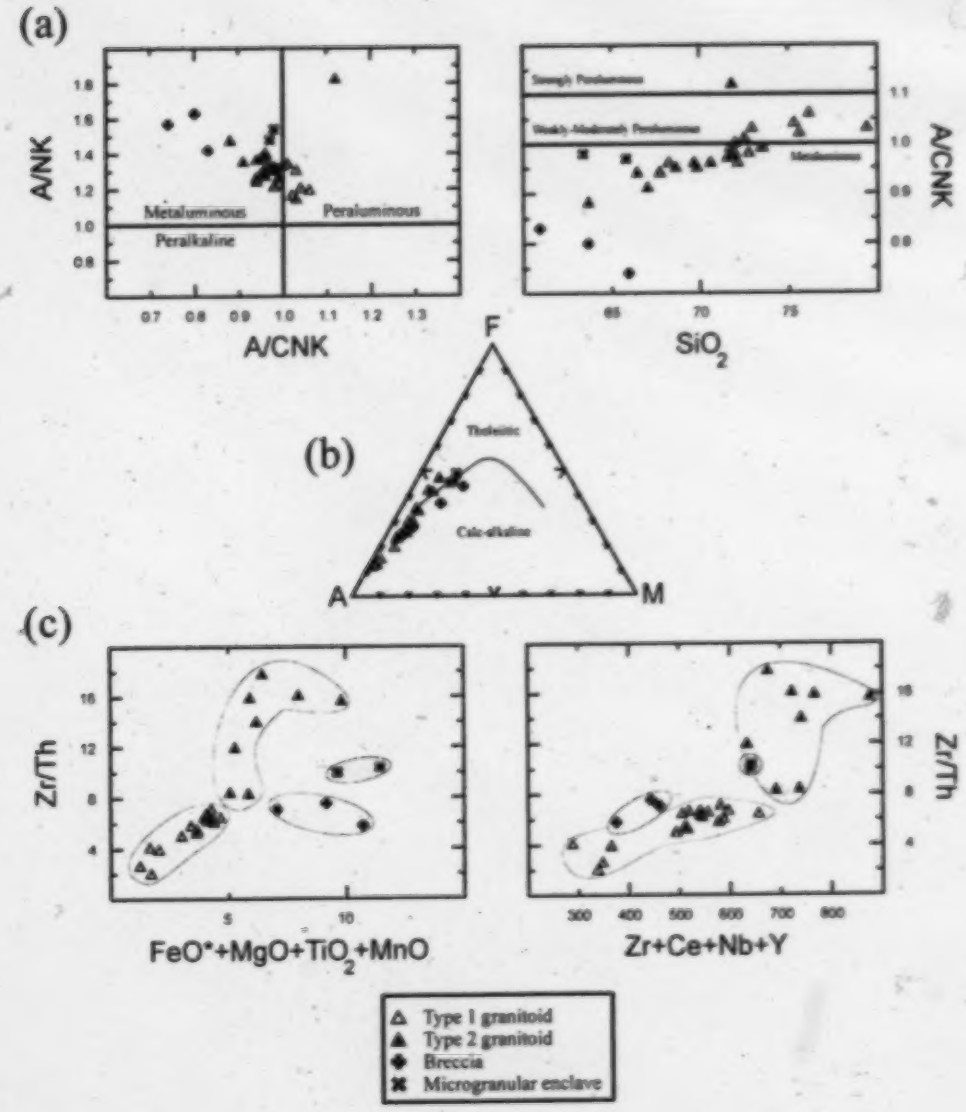

Figure 4.4: **(a)** ASI (alumina-saturation index) diagrams. A/CNK = molar ratio Al/(Ca + Na + K); A/NK = molar ratio Al/(Na + K). **(b)** AFM ternary diagram after Irvine and Baragar (1971). A = $Na_2O + K_2O$; F = FeO (total Fe); M = MgO. **(c)** Comparative multi-elemental diagrams for the Creighton pluton incorporating major-, trace- and rare-earth elements.

As with major-element composition discussed above, the granitoid populations of the Creighton pluton show significant differences in trace element contents and distinct fractionation slopes. Relative to the Type 1 granitoids, the Type 2 samples show higher Ba, Ce, Sc, Zn and Zr (weakly higher Hf, Ga, Sr) and lower Rb, Th and U content. Comparative diagrams of Zr/Th vs. $FeO^*+MgO+MnO+TiO_2$ and Zr/Th vs. Zr+Ce+Y+Nb incorporating differences in both major and trace elements identify well-defined discrimination boundaries between all rock types in the Creighton pluton (Figure 4.4c).

The microgranular enclaves and hydrothermal breccias are compositionally similar, metaluminous and plot along the calc-alkaline – tholeiitic boundary of the AFM ternary diagram (Figure 4.3). Both have elevated values of FeO*, MgO and MnO with lower K_2O and Ba compared to the granitoids. The enclaves are enriched in Na_2O, Ga and Zn whereas the breccias have higher CaO values. The "Sudbury" breccias exhibit opposite fractionation trends to the granitoids for a number of elements. With respect to silica content CaO, TiO_2, Ga and Sr increase whereas K_2O decreases (Figure 4.2, 4.3). Many of these elements are mobile under metamorphic and hydrothermal conditions and can easily be disturbed by these processes.

Rare-earth-element chemistry

Despite differences in major- and trace-element concentrations, the Creighton pluton exhibits similar rare-earth-element patterns for all rock types (Figure 4.5). The intrusion has light rare-earth-element (LREE) enrichment (average $La_N/Yb_N = 8.16$), a slight negative Eu anomaly (average $Eu/Eu^* = 0.41$), and a relatively flat heavy rare-

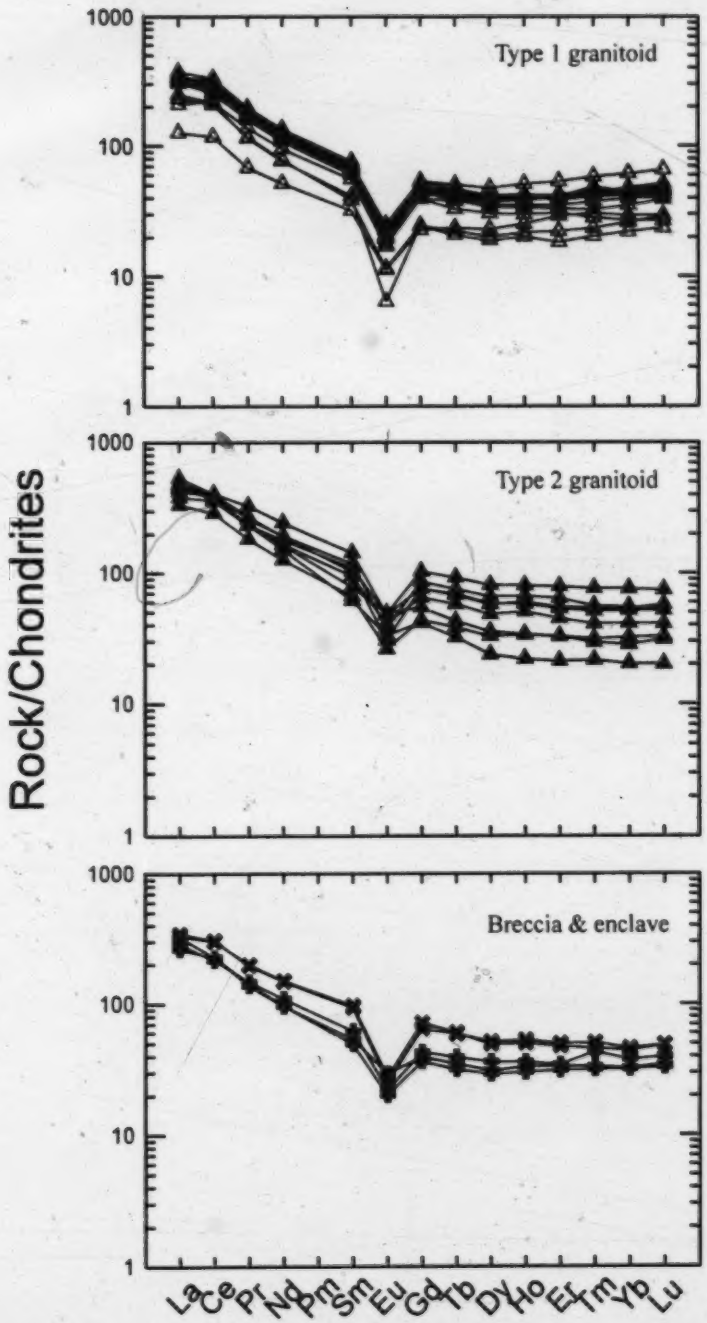

Figure 4.5: Chondrite normalized rare-earth element diagrams for the Creighton pluton. Normalization values are after Sun and McDonough (1989).

earth-element (HREE) pattern (average Gd_N/Yb_N = 1.19). The less felsic Type 2 granitoids tend to be more LREE-enriched, which is the reverse of normal igneous trends. Primitive mantle and MORB-normalised spidergrams also illustrate the similar characteristics of all rock types in the Creighton pluton (Figure 4.6). Relative depletions in Ba, Nb, P, Sr, and Ti are typical with the Type 1 granitoid depletions being more pronounced. Relative enrichments of Rb, Pb, Th and U, equal abundance of Ta-Nb-Ce and flat MORB-like values of Zr-Hf-Sm-Y-Yb are characteristic of the granitic intrusion.

Discussion

The geochemistry further supports the initial claim based on the mineralogy that there are two distinct phases within the Creighton pluton. The geochemical similarities and continuous chemical trends between the two types of granitoids (e.g. ASI, REE pattern) indicate that they could be the products of the same parental magma or source. The minor differences suggest that each possess a slightly different petrogenetic history. The geochemical zones identified here roughly correspond to previous geophysical (Popelar, 1972; cf. Dutch, 1979) and structural (Dutch, 1976; 1979) data that were interpreted to indicate the Creighton pluton is composed of two separate intrusive centres. Anomalous values in certain major elements (Na_2O, K_2O) occurred in samples located near the Sudbury Irruptive contact and likely resulted from element mobility during this geological event.

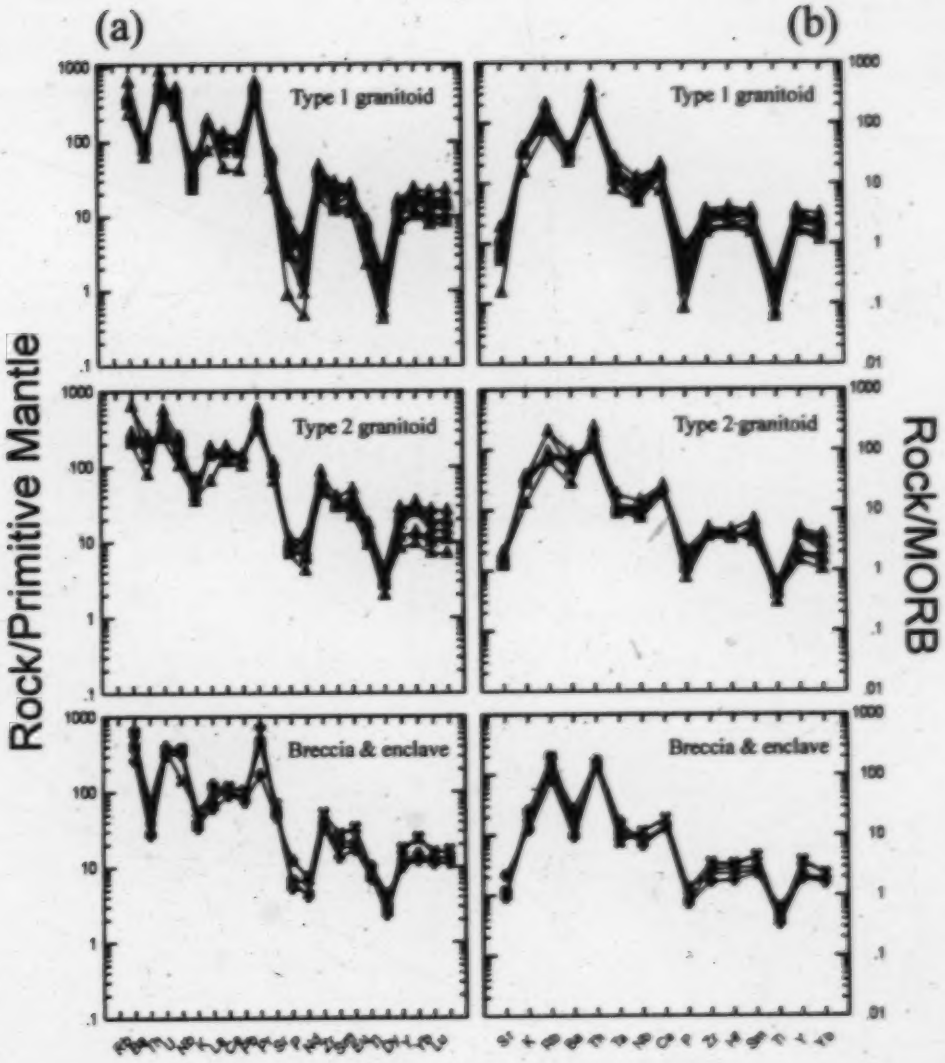

Figure 4.6: **(a)** Primitive mantle normalized multi-element spidergram for the Creighton pluton. Normalization values are after Sun and McDonough (1989). **(b)** MORB (Mid-Ocean Ridge Basalt) normalized multi-element spidergram for the Creighton pluton. Normalization values are after Pearce (1983).

CHAPTER 5: GEOCHRONOLOGY

Introduction

A U-Pb geochronology study was conducted on two samples (LH98-63 and MS99-50) from the Creighton pluton to constrain the precise timing of granite emplacement and facilitate temporal comparisons with other Matachewan Igneous Events in the Southern Superior and Grenville Provinces. The two samples were selected to represent each of the two distinct mineralogical and chemical phases within the granitic body, to test whether they have identical emplacement ages.

The U-Pb zircon age data for a total of 14 analyses from the Creighton pluton are presented in Table 5.1 with corresponding concordia diagrams in Figures 5.1b, 5.5b, 5.8 and 5.9. In addition, three U-Pb zircon analyses from Frarey et al., (1982) are shown for comparison. Complete zircon fraction descriptions are given in Table 5.2 and sample locations in Figure 4.1.

Analytical procedures for the mineral separation of zircon and the determination of the isotopic composition of uranium and lead are outlined in Appendix C. All U and Pb isotopic analyses were determined in single collector (Daly) mode with either a VG354 or Micromass Sector 54 mass spectrometer. Discordia line calculations were performed using the ISOPLOT/Ex program of Ludwig (1998).

Table 5.1: Complete U-Pb data from Creighton pluton.

Description		Concentrations (ppm)					Atomic Ratios[3] ± 1 σ error (Ma)				Apparent Age ± 1 σ error (Ma)			
#	Wt (mg)	U	Pb	Th[1]	Th/U	Pb_C[2] (pg)	$^{206}Pb/^{204}Pb$	$^{206}Pb/^{238}U$	$^{207}Pb/^{235}U$	$^{207}Pb/^{206}Pb$	$^{206}Pb/^{238}U$	$^{207}Pb/^{235}U$	$^{207}Pb/^{206}Pb$	PD[4]
Frarey														
F1	1.5500	550	239				1670	0.3949	8.0749	0.1483	2146.0	2239.0	2326.0	7.74
F2	0.9200	464	198				1368	0.3942	8.0316	0.1478	2142.0	2235.0	2320.0	7.67
F3	2.3800	585	241				1394	0.3773	7.6847	0.1477	2064.0	2195.0	2319.0	11.00
LH98-63														
1*	0.0009	225	115	140	0.62	2.5	2249	0.4415 ± 10	9.535 ± 25	0.1566 ± 2	2357.4 ± 4.5	2391.0 ± 2.4	2419.7 ± 2.0	3.08
2*	0.0020	313	158	169	0.54	8.5	1001	0.4292 ± 9	9.264 ± 23	0.1566 ± 2	2302.0 ± 4.2	2364.5 ± 2.4	2418.8 ± 1.8	5.74
3	0.0010	202	110	127	0.63	8.4	687	0.4486 ± 11	9.640 ± 27	0.1558 ± 2	2389.2 ± 4.7	2401.0 ± 2.7	2411.0 ± 2.2	1.08
4	0.0062	84	38	44	0.52	9.4	1370	0.3902 ± 8	8.246 ± 19	0.1533 ± 1	2123.8 ± 3.7	2258.3 ± 2.2	2382.6 ± 1.3	12.74
5	0.0010	473	242	262	0.55	14.1	921	0.4312 ± 10	9.200 ± 23	0.1547 ± 2	2311.1 ± 4.3	2358.1 ± 2.4	2399.0 ± 1.7	4.36
MS99-50														
2*	0.0010	75	36	34	0.45	1.5	1345	0.4339 ± 17	9.122 ± 42	0.1525 ± 3	2323.2 ± 7.5	2350.2 ± 4.2	2373.7 ± 3.8	2.53
3*	0.0020	37	8	6	0.16	1.7	679	0.2161 ± 8	3.724 ± 25	0.1250 ± 6	1261.5 ± 4.2	1576.5 ± 5.3	2028.2 ± 9.0	41.54
4*	0.0017	207	101	82	0.40	7.8	1237	0.4339 ± 9	9.144 ± 21	0.1528 ± 1	2323.4 ± 3.8	2352.5 ± 2.1	2377.9 ± 1.5	2.73
5	0.0020	337	155	105	0.31	4.5	3986	0.4277 ± 8	8.953 ± 18	0.1518 ± 1	2295.5 ± 3.5	2333.2 ± 1.9	2366.4 ± 1.1	3.56
6	0.0024	326	325	1096	3.36	145.3	170	0.4634 ± 10	9.747 ± 42	0.1526 ± 5	2454.4 ± 4.4	2411.1 ± 4.7	2374.8 ± 6.0	-4.03
7	0.0001	278	137	148	0.53	1.4	553	0.4373 ± 43	9.208 ± 104	0.1527 ± 8	2338.7 ± 19.2	2358.9 ± 10.3	2376.5 ± 8.7	1.89
8	0.0022	113	53	34	0.30	2.2	3084	0.4370 ± 9	9.322 ± 22	0.1547 ± 2	2337.3 ± 4.0	2370.2 ± 2.2	2398.5 ± 1.6	3.04
9	0.0043	310	144	111	0.36	4.4	8219	0.4271 ± 8	9.027 ± 18	0.1533 ± 1	2292.5 ± 3.4	2340.8 ± 1.8	2383.0 ± 0.9	4.51
10	0.0132	261	134	105	0.40	172.1	553	0.4299 ± 8	9.037 ± 23	0.1525 ± 2	2305.3 ± 3.7	2341.7 ± 2.5	2373.7 ± 2.5	3.43

All samples analyzed on VG354 except those denoted by an * which were analyzed by the Sector 54 and 3 analyses from Frarey et al., (1982)

[1] Model Th/U concentration calculated based on ^{208}Pb and $^{207}Pb/^{206}Pb$ age

[2] Pb_c = Common Pb = Initial + blank Pb

[3] Atomic ratios corrected for blank (Pb = 2 pg +/- 50% and U = 0.5 pg +/- 20%) and initial common Pb (Stacey and Kramers, 1975)

[4] Discordance values (%) for Frarey et al., (1982) calculated based on apparent ages

Fractions		Grain Size	Description[1]
#	Wt (mg)	(μm)	
LH98-63			
1	0.0009	100	1 gr, tan prism, ab, frac
2	0.0020	100	1 gr, tan prism, ab, frac
3	0.0010	125	1 gr, tan prism, ab, frac
4	0.0062	60	4 gr, tan prism, ab, frac
5	0.0010	100	1 gr, tan prism, ab, frac
MS99-50			
2	0.0010	80	1 gr, tan prism, small, ab, frac
3	0.0020	125	1 gr, brown equant, ab, incl, frac
4	0.0017	125	1 gr, brown equant, ab, incl, frac
5	0.0020	125	1 gr, brown equant, ab, frac, clear tip
6	0.0024	100	1 gr, trans brown equant, ab, frac
7	0.0001	80	1 gr, clear trans prism, ab, incl, frac
8	0.0022	80	2 gr, trans brown equant, ab, incl, frac
9	0.0043	80-100	8 gr, brown equant, ab, incl, frac
10	0.0132	100-125	12 gr, large, brown equant, ab, frac

[1] All Creighton pluton zircon samples separated out are non-magnetic at 1.8A and 15° inclined tilt

Gr: grain; Ab: air abraded; Frac: fractures; Incl: inclusions; Trans: transparent

Table 5.2: Complete zircon fraction descriptions from the Creighton pluton.

LH98-63

Sample LH98-63 is gray, coarse-grained porphyritic granite located in the south-central region of the pluton along Highway 144 (Figure 5.1a). It is a Type 1 granitoid with minor amounts of biotite and accessory minerals. Four abraded single grain and one multi-grain zircon fraction were analyzed from this sample.

The zircon crystals are cloudy to transparent tan prisms that are euhedral to subhedral in form (width:length = 4:1). The larger grains (75-150 microns) tend to be more mottled with abundant mineral inclusions and fractures and show signs of resorption. Backscatter electron images illustrate these features, as well as compositional zoning and structure within the zircon grains (Figure 5.2). A characteristic common to some of the crystals seen in secondary electron images (Figure 5.3) are parallel planar fractures that have been interpreted as shock induced PDF (planar deformation features) similar to those found in the nearby 2477 ± 9 Ma Murray pluton (Krogh et al., 1996). The smaller transparent (30-60 microns) tan prisms are generally less fractured with fewer inclusions and were carefully selected for U-Pb analyses (Figure 5.4).

All analyzed fractions are slightly to moderately discordant (1.1 – 12.7%) and yield a scattered pattern (Figure 5.1b). Th/U ratios are consistent (0.52 – 0.63) with four samples having a uranium concentration range of 202 – 473 ppm. $^{207}Pb/^{206}Pb$ ages are all near 2400 Ma with a range from 2382.6 Ma to 2419.7 Ma. The most discordant sample corresponds to the anomalous low uranium concentration (#4 – 84.1 ppm) and the youngest $^{207}Pb/^{206}Pb$ age. The scatter is likely to represent a complex Pb-loss history and

(a)

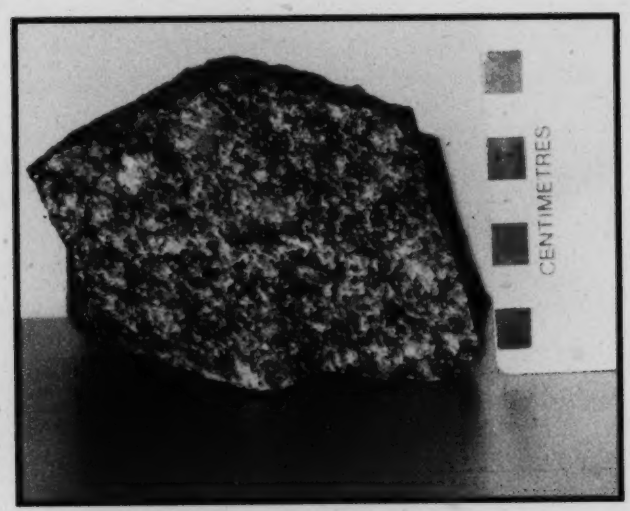

(b)

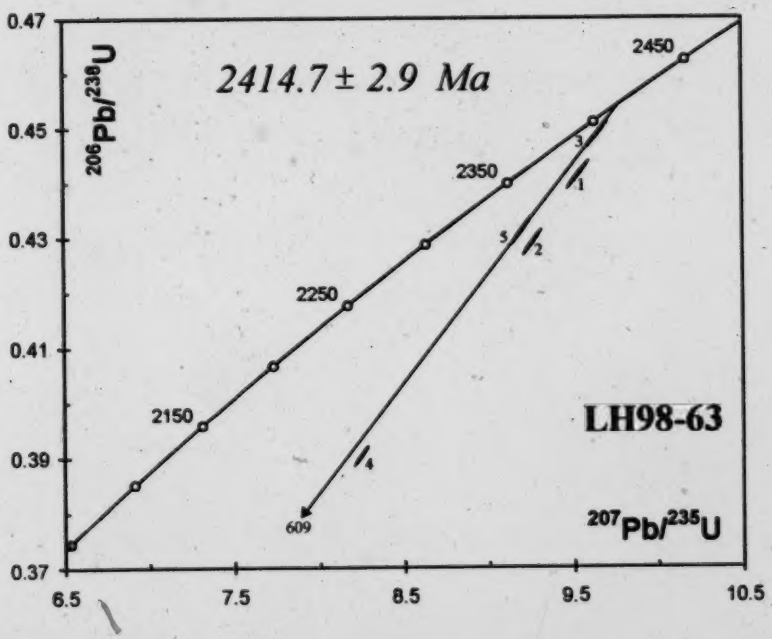

Figure 5.1: **(a)** Photograph of Type 1 sample LH98-63. **(b)** U-Pb concordia diagram showing results from sample LH98-63. Regression line plots through the two single grain analyses with similar $^{207}Pb/^{206}Pb$ ages (#1 and #2). Numbers beside error ellipses refer to analysis number in Table 5.1. Error ellipses are shown at 1σ.

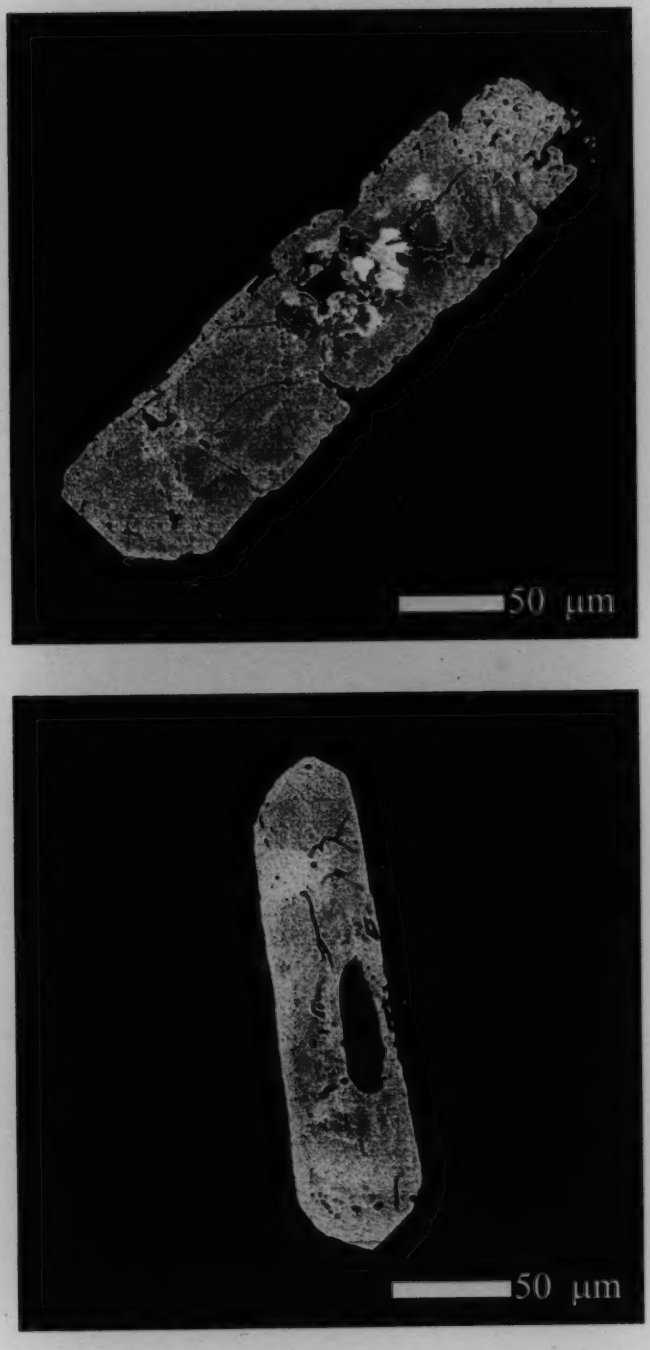

Figure 5.2: Backscatter electron images of zircons from LH98-63.

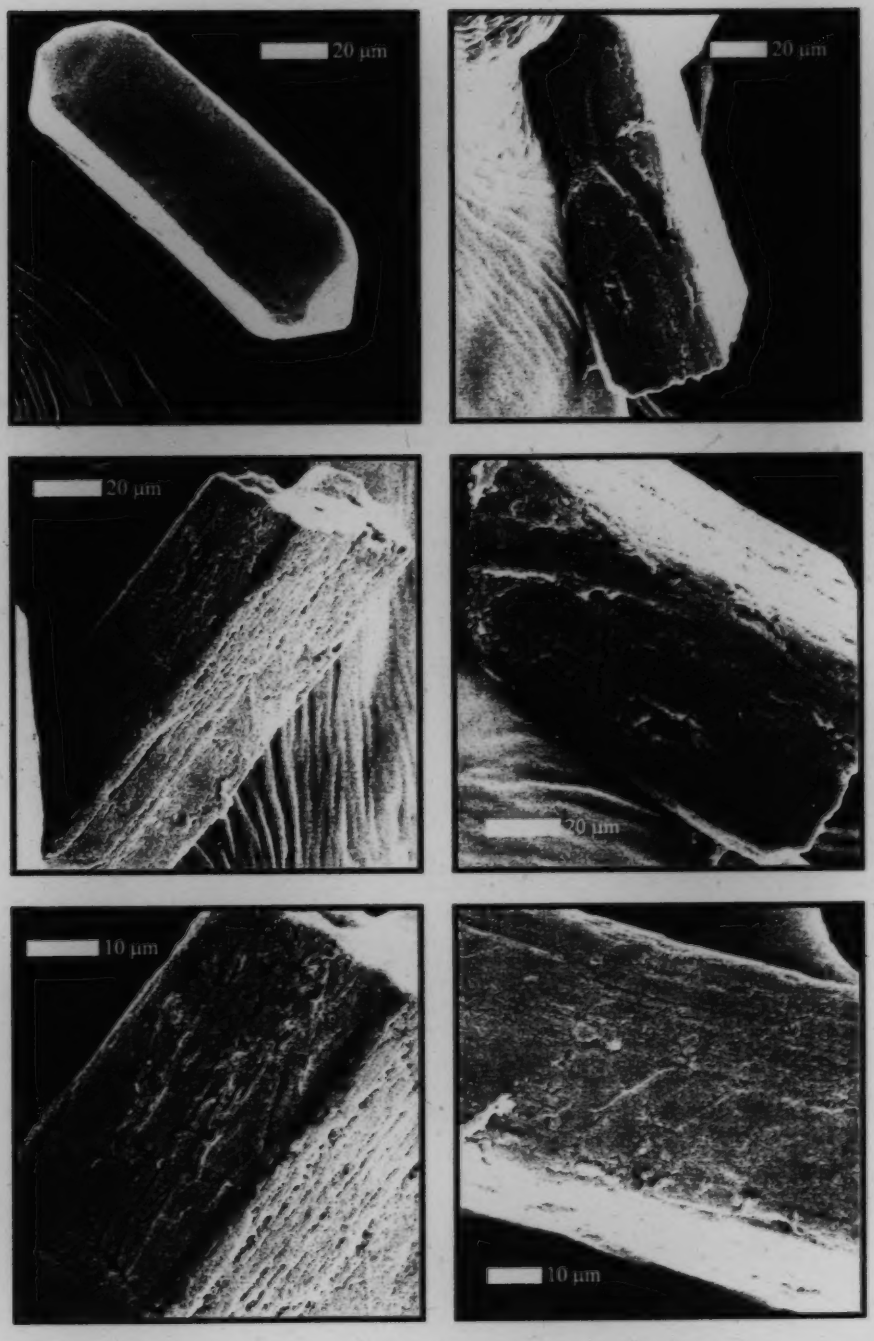

Figure 5.3: Secondary electron images of shocked zircons from the Creighton pluton (sample LH98-63) displaying PDF (planar deformation features).

Figure 5.4: Photographs of zircon fractions from LH98-63. Magnification is x100.

no precise emplacement age can be determined through linear regression. However, a minimum crystallization age of 2411 Ma can be assigned to the Creighton pluton using the $^{207}Pb/^{206}Pb$ age of the least discordant fraction (#3 – 1.08%). Regression of analyses #3 and #5 yield an upper intercept age of 2414.7 ± 2.9 Ma with the three other analyses (#1, #2, #4) falling slightly to the right of this line. These fractions may simply be showing slight inheritance from earlier (ca. 2450 – 2490 Ma) Paleoproterozoic magmatism. These data show that the Creighton pluton is nearly 100 Ma older than age interpretations based on previous radiometric determinations (Stockwell, 1982; Frarey et al., 1982).

MS99-50

Sample MS99-50 is dark grey, foliated, coarse-grained granite located in the northeastern portion of the pluton near the contact with the Sudbury Structure (Figure 5.5a). It is a Type 2 granitoid with abundant biotite and accessory minerals (epidote, zircon) and minor hornblende. Six abraded single grain and three multi-grain zircon analyses from this sample are reported in Table 5.1.

This granitoid sample possesses two morphologically distinct populations of zircon. The first are tan prisms similar in size and appearance to those in sample LH98-63. The second population is small (60-80 microns), brown, subhedral equant (width: length = 2:1) grains that are cloudy to transparent. Backscatter electron images show inclusions, abundant fractures and a well-defined oscillatory zoning within the crystals (Figure 5.6). Fractures interpreted as PDF are common and can be easily viewed using a

(a)

(b)

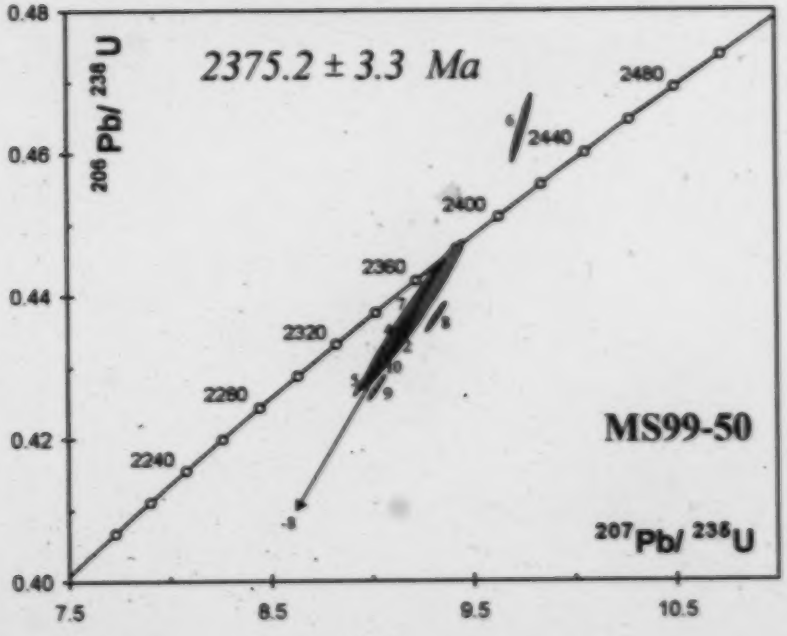

Figure 5.5: **(a)** Photograph of Type 2 sample MS99-50. **(b)** U-Pb concordia diagram showing results from sample MS99-50. Regression line plots through five analyses (#2, #4, #6, #7, #10). Numbers beside error ellipses refer to analysis number in Table 5.1. Error ellipses are shown at 1σ.

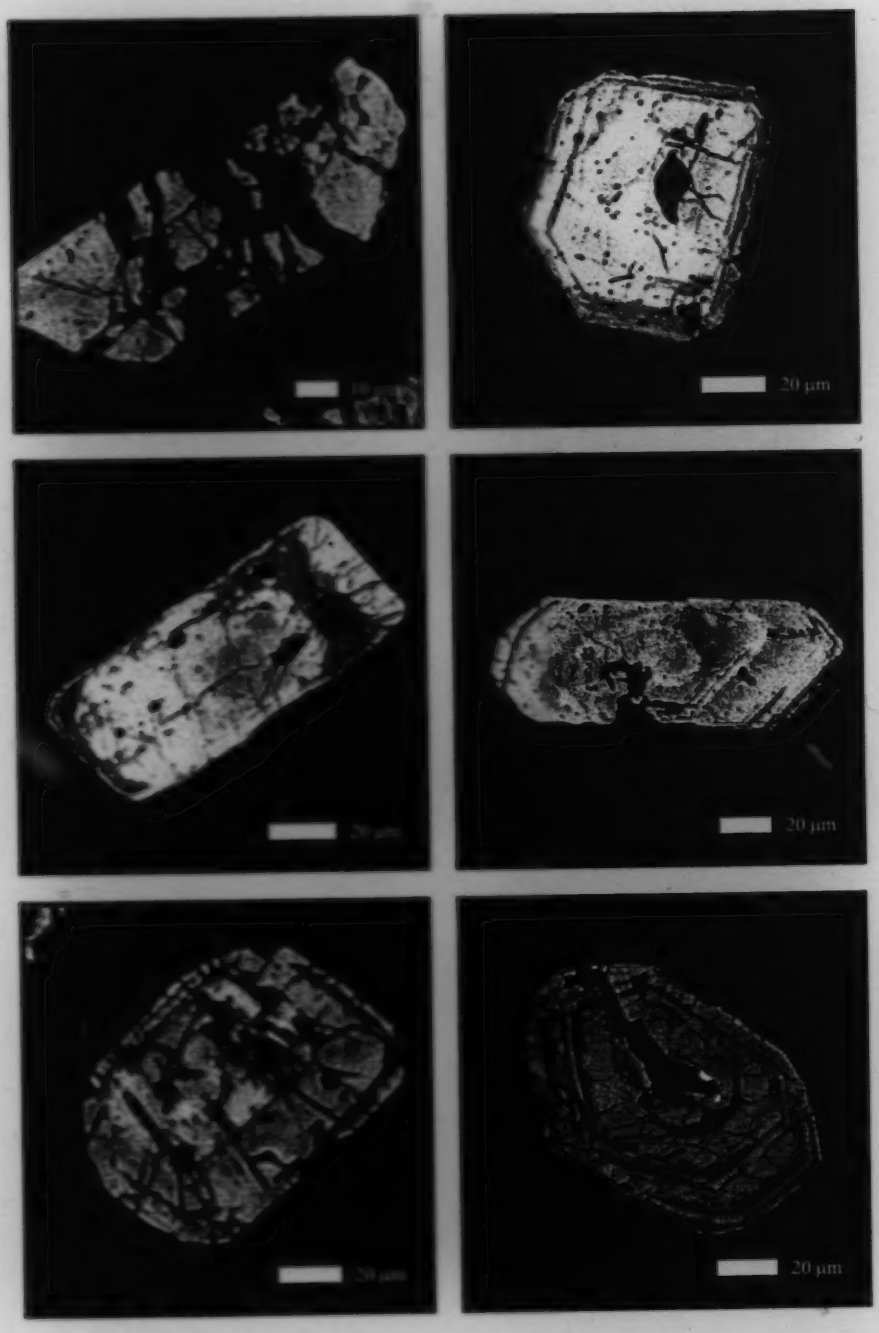

Figure 5.6: Backscatter electron images of zircons from MS99-50.

reflected light microscope. Zircon grains from both the tan prisms and brown equant populations were selected for U-Pb radiometric analyses (Figure 5.7).

Although most of the U-Pb zircon analyses are moderately discordant (1.89 – 4.51%), similar to sample LH98-63, the data for MS99-50 produced a cluster pattern (Figure 5.1b). With the exception of two fractions, the Th/U ratios are generally consistent (0.30 – 0.53) with a uranium concentration range from 75 to 337 ppm. Unlike LH98-63, there is no correlation between uranium concentration and degree of discordance. The most discordant fraction (#3) possesses anomalous concentrations of model Th (6 ppm), U (36.9 ppm), Pb (8.3 ppm) and a low Th/U ratio of 0.160. This fraction was not used in any U-Pb age calculations because of apparent U and Pb mobility and is not shown in Figure 5.5b. Fraction #6 possesses high concentrations of model Th (1095.8 ppm) and common Pb (145.3 pg) with a Th/U ratio of 3.36. The analysis is reversely discordant which may be the result of incomplete dissolution of the sample. Five of the fractions (#2, #4, #6, #7 and #10) yielded consistent $^{207}Pb/^{206}Pb$ ages ranging from 2373.7 Ma to 2377.9 Ma. Two of the multi-grain fractions (#8 and #9) have slightly older $^{207}Pb/^{206}Pb$ ages of 2398.7 Ma and 2383.0 Ma, respectively, with single grain fraction #5 having a younger $^{207}Pb/^{206}Pb$ age of 2366.4 Ma. A weighted average $^{207}Pb/^{206}Pb$ calculation of the five similar fractions (#2, #4, #6, #7 and #10) yields an age of 2376.3 ± 2.3 (MSWD = 0.69). A regression line through these five points produces a similar age of 2375.2 ± 3.3 Ma with a lower intercept of -8 Ma (MSWD = 3.2) (Figure 5.5b). Analyses #8 and #9 could have slight inheritance from either the Creighton Type 1 granitoid intrusion or older Paleoproterozoic material.

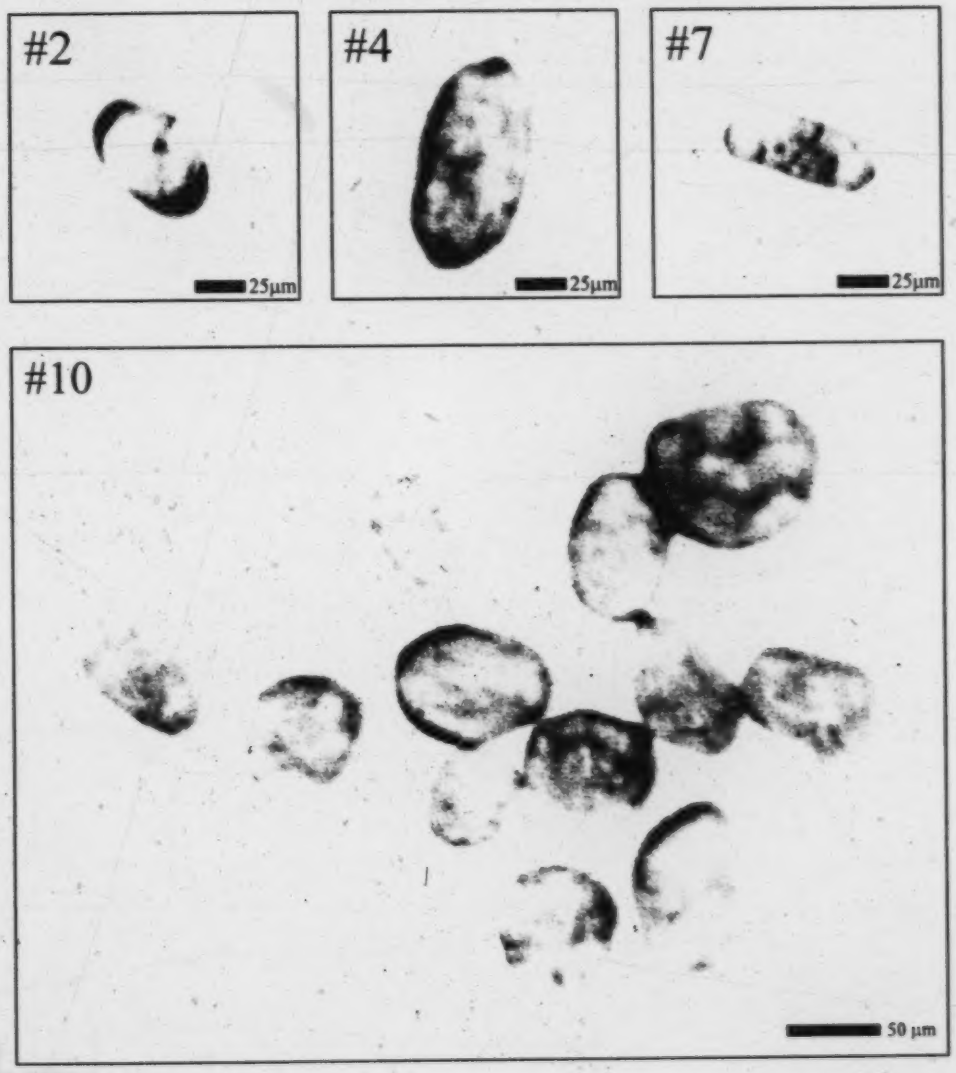

Figure 5.7: Photographs of zircon fractions from MS99-50. Magnification is x100.

Discussion

To assess all of the U-Pb geochronology data (Figure 5.8) and determine the best age estimate for the Creighton pluton phases, a number of factors must be considered. The two samples produce different initial age estimates (2414.7 ± 2.9 Ma and 2376.3 ± 2.3 Ma) with the fractions from MS99-50 generally yielding tightly constrained and younger $^{207}Pb/^{206}Pb$ ages. Sample LH98-63 yields a scattered pattern suggesting a complex, multiple Pb-loss history, whereas MS99-50 yields a cluster pattern suggesting a similar Pb-loss history and similar degree of Pb-loss. The multi-grain zircon analyses (#8, #9, and #10) from MS99-50 are slightly more discordant but not as much as the multi-grain analysis (#4) from LH98-63. The well-documented 1850 Ma Sudbury Impact related Pb-loss event in the nearby Murray pluton (Krogh et al., 1996) does not seem as prevalent in the Creighton pluton despite the presence of fractures interpreted as PDFs in the zircon crystals. Although rare, there are two studies that document relatively nearby geological events at ca. 2.4 Ga. The first is a 2408 ± 3 Ma meta-diabase dike located in the Grenville Province (Krogh, 1994) and the second is a 2416 ± 30 Ma metamorphic zircon overgrowth from a granulite-grade meta-anorthosite recovered in a Jurassic kimberlite pipe near Kirkland Lake, Ontario (Moser and Heaman, 1997).

The possibility of an 1850 Ma component of Pb-loss that is prevalent in the zircon from the nearby Murray granite cannot be discounted for the Creighton granite zircon. A closer inspection of the fractions from LH98-63 appears to show three separate trends that all suggest a similar upper intercept age (Figure 5.9a). Fraction #3 can be interpreted to

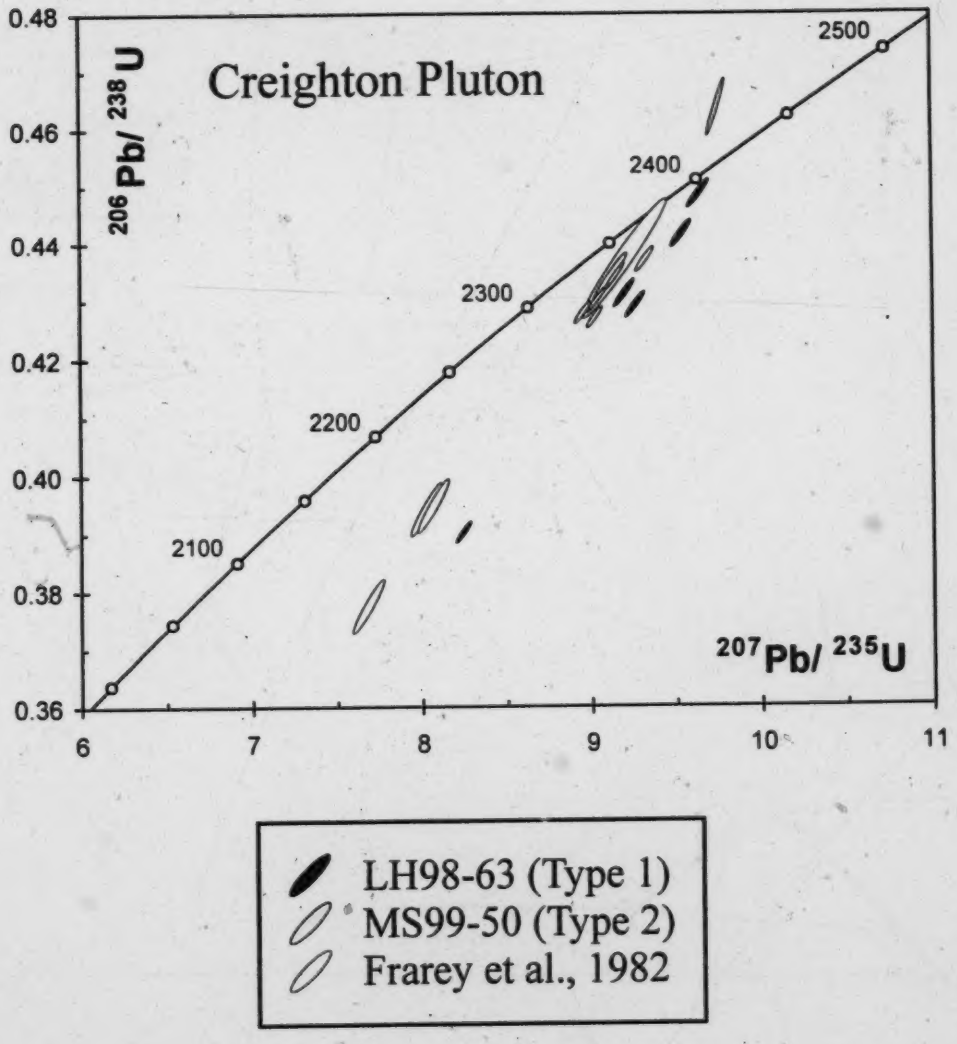

Figure 5.8: U-Pb concordia diagram showing results from all zircon analyses for the Creighton pluton. Numbers beside error ellipses refer to analysis number in Table 5.1. Error ellipses are shown at 1σ.

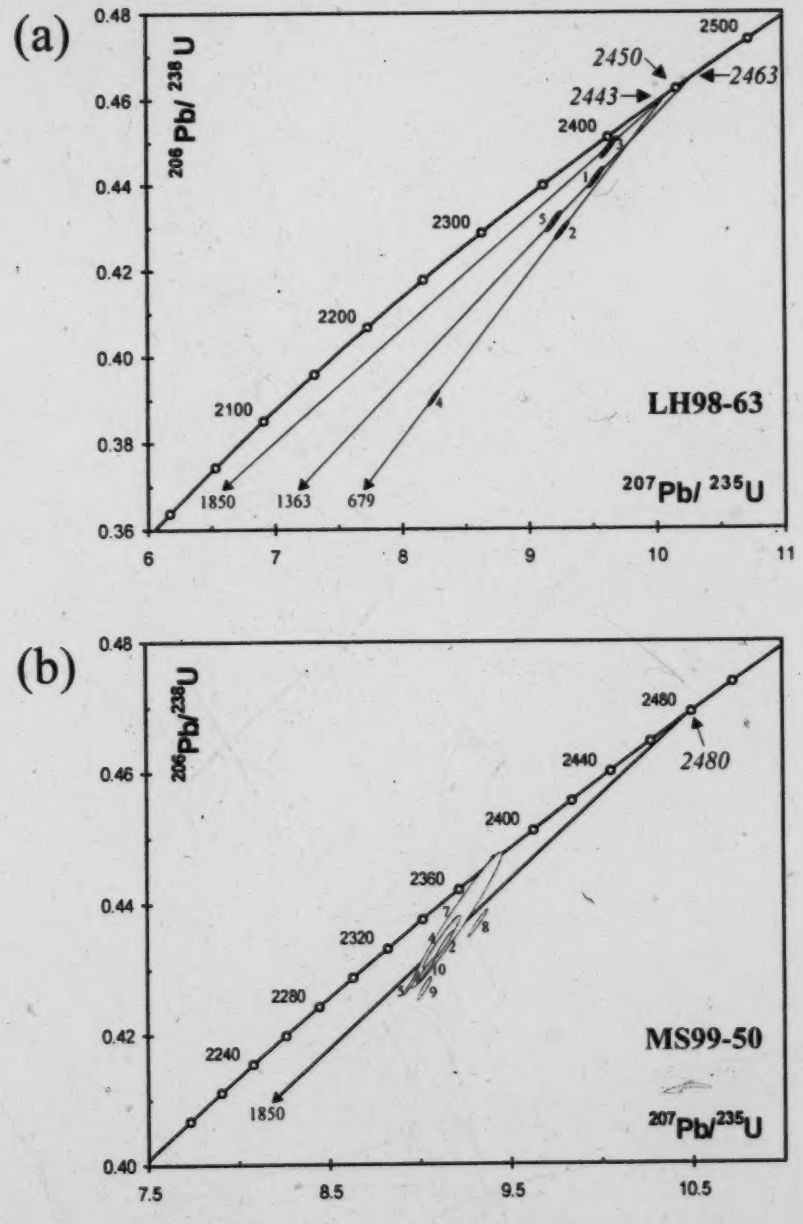

Figure 5.9: **(a)** U-Pb concordia diagram showing results from sample LH98-63. The three separate regression treatments are plotted with corresponding upper and lower intercepts. **(b)** U-Pb concordia diagram showing results from sample MS99-50. The reference line plots from 2480 Ma to 1850 Ma. Some of the analyses plot near this inferred Pb-loss line. Numbers beside error ellipses refer to analysis number in Table 5.1. Error ellipses are shown at 1σ.

lie along a discordia line between 1850 Ma to 2450 Ma. Fractions #2 and #4 yield an upper intercept of ca. 2440 Ma and fractions #1 and #5 yield an upper intercept of ca. 2460 Ma. Each grouping has a different lower intercept that may reflect a combination of separate Pb-loss events. Further examination of sample MS99-50 indicates three of the single zircon grain analyses lie along an 1850 Ma – ca. 2480 Ma discordia line with the fourth single grain and multi-grain analyses falling only slightly below this reference line (Figure 5.9b). Unfortunately, in both cases the data do not allow construction of a robust regression line making it difficult to identify any 1850 Ma Pb-loss event. The best age estimate for the Type 1 granitoids is 2415 Ma with an assigned error of ± 5 Ma to encompass the $^{207}Pb/^{206}Pb$ age of the least discordant analysis (#3) and for the Type 2 granitoid intrusion, 2376.3 ± 2.3 Ma. The Type 2 lower intercept age of ca. 0 Ma may simply reflect a recent Pb-loss event.

The interpreted ages of crystallization for the Type 1 and 2 granitoids are 2415 ± 5 Ma and 2376.3 ± 2.3 Ma, respectively. Different $^{207}Pb/^{206}Pb$ ages and Pb-loss patterns combined with the mineralogical and geochemical variances support the hypothesis that the two distinct geochemical zones of granitoid within the Creighton pluton represent temporally discrete pulses of felsic magmatism separated by ca. 40 Ma.

CHAPTER 6: TRACER ISOTOPES

Introduction

Tracer isotope Rb-Sr, Sm-Nd and common Pb-feldspar studies were conducted on seven representative samples from the Creighton pluton. The purpose of these isotopic studies is to complement the existing geochemical studies and provide more diagnostic information that may help to elucidate the origin of the felsic magmatism. Radiogenic isotopes are excellent geologic tools to gain information on the petrogenesis of granitic rocks because their ratios remain unchanged during subsequent fractionation events. This enables the identification of characteristic isotopic source reservoirs or the mixing between distinct sources. Common Pb-feldspar studies have been demonstrated to be a sensitive indicator for identifying ancient crustal signatures (e.g. Yamashita et al., 1999).

A typical suite from the Creighton pluton based on geography and geochemistry was selected for analysis of Rb-Sr, Sm-Nd and common Pb-feldspar. Four whole rock samples of Type 1 granitoid, one of Type 2 granitoid, one breccia and one enclave were chosen for Rb-Sr and Sm-Nd isotopes. Potassium feldspar mineral separates were selected from the same samples for Pb isotope analysis. The two samples used for U-Pb zircon radiometric dating (LH98-63, MS99-50) had duplicate analyses run on both residues and leachates. A complete summary of the tracer isotope data is presented in Tables 6.1, 6.2 and 6.3.

Table 6.1: Summary of Rb-Sr whole rock and apatite data from the Creighton pluton.

Sample	Rock Type[1]	Age (Ma)	Rb (ppm)	Sr (ppm)	Rb/Sr	$^{87}Rb/^{86}Sr$	$^{87}Sr/^{86}Sr \pm 2\sigma$ err (@ 0 Ma)	$^{87}Sr/^{86}Sr_i$ (@ T Ma)
LH98-63	CG1	2415	265.33	73.83	3.59	10.76	1.063224 ± 17	0.68779
MS99-31	CG1	2415	260.11	15.99	16.27	55.82	2.602493 ± 22	0.65521
MS99-38	CG1	2415	229.70	79.90	2.87	8.54	0.984908 ± 13	0.68681
MS99-46	CG1	2415	254.20	59.87	4.25	12.80	1.135969 ± 13	0.68937
MS99-50	CG2	2376	157.23	134.60	1.17	3.42	0.820966 ± 17	0.70368
MS98-2	Br	(2415)	268.22	109.58	2.45	7.23	0.925050 ± 13	0.67268
MS99-57	En	2415	258.38	86.79	2.98	8.84	0.980608 ± 14	0.67203
LH98-63	ap	2415	2.06	76.69	0.03	0.0785	0.833256 ± 54	0.83052
MS99-50	ap	2376	2.62	128.36	0.02	0.0592	0.750818 ± 21	0.74879

[1] Rock Type legend

CG1 = Type 1 granitoid
CG2 = Type 2 granitoid
Br = Breccia
En = Felsic microgranular enclave
ap = mineral apatite

^{87}Rb decay constant = 1.42×10^{-11} a^{-1}

Sample	Rock Type[1]	Age (Ma)	Sm (ppm)	Nd (ppm)	Sm/Nd	$^{147}Sm/^{144}Nd$	$^{143}Nd/^{144}Nd \pm 2s$ err (@ 0 Ma)	ε_{Nd} (@ 0 Ma)	ε_{Nd} (@ T Ma)	$f^{Sm/Nd}$	T_{DM}^2 (Ma)
LH98-63	CG1	2415	10.33	55.77	0.19	0.1120	0.511197 ± 19	-28.10	-1.83	-0.43	2790
MS99-31	CG1	2415	5.93	32.23	0.18	0.1112	0.511155 ± 9	-28.90	-2.40	-0.43	2828
MS99-38	CG1	2415	10.43	57.00	0.18	0.1106	0.511148 ± 7	-29.10	-2.34	-0.44	2822
MS99-46	CG1	2415	9.31	48.28	0.19	0.1166	0.511140 ± 8	-29.20	-4.38	-0.41	2999
MS99-50	CG2	2376	22.73	115.63	0.20	0.1189	0.511304 ± 8	-26.00	-2.26	-0.40	2820
MS98-2	Br	(2415)	9.47	50.65	0.19	0.1131	0.511214 ± 7	-27.80	-1.83	-0.42	2795
MS99-57	En	2415	13.72	66.99	0.20	0.1239	0.511333 ± 8	-25.40	-2.85	-0.37	2922

[1] Rock type legend
CG1 = Type 1 granitoid
CG2 = Type 2 granitoid
Br = Breccia
En = Felsic microgranular enclave

[2] T_{DM} calculated using the mantle evolution model of Goldstein et al., 1984
Present day CHUR parameters are $^{147}Sm/^{144}Nd = 0.1967$, $^{143}Nd/^{144}Nd = 0.512658$
Depleted Mantle parameters are $^{147}Sm/^{144}Nd = 0.2186$, $^{143}Nd/^{144}Nd = 0.51316$
^{147}Sm decay constant = 6.54×10^{-12} a^{-1}

Table 6.2: Summary of Sm-Nd whole rock data from the Creighton pluton.

Sample[1]	Rock Type[2]	Separate Type[3]	$^{208}Pb/^{204}Pb$	$^{207}Pb/^{204}Pb$	$^{206}Pb/^{204}Pb$
LH98-63	CG1	R	36.662	15.862	17.447
		L1	41.177	16.198	20.221
LH98-63D	CG1	R	36.606	15.845	17.438
		L4	38.015	15.938	18.877
		L1	44.410	16.337	21.538
MS99-31	CG1	R	37.901	15.929	17.588
MS99-38	CG1	R	36.676	15.809	17.126
MS99-46	CG1	R	36.290	15.759	16.900
MS99-50	CG2	R	36.226	15.390	15.658
		L4	36.779	15.379	16.381
		L1	39.005	15.525	16.740
MS99-50D	CG2	R	36.283	15.399	15.672
		L4	37.259	15.564	16.779
		L1	39.562	15.524	16.801

Pb isotopic ratios were corrected for mass discrimination based on values obtained for NBS-981 (n = 4) and normalized to the value reported by Todt et al., (1996).

[1] "D" denotes duplicate analysis

[2] Rock type legend

CG1 = Type 1 granitoid

CG2 = Type 2 granitoid

3) Potassium feldspar separate type legend

R = Residue

L1 = Leachate 1

L4 = Leachate 4

Table 6.3: Summary of common Pb-feldspar data from the Creighton pluton.

Mineral separation techniques and Rb-Sr and Sm-Nd isotope dilution techniques are outlined in Appendix D and are primarily based on procedures described by Creaser et al. (1997). Common Pb-feldspar leaching procedures and Pb purification by ion exchange chromatography follow Cumming and Krstic (1987), Housh and Bowring (1991) and Lugmair and Galer, (1992). Rb and Sm concentrations were determined by isotope dilution using a Micromass30 in single collector mode with Sr, Nd and Pb isotopic ratios and concentrations determined on a VG354 mass spectrometer. Pb isotopic ratios were corrected for mass discrimination based on values obtained for NBS-981 (n = 4; $^{208}Pb/^{204}Pb$ = 36.511; $^{207}Pb/^{204}Pb$ = 15.435; $^{206}Pb/^{204}Pb$ 16.881) and normalized to the values reported by Todt et al., (1996).

Rb-Sr

The suite of samples analyzed from the Creighton pluton produce a range of initial $^{87}Sr/^{86}Sr$ ratios of 0.65521 to 0.70368. Except for sample MS99-50, all initial ratios are lower than any reasonable terrestrial values. The lowest of the initial Sr values (t = 2415 Ma) is from the most felsic sample (MS99-31) with the remaining Type 1 samples having compositions consistently near 0.69. The breccia and microgranular felsic enclave have similar low initial Sr values of just above 0.67. The Type 2 granitoid sample yields the only realistic value with an initial $^{87}Sr/^{86}Sr$ ratio (t = 2376 Ma) of 0.70368. With the exception of the Type 2 sample all the reported data are implausibly low (e.g. below the most primitive ratios known in our solar system) and can have no petrogenetic significance. In an attempt to verify that the Rb-Sr whole rock system could be disturbed,

Sr isotope analyses on two apatite mineral separates (LH98-63 and MS99-50) were conducted. Apatite has been shown to record a minimum initial $^{87}Sr/^{86}Sr$ ratio where the whole rock values were too low (Creaser and Gray, 1992). However the initial $^{87}Sr/^{86}Sr$ values from the two-apatite analyses are very radiogenic (0.83052 and 0.74879) and likely reflect post-crystallization exchange with a radiogenic reservoir, similar to results obtained for granitic rocks of the World Beater Complex (Lanphere et al., 1964).

Sm-Nd

The analyzed samples from the Creighton pluton yield a narrow range of Sm/Nd ratios, ε_{Nd} values, and depleted mantle ages irrespective of rock type. The Sm/Nd ratios range from 0.18 to 0.20, $f^{Sm/Nd}$ from -0.37 to -0.44 and ε_{Nd} (t = 2376 and 2415 Ma) values from –1.8 to –2.4. Calculated depleted mantle model ages (Goldstein et al., 1984), representing the time the sample has been separated from the mantle, are Mesoarchean between 2790 – 2830 Ma. (Figure 6.1). The exceptions are sample MS99-46 and the enclave which possess slightly lower ε_{Nd} (t = 2415) values of –4.4 and –2.9 respectively, and an older T_{DM} of 2.9 - 3.0 Ga. Overall these data are consistent with the single Sm-Nd analysis (Sm/Nd = 0.18, ε_{Nd} (t = 2415) = -2.2, $f^{Sm/Nd}$ = -0.43) calculated from data reported in Dickin (1998).

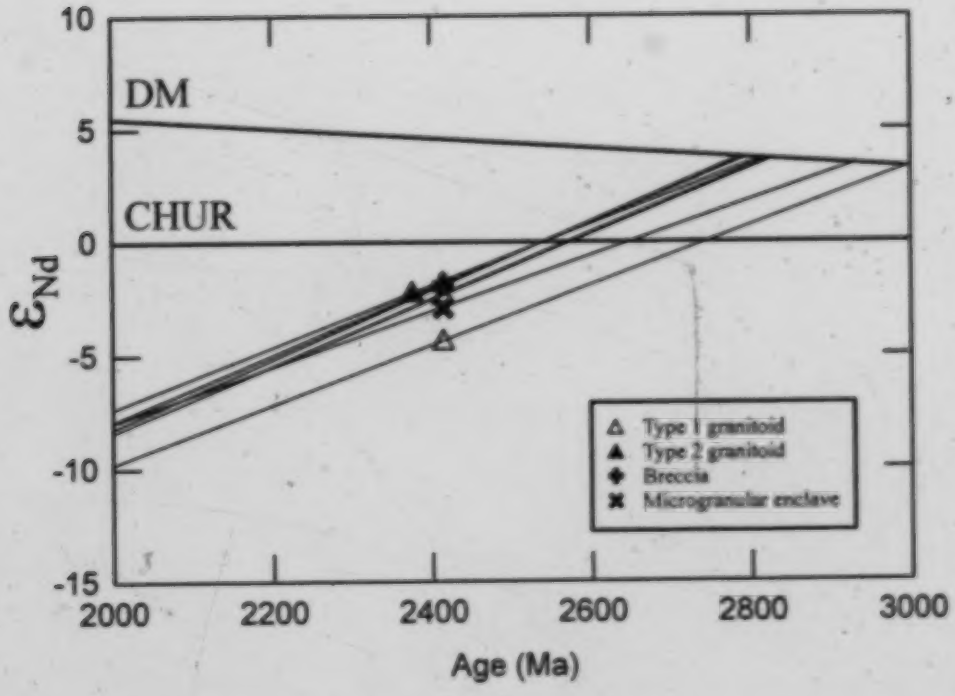

Figure 6.1: ε_{Nd} vs. time (Ma) diagram of Creighton pluton samples with respect to CHUR (CHondritic Uniform Reservoir) and Depleted Mantle (DM) after Goldstein et al., (1984).

Common Pb-feldspar

The Pb isotopic data obtained for potassic feldspar residues have a wide range of isotopic ratios. The Type 1 granitoid $^{208}Pb/^{204}Pb$ values range from 36.290 to 37.901, the $^{207}Pb/^{204}Pb$ from 15.759 to 15.929 and the $^{206}Pb/^{204}Pb$ from 16.900 to 17.588. The Type 2 granitoid possesses less radiogenic values of $^{208}Pb/^{204}Pb$ from 36.226 to 36.283, the $^{207}Pb/^{204}Pb$ from 15.390 to 15.399 and the $^{206}Pb/^{204}Pb$ from 15.658 to 15.672. Attempts to measure the Pb isotopic composition for the breccia and the enclave were unsuccessful due to a lack of measurable lead in the small feldspar separate. The granitoid residue compositions appear too radiogenic for Paleoproterozoic samples and may have had addition of Pb by a later geological event.

Discussion

The isotopic data from the Creighton pluton indicate a complex system that is partially disturbed by later geological events. There is no significant variation in the ε_{Nd} values or T_{DM} ages for the Creighton pluton, suggesting a similar isotopic source reservoir for all the samples. The values reflect neither a pure mantle nor pure crustal source but are likely the result of mixing of the two sources and will be used in conjunction with the geochemistry to identify possible source materials for the Creighton pluton.

The impossibly low initial Sr values for the Type 1 samples from the Creighton pluton imply that the data do not provide any direct petrogenetic constraints to the

Creighton pluton, but may help in assessing the effects of geological events in the region. A close correlation between the Rb/Sr ratio and the initial $^{87}Sr/^{86}Sr$ ratio shows that samples with a higher Rb/Sr ratio are more disturbed (Figure 6.2a). A whole rock isochron diagram of the four Type 1 samples yields an age of 2367 ± 37 Ma (MSWD = 8.2) with a lower intercept of 0.695 ± 0.010 (Figure 6.2b). This whole rock Rb-Sr isochron age is identical within error to the U-Pb zircon age of 2376 ± 2.3 Ma for the Type 2 granitoid. The significance of this isochron age is that it demonstrates that the Rb-Sr system in the Creighton pluton has not been reset by younger events such as the 1850 Ma Sudbury Event nor the 1.7 Ga K-metasomatism common to the Huronian sediments (Fairbairn et al., 1965; Roscoe et al., 1992; Schandl et al., 1994; Fedo et al., 1997). The most likely explanation is Rb addition ca. 40 Ma after emplacement of the Type 1 granitoid. The isochron age of the Type 1 samples seems to be recording the intrusion of the Type 2 granitoid body, with low initial Sr ratios as a result of Rb or Sr migration during its emplacement. The fact that the Rb-Sr system in the Type 1 samples shows little evidence of later geological disturbances suggests that similar circumstances have occurred in the Type 2 sample. This would imply that the initial $^{87}Sr/^{86}Sr$ value from the Type 2 sample might have some petrogenetic significance. The low initial Sr ratio of the Type 2 granitoid indicates that it is unlikely that mixing with a highly radiogenic (high $^{87}Sr/^{86}Sr$) Archean mid- to upper crustal component occurred during crystallisation. The initial $^{87}Sr/^{86}Sr$ value of 0.70368 for the Type 2 granitoid would suggest a depleted mantle source, if reliable.

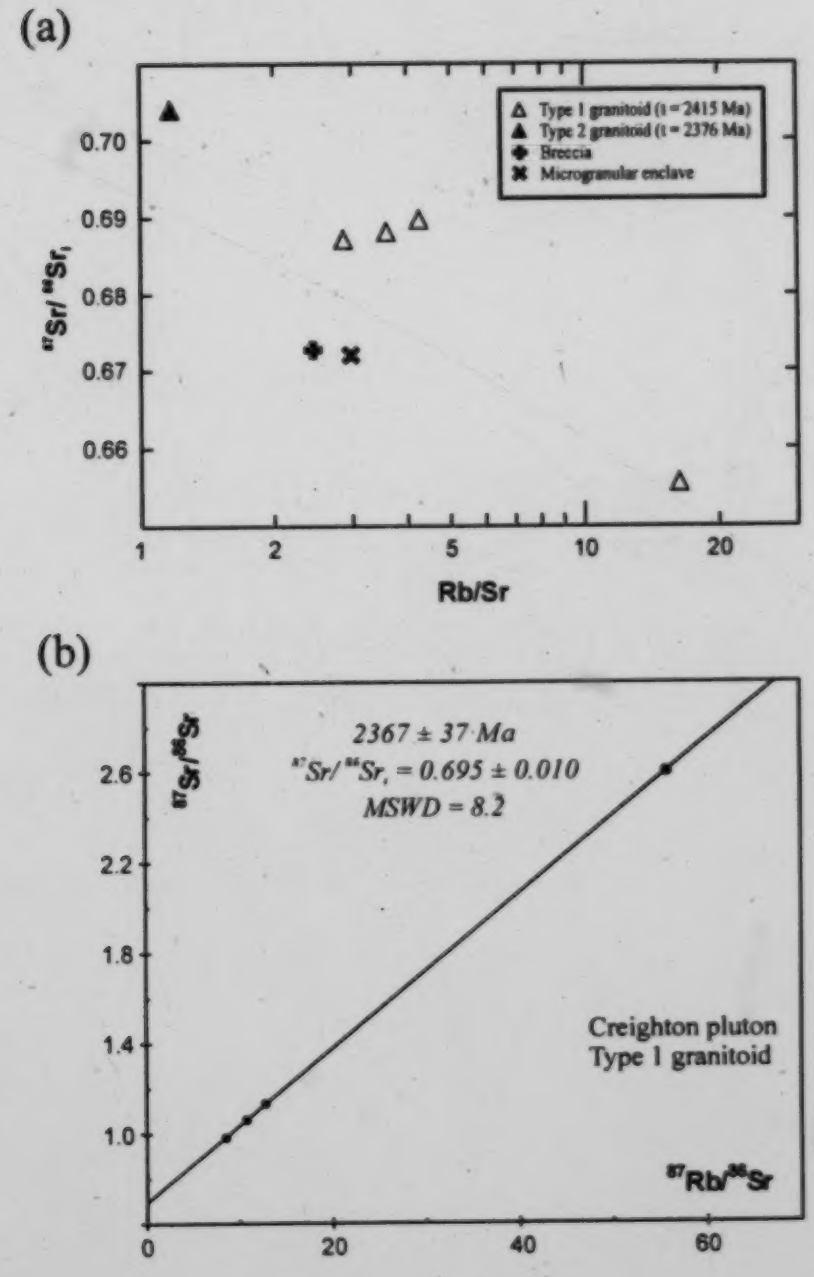

Figure 6.2: **(a)** Rb/Sr vs. initial $^{87}Sr/^{86}Sr$ ratio. **(b)** Rb-Sr isochron diagram of four Type 1 granitoid samples from the Creighton pluton.

The Pb isotopic signatures show evidence of an open system because the leachates and residues from the two samples do not plot parallel to a 2400 Ma reference isochron (Figure 6.3). The Pb leachate-residue isochrons from both granitoid types show similar regression slope results. The Type 1 samples yield an age of 1962 ± 360 Ma (MSWD = 19) (Figure 6.4a) and the Type 2 sample (MS99-50) an age of 1956 ± 140 Ma (MSWD = 1.3) (Figure 6.4b) with the two anomalous leachate points ignored. Although the two granitoids have different Pb isotopic compositions, it appears that the Pb systems were disturbed by the same Mesoproterozoic event. Both ages agree within the uncertainty to the 1850 Ma Sudbury Impact event responsible for Pb-loss in the nearby Murray pluton (Krogh et al., 1996). A plot of the residues compared to the Pb evolution model of Stacey and Kramers (1975) ($\mu = 9.74$) shows that all the samples do not plot at ca. 2.4 Ga on any evolution curve. They would require a long residence time in a high U/Pb reservoir to generate the required high radiogenic Pb isotope compositions (Figure 6.5). Unlike the Nd isotopes, the Pb isotopic compositions are different for each granitoid intrusion. This data supports the U-Pb zircon geochronology indicating that there are two temporally separate bodies and combined with the geochemical differences, this may imply a slightly different petrogenetic origin.

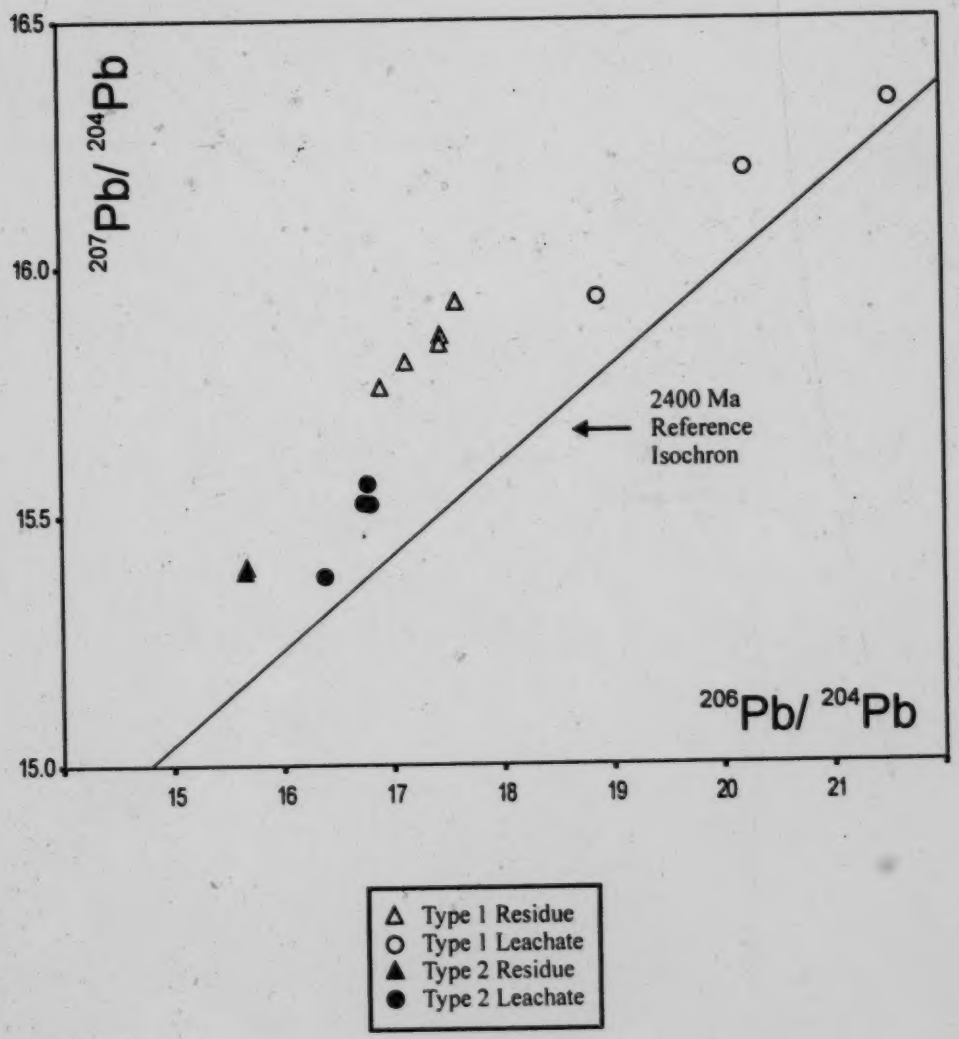

Figure 6.3: Pb isochrons for the two U-Pb ages of the Creighton pluton plotted with corresponding potassium feldspar residues and leachates.

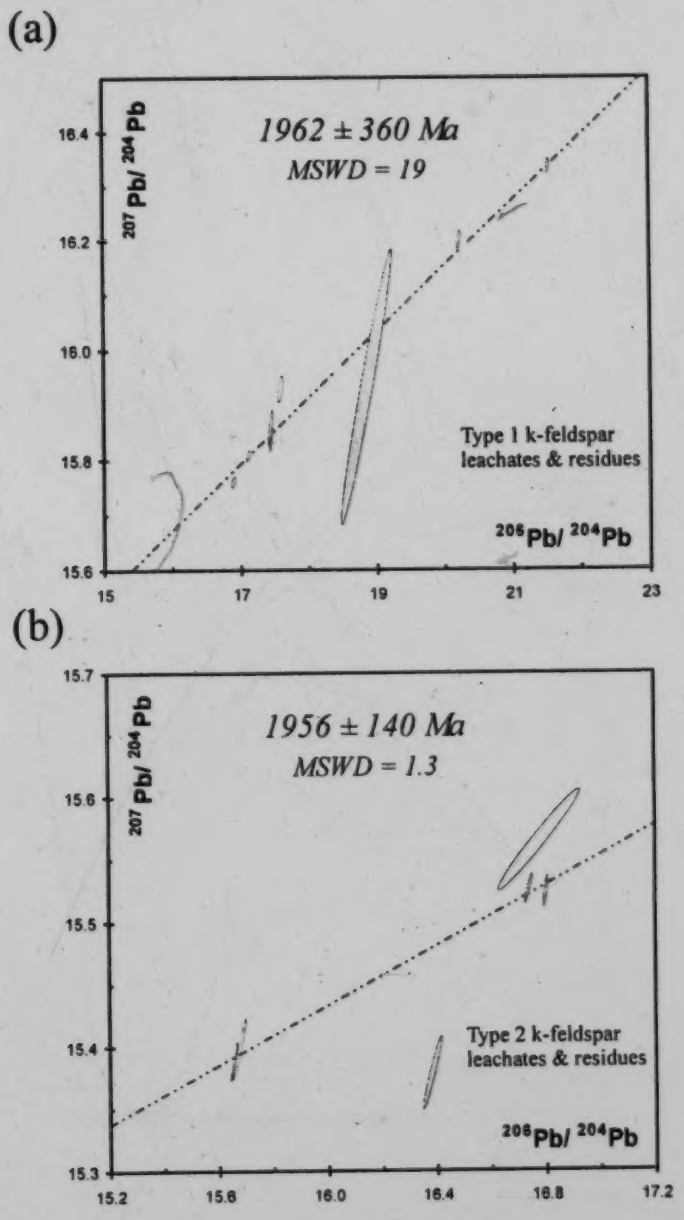

Figure 6.4: Pb isochron diagrams from the Creighton pluton. Shaded ellipses represent leachates and empty ellipses residues. Error ellipses are shown at 2σ. **(a)** Pb isochron from residues and leachates from Creighton Type 1 granitoid samples. **(b)** Pb isochron from residues and leachates from Creighton Type 2 granitoid sample MS99-50. The two L4 samples (large error ellipses) were not used in the regression treatment.

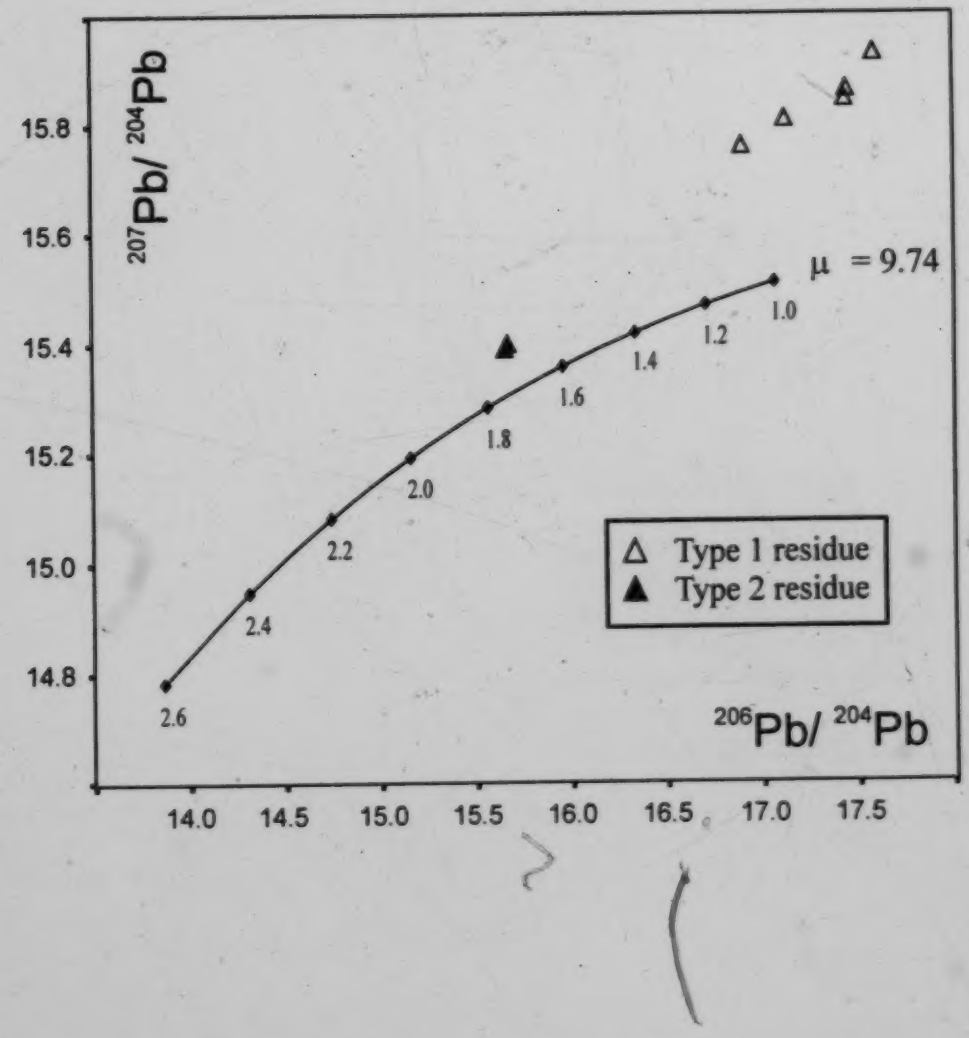

Figure 6.5: Pb evolution curve (μ = 9.74) from Stacey and Kramers (1975) plotted with k-feldspar residues from Creighton pluton.

CHAPTER 7: TECTONO-MAGMATIC SETTING

Introduction

Unlike their volcanic counterparts, identifying source components and the tectonic setting of granitic magmatism based solely on geochemistry commonly gives ambiguous results. The complexity of granites is due to a complicated petrogenetic history that is the product of a diversity of origins, sources and subsequent geological processes (i.e. crustal contamination) that can alter their chemistry. Numerous classification techniques designed using field relations, mineralogy/petrography or chemistry have been proposed to address the issue of determining the tectonic environment of granitic emplacement (e.g. Chappell and White, 1974; Pearce et al., 1984; Whalen et al., 1987; Maniar and Piccoli, 1989; Batchelor and Bowden, 1985). Unfortunately, many problems arise when attempting to use these classification schemes because of the complex nature of granites. Most systems are empirically based on Phanerozoic granites with the resulting well-defined boundaries and simple tectonic correlation not necessarily valid for granite magmatism throughout Earth's evolution.

In an attempt to decipher the complex features of the Creighton pluton, an integrated approach using field relationships, mineralogy/petrography, chemistry and isotopic characteristics will be employed in an attempt to constrain the source components and tectonic setting. This type of synthesis will incorporate many of the existing granite petrogenetic classifications. The advantages to this approach are that it

does not solely rely on one set of criteria or one type of methodology that may have been adversely affected by subsequent geological events. Exceptional mineral occurrences and anomalous geochemical values can be correctly identified, allowing the evaluation of their importance, thus minimizing the chance of any potential misinterpretations.

Field relations

Prior to any attempts to classify granitic magmatism mineralogically or chemically, the field relationships must be considered first. Petrographically, the Creighton pluton consists of granites to monzogranites and is associated with mafic dike swarms, extensive basaltic to rhyolitic volcanism and a number of gabbro-anorthosite intrusions (Krogh et al., 1984; Ashwal and Wooden, 1989; Prevec, 1993; Heaman, 1997; Corfu and Easton, 2001). Felsic microgranular enclaves are present along with two large mafic enclaves of the surrounding volcanic formations. These characteristics are common to granitoids located in a wide range of geological settings such as rifts, volcanic arcs or post-orogenic zones.

Mineralogy

The Creighton pluton is a typical two feldspar-quartz granite containing minor amounts of biotite + epidote ± amphibole. Accessory minerals of apatite + zircon + ilmenite ± allanite ± titanite are common as well. Type 2 granitoids contain calcic amphibole and a higher modal abundance of the accessory minerals. Pyroxene is absent

and muscovite was identified in only one highly silicic sample (MS99-31). Epidote and titanite are likely to be secondary in origin having crystallized as a result of later hydrothermal alteration or metamorphism.

Chappell and White (1974, 1992) proposed and modified a classification scheme to distinguish between I-type (intracrustal/igneous) and S-type (supracrustal/sedimentary) using both mineralogy/petrography and geochemistry based on extensive work on the Australian Lachan Fold Belt granites. The S-type intrusions have a peraluminous nature and contain specific minerals (e.g. cordierite, Al-polymorphs, garnet, muscovite) not found in a mixed or mantle generated granite. The Creighton pluton is metaluminous to weakly peraluminous and lacks these common Al-rich minerals associated with crustal anatexis. The simple mineralogy of the intrusion with biotite as the dominant mafic mineral is consistent with I-type granites.

Geochemistry

Major-element chemistry has been applied to provide a descriptive nature for granitoids and identify the tectonic setting. Maniar and Piccoli (1989) utilise the major elements in a series of discrimination diagrams to distinguish granites into appropriate tectonic environments. Most of the Creighton pluton samples plot in the POG (post-orogenic granite) field of the SiO_2 vs. FeO*/FeO*+MgO diagram with a number of the Type 2 granitoids located in the RRG (rift-related granite) field (Figure 7.1a). The multi-cationic system of Batchelor and Bowden (1985) that was designed based on the R1-R2 diagram of de la Roche et al., (1980) shows the Creighton pluton samples plot mainly in

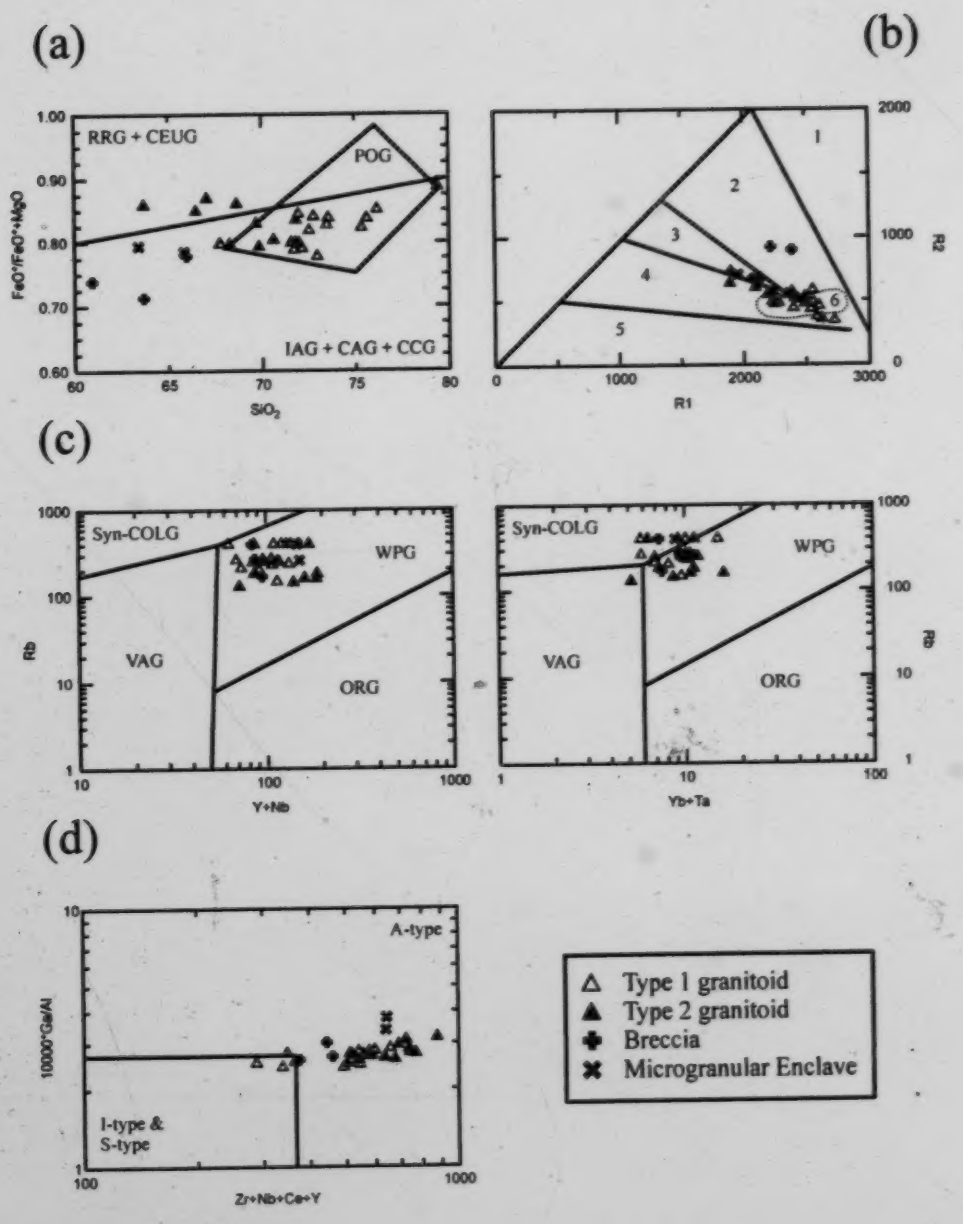
(a)
(b)
RRG + CEUG
POG
IAG + CAG + CCG
FeO*/FeO*+MgO
SiO2
1
2
3
4
5
6
R1
R2
(c)
Syn-COLG
WPG
VAG
ORG
Rb
Y+Nb
Yb+Ta
(d)
A-type
I-type &
S-type
10000*Ga/Al
Zr+Nb+Ce+Y
Type 1 granitoid
Type 2 granitoid
Breccia
Microgranular Enclave

Figure 7.1: Granitoid tectonic discrimination diagrams. **(a)** SiO_2 vs. FeO*/(FeO*+MgO) diagram of Maniar and Piccoli (1989). IAG = island arc granitoids; CAG = continental arc granitoids; CCG = continental collision granitoids; POG = post orogenic granitoids; RRG = rift-related granitoids; CEUG = continental epeirogenic uplift granitoids. **(b)** R1 vs. R2 diagram of Batchelor and Bowden (1985). Group 1 = mantle fractionates; group 2 = pre-plate collision granitoids; group 3 = post-collision uplift granitoids; group 4 = late-orogenic granitoids; group 5 = anorogenic granitoids; group 6 = syn-collision granitoids. R1 = 4Si – 11(Na+K) – 2(Fe+Ti); R2 = 6Ca + 2Mg + Al. **(c)** Rb vs. Y + Nb and Rb vs. Yb + Ta diagrams of Pearce et al., (1984). WPG = within-plate granite; VAG = volcanic arc granite; ORG = ocean ridge granite; syn-COLG = syn-collisional granite. **(d)** A-type granite discrimination diagram of Whalen et al., (1987). A-type = anorogenic granite; I-type = intracrustal/igneous derived granite; S-type = supracrustal/sedimentary derived granite.

the syn-collisional field, but there is considerable data scatter (Figure 7.1b). Unfortunately, the use of major elements such as Na, K and Ca is suspect because they are considered highly mobile under metamorphic or hydrothermal conditions and may have been modified by the 1.85 Ga Penokean Orogeny or 1.7 Ga metasomatism.

Pearce et al. (1984) also used trace-element chemistry to define tectonic boundaries in Rb-Y-Nb and Rb-Yb-Ta space modelled on the basis of the petrogenetic histories of different granites. All samples from the Creighton pluton are well constrained to the WPG (within-plate granite) field on the Rb vs. Y+Nb diagram with a few samples straying into the syn-COLG (syn-collisional granite) field on the Rb vs. Yb+Ta diagram (Figure 7.1c). This may be the result of post-emplacement Rb addition that was also observed in the Rb-Sr isotope data. The pluton shows many characteristics of the subset category 'b' of the within-plate granites (metaluminous, calcic amphiboles) that are associated with dike swarms (Pearce et al. 1984). On an ORG-normalised plot the granitoids exhibit relative Rb and Th enrichments, slight Ce and Sm enrichments, a negative Ba anomaly and a flat Hf-Zr-Y-Yb pattern that are common for a crustal dominated pattern. The disadvantage to these diagrams is that they do not readily identify post-orogenic characteristics.

Although mineralogically consistent with I-type granites of Chappell and White (1974), geochemically the Creighton pluton has high values of Na_2O+K_2O, Zr, Nb, Ga, Y and REE with low Sr that are signatures of A-type (anorogenic) granitoids. Whalen et al. (1987) designed a number of graphical plots to distinguish A-type granites primarily using the major elements, the immobile high-field strength elements and the Ga/Al ratio. On these diagrams the Creighton pluton plots in the A-type field with a number of the

Type 1 samples lying along the border with fractionated I-type granites (Figure 7.1d, Figure 7.2). Despite the good correspondence, the Creighton pluton shows several deviations from the expected A-type magma chemistry having unusually high contents of CaO, Ba and Th with lower SiO_2 and Fe/Mg.

Studies by Kilpatrick and Ellis (1992) have identified C-type (charnockite) magmatism that can be distinguished from I-type and A-type granites by distinct geochemical signatures. This magmatic type is generally expressed by the presence of charnockites (orthopyroxene-bearing granites), but can have granites and felsic volcanics that exhibit the same chemical features inherited from their parental magma. Although similar in many features to A-type granitoids, the C-type magmatism is characterized by a lower (and wider range) SiO_2 values, higher TiO_2, P_2O_5 and K_2O at a given SiO_2 level and a lower ratio of Mg#. Multi-element diagrams normalized to average I-type (n = 991) and A-type granites (n = 148) (Whalen et al., 1987) (Figure 7.3) provide an effective tool to compare C-type magmatism (SiO_2 = 66.37% and 70.75%) (Kilpatrick and Ellis, 1992) and the Creighton pluton. In both diagrams the Creighton pluton and Ardery Charnockites possess comparable patterns of relative elemental enrichments and depletions. The similarity is more striking on the plot normalized to average A-type granite with lower Zr and higher Ca, Ba, P and Mg#. One key chemical feature of C-type magmatism that distinguishes it from either A-type or I-type granites is the Fe/Mg ratio (Kilpatrick and Ellis, 1992). C-type magmas generally possess a wide range of Mg# values from 25-40, whereas A-type granites are commonly <10 and I-type granites around 45. The average Mg# for the Creighton pluton Type 1 and Type 2 granitoids are 29 and 26 respectively, plotting in the C-type range.

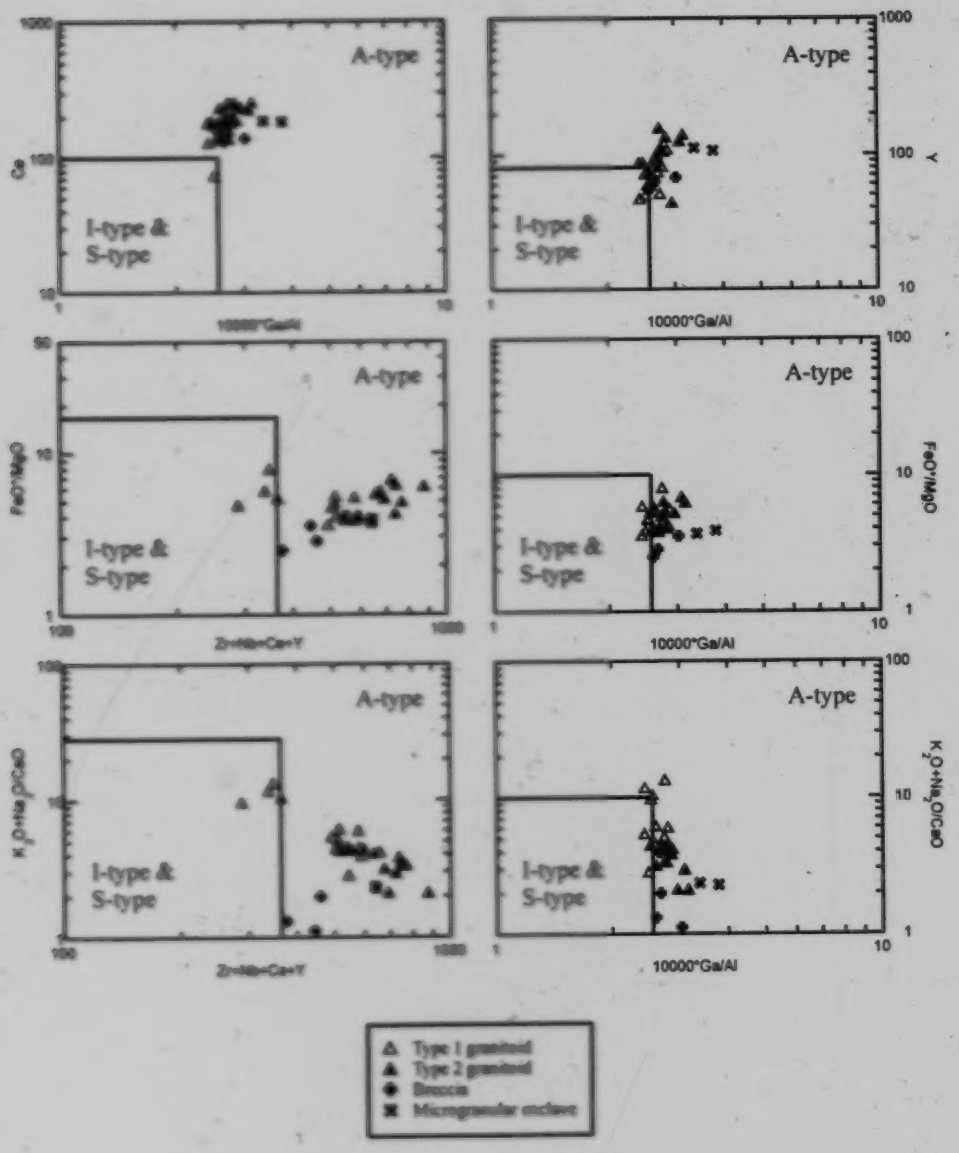

Figure 7.2: Various A-type granite tectonic discrimination diagrams (Whalen et al., 1987). A-type = anorogenic granite; I-type = intracrustal/igneous derived granite; S-type = supracrustal/sedimentary derived granite.

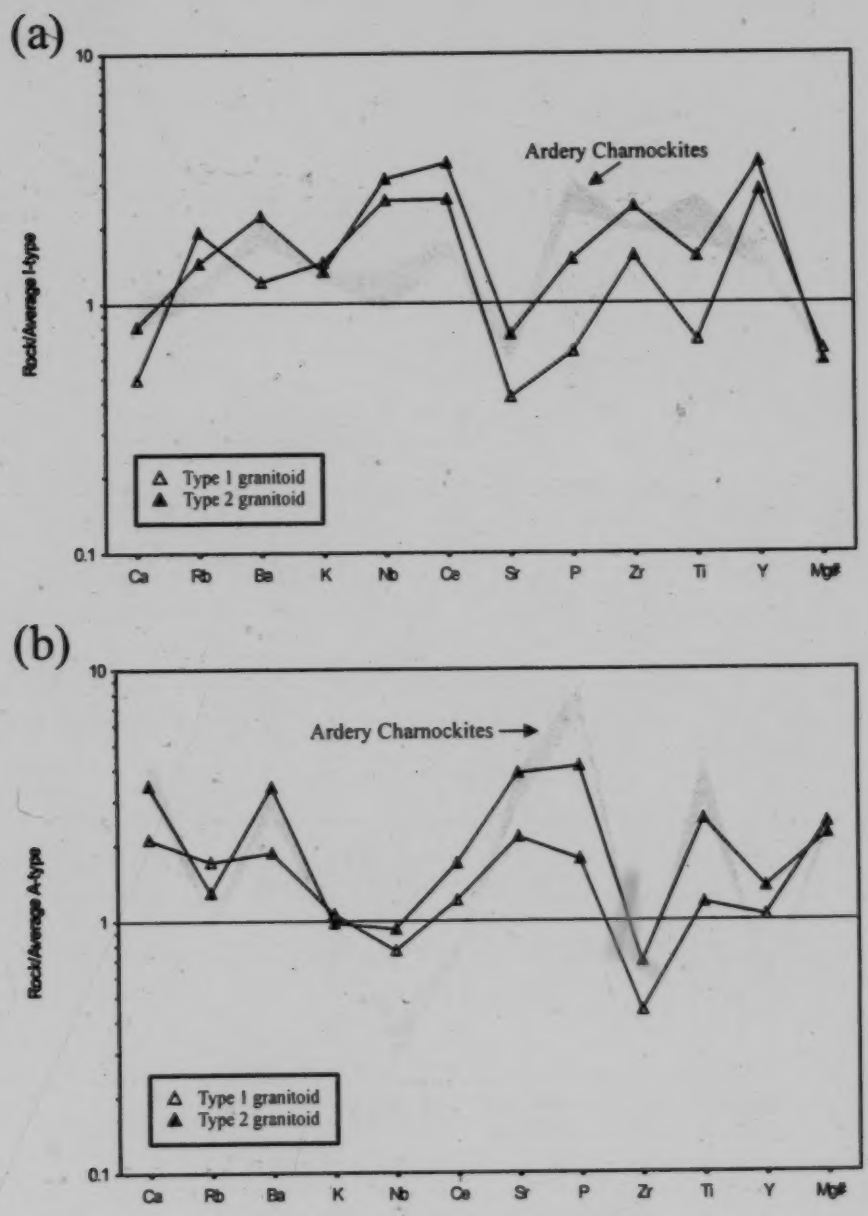

Figure 7.3: Multi-element profile diagrams comparing the Creighton pluton granitoids and the C-type Ardery Charnockites (Kilpatrick and Ellis, 1992). **(a)** Normalization to average I-type granite (Whalen et al., 1987). **(b)** Normalization to average A-type granite (Whalen, et al., 1987).

Isotopes

Although tracer isotopes are not generally used to specify the tectonic setting of granites, they are extremely useful for identifying source reservoirs of the parental magma. Unfortunately, the Creighton pluton possesses a complex isotopic history having been affected by many post-emplacement geological events. This makes it difficult to provide unequivocal evidence of the source components.

Both the Rb-Sr and common Pb-feldspar analyses show evidence of an open system but still can be used in conjunction with other data to eliminate certain possibilities. The low initial $^{87}Sr/^{86}Sr$ values from the Type 2 Creighton pluton sample show that the intrusion was not derived solely from an evolved Archean crustal source such as the Cartier Batholith or Levack Gneiss. Common Pb-feldspar data from the Creighton pluton is generally consistent with the rest of the ca. 2.45 Ga Huronian felsic and mafic magmatism with the Type 1 residues lying slightly above the reference field (Figure 7.4). None of the Pb isotope compositions from ca. 2.45 Ga magmatism overlap the field of Archean compositions that represent the depleted mantle at approximately 2.7 Ga. Similar to the findings for the River Valley anorthosite by Ashwal and Wooden (1989), the source reservoir for the Creighton pluton is not likely to be late Archean crustal rocks nor the typical depleted mantle from which they were derived. In order to evolve to the Pb isotopic values of the Creighton pluton from the Archean field, the magma would require a very high U/Pb (μ = 13 - 15) ratio. Although not providing any

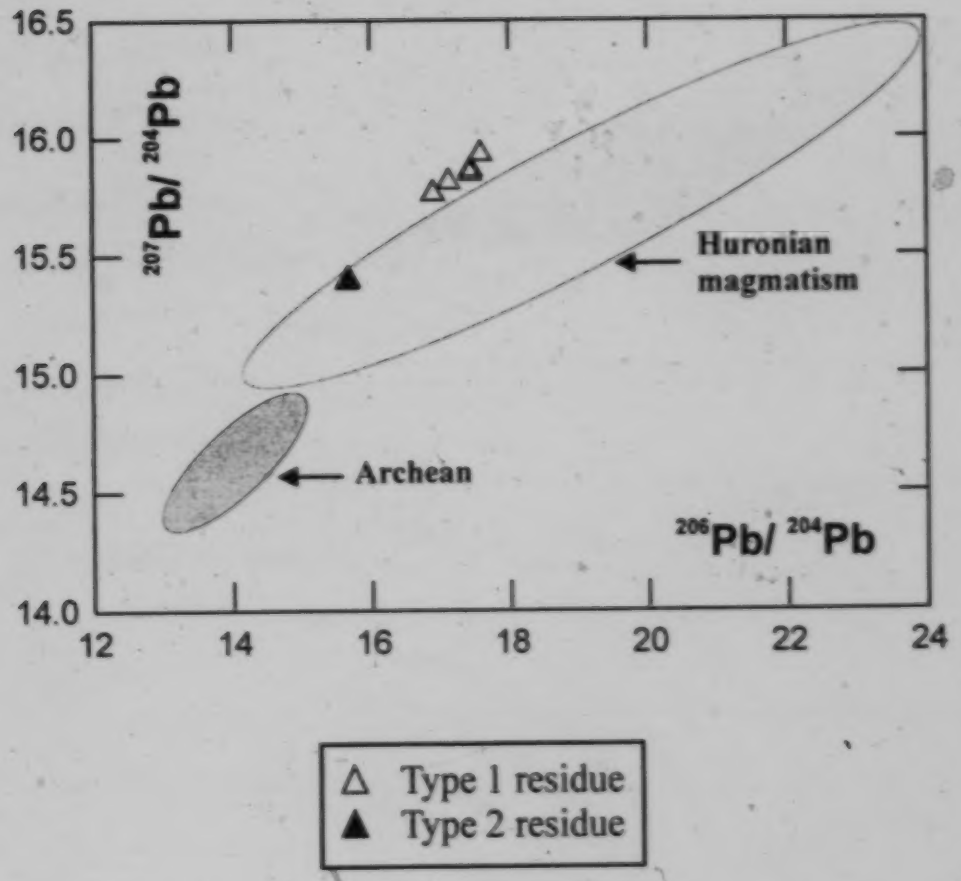

Figure 7.4: $^{207}Pb/^{204}Pb$ vs. $^{206}Pb/^{204}Pb$ diagram of the Creighton pluton k-feldspar residues and potential source materials. Archean field includes komatiite minerals (Tilton, 1983), granitoid k-feldspar residues (Gariepy and Allegre 1985; Stevenson et al., 1999) and Levack gneiss (Prevec, 1993; Dickin, 1998). Huronian Magmatism field includes River Valley Anorthosite (Ashwal and Wooden, 1989), Hearst dikes (Smith et al., 1992), gabbro-anorthosite intrusions (Prevec, 1993) and Murray pluton (this study).

direct evidence for the source components of the Creighton pluton, the Rb-Sr and common Pb-feldspar systems seem to rule out late Archean materials as the primary source reservoirs.

The Sm-Nd system appears to be the only isotopic system that is robust enough in the Creighton pluton to make petrogenetic interpretations. Overall, the ε_{Nd} and $f^{Sm/Nd}$ values reported from the Creighton pluton are consistent with the field for the Huronian magmatism with a small overlap with late Archean granitoid rocks (Figure 7.5a). The slightly negative ε_{Nd} values make it unlikely that it is a melt from a pure mantle or pure crustal source with the negative $f^{Sm/Nd}$ showing its LREE enriched nature. A simple interpretation would be that the values are the result of LREE enriched mantle magma with variable amounts of crustal contamination. The difficulty lies in correctly identifying the isotopic nature of the "Huronian" mantle at ca. 2.45 Ga and the crustal contaminant. Prevec et al. (1995) and Tomlinson (1996) have indicated that the mantle beneath the Southern Superior Province at this time is likely very chondritic in nature, or relatively uniformly enriched. This seems plausible in that the Hearst-Matachewan dikes have near chondritic values (average $\varepsilon_{Nd} = 0.9$, n = 7) (Boily and Ludden, 1991) and may represent the most primitive source magma of the ca. 2.45 Ga MIE. A multi-element spidergram comparing average Creighton pluton to average Hearst-Matachewan dike shows a very similar pattern, with the granites being more enriched in many of the elements (Figure 7.6a/7.6b). A suitable contaminant that is exposed in the region with Nd isotopic data is the Levack Gneiss. Attempts at AFC (assimilation-fractional crystallization) calculations (DePaolo, 1981) involving the Hearst-Matachewan dikes (Nd = 10 ppm, $\varepsilon_{Nd} = 1.3$ at t = 2400 Ma) and Levack Gneiss (Nd = 40 ppm, $\varepsilon_{Nd} = -2.3$ at t =

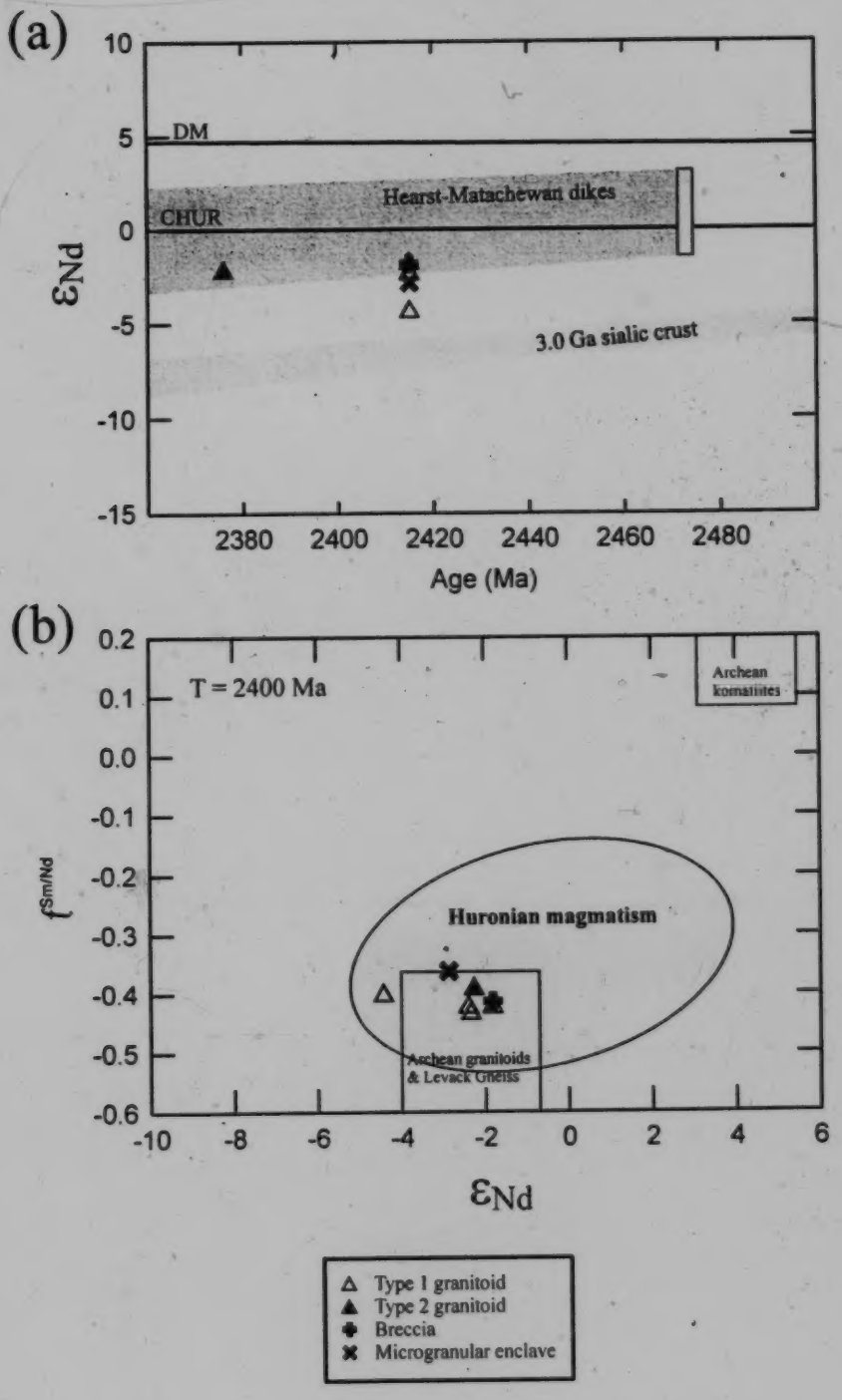
(a)
10
5
0
-5
-10
-15
εNd
DM
CHUR
Hearst-Matachewan dikes
3.0 Ga sialic crust
2380
2400
2420
2440
2460
2480
Age (Ma)
(b)
0.2
0.1
0.0
-0.1
-0.2
-0.3
-0.4
-0.5
-0.6
fSm/Nd
T = 2400 Ma
Archean komatiites
Huronian magmatism
Archean granitoids & Levack Gneiss
-10
-8
-6
-4
-2
0
2
4
6
εNd
Type 1 granitoid
Type 2 granitoid
Breccia
Microgranular enclave

Figure 7.5: **(a)** ε_{Nd} vs. time (Ma) diagram of Creighton pluton samples and potential source material with respect to CHUR (CHondritic Uniform Reservoir) and Depleted Mantle after Goldstein et al., (1984). Hearst-Matachewan dikes values from Boily and Ludden (1991) and 3.0 sialic crust from Stern et al. (1994). **(b)** ε_{Nd} vs. $f^{Sm/Nd}$ diagram of the Creighton pluton samples and potential source materials. Archean komatiite field from Dupre et al. (1984), Archean granitoids from Shirey and Hanson (1986) and Stevenson et al. (1999) and Levack Gneiss from Prevec (1993) and Dickin (1998). Huronian magmatism field includes the Hearst-Matachwean dikes (Boily and Ludden, 1991), Thessalon volcanics (Jolly et al., 1992), gabbro-anorthosite intrusions (Prevec, 1993) and Murray pluton (this study).

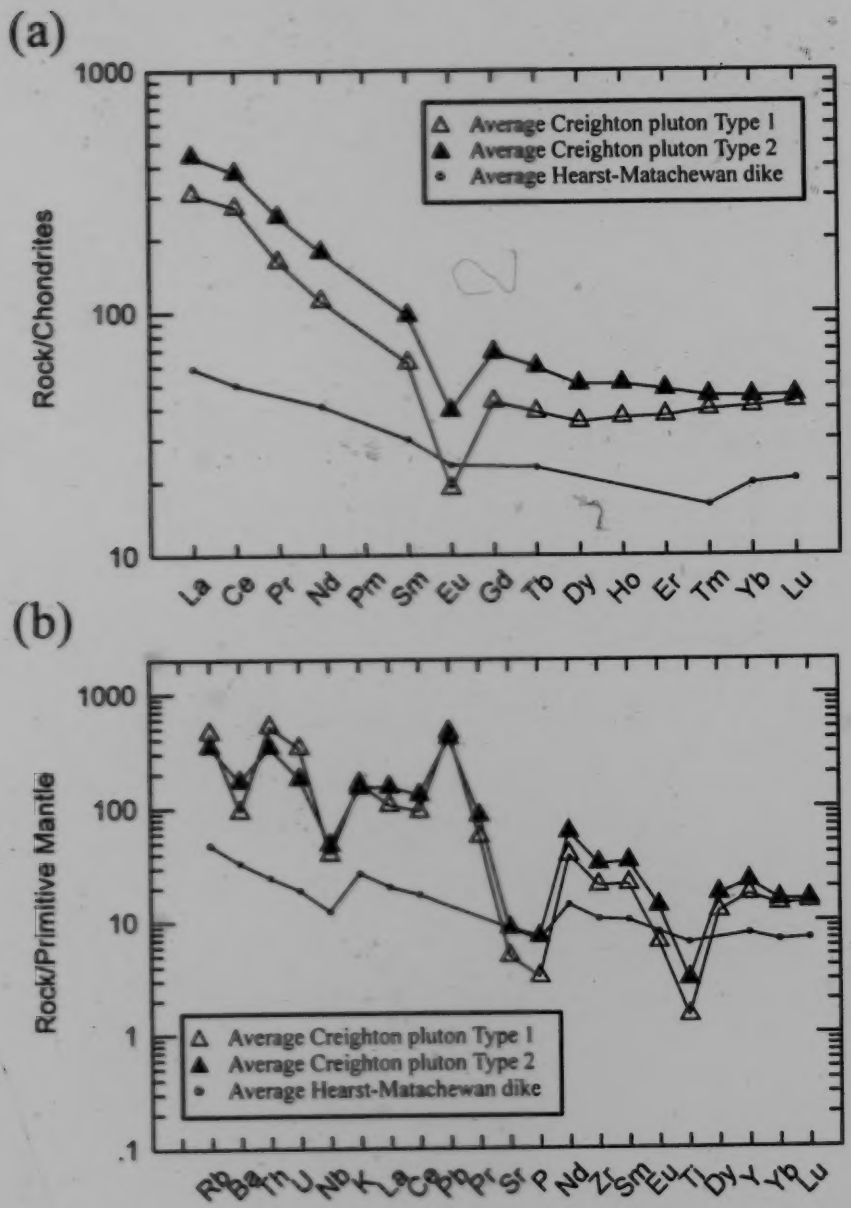

Figure 7.6: Multi-element spidergrams comparing average Creighton pluton Type 1 (n=18) and Type 2 (n=8) granitoids to average Hearst-Matachewan dike (n=33) (Condie et al., 1987; Nelson et al., 1990; Boily and Ludden, 1991). Normalization values from Sun and McDonough (1989). **(a)** Chondrite normalized rare-earth element diagram. **(b)** Primitive mantle normalized diagram.

2400 Ma) show that an unrealistic bulk distribution coefficient for the basaltic magma (0.75) is required to generate the Nd concentration and ε_{Nd} values of the Creighton pluton. However, if 3.0 Ga average Superior sialic crust (Nd = 25 ppm, ε_{Nd} = -7.0 at t = 2400 Ma) (Stern et al., 1994) is substituted as the contaminant it is possible to generate the values of the Creighton pluton with 30% of the original mafic magma remaining. For the model, a distribution coefficient of 0.2 for the basaltic magma and an *r*-value of 0.33 corresponding to the assimilation of cool crust, was used. This is not to say with certainty that 3.0 Ga sialic crust is the contaminant, only that if the Creighton pluton formed under AFC conditions then an older, more enriched contaminant than is exposed at surface is required. Other authors that have conducted isotopic studies of the MIE magmatism have also made note that older crust is necessary to explain AFC processes (Ashwal and Wooden, 1989; Boily and Ludden, 1991). This type of meso-Archean source component may be found at depth underlying the Southern Superior Province with the T_{DM}s of 2.79 – 2.83 Ga, supporting involvement with a major melting event at this time.

Discussion

The Creighton pluton is a small granitic intrusive body that has surprisingly complicated geochemical and isotopic characteristics. The difficulty lies in providing the most plausible explanation for the source components and tectonic setting of the Creighton pluton based on the existing evidence. In constructing a viable tectonic model, only elements and isotopic systems that seem unaffected will be used.

The first conclusion is that the Creighton pluton does not appear to be the product of a pure crustal nor pure mantle source. It does not contain the correct mineralogy nor does it have the necessary chemical or isotopic signatures to be the result of melting of exposed late Archean crust. The pluton also does not possess the mineralogy, geochemistry nor isotopic characteristics of a granitoid that derived solely from a mantle reservoir. It is also unlikely to be a local magmatic episode of the proposed 2.4 – 2.2 Ga Blezardian Orogeny (Riller et al., 1999) because it shows none of the characteristics of a syn-orogenic granite. The Creighton pluton appears to have occurred in a geodynamic environment that could facilitate the mixing of mantle and crustal source components.

The favored explanation is that the Creighton pluton is similar to the C-type magmatism as described by Kilpatrick and Ellis (1992). The lack of charnockites in the Southern Superior Province appears to be a problem, but this style of magmatism can be expressed solely by extrusive or granitoid equivalents (Kilpatrick and Ellis, 1992) and the charnockites could be found at depth. C-type magmatism can occur due to the input of large volumes of basalt into stabilized fertile lower crustal granulites with subsequent dry partial melting (Kilpatrick and Ellis, 1992). Although there is no surficial expression of any Paleoproterozoic granulites in the southern Superior Province, there is evidence of a significant granulite grade metamorphic event between 2.50 and 2.40 Ga from kimberlite-borne mafic granulite xenoliths, near Kirkland Lake under the Abitibi Province (Moser and Heaman, 1997). This metamorphic event is interpreted to have occurred under anhydrous conditions and is the result of heat supplied by the underplating Huronian-aged magmas in a rift setting (Moser and Heaman, 1997). It is possible that similar Paleoproterozoic-aged granulite-grade metamorphic rocks underlie the southern Superior

Province. The extended period of granulite metamorphism (2.50 – 2.40 Ga) and mafic magmatism (2.48 – 2.44 Ga) would imply the existence of granulitic crust prior to emplacement of the Creighton pluton. The 2416 ± 30 Ma metamorphic age (Moser and Heaman, 1997) suggests a period of heating and melting that might be coeval with the crystallization of the Creighton pluton. The granitoid intrusive would be the result of the melting of the enriched granulite-grade intermediate to mafic material (Hearst-Matachewan dikes or Elliot Lake volcanics equivalent) with the incorporation of some of the pre-existing (granulitic?) lower crust. If AFC (assimilation-fractional crystallization) processes and crustal contamination are involved, then this crustal material may have Nd isotopic signatures similar to 3.0 Ga sialic crust that is only exposed at depth.

This tectonic model involving the partial melting of two different types of components explains the discrete differences between the two types of granitoids in the Creighton pluton. The bodies are temporally separate and based on a number of lines of evidence (mineralogy, geochemistry, geophysics, structure, tracer isotopes), resulted from two distinct pulses of magma. These pulses must have come from a similar parental source because of similar Nd isotope signatures and rare-earth-element patterns. The differences in geochemistry and common Pb-feldspar isotopes may reflect the variability in the amount and nature of the lower crustal material being incorporated, or open system processes. The felsic microgranular enclaves are interpreted to represent a more primitive stage of crystallization of the granitic magma based on their similar geochemical patterns and isotopic characteristics.

CHAPTER 8: MATACHEWAN IGNEOUS EVENTS

Introduction

The Creighton pluton possesses unusual chemical and isotopic characteristics making it important to compare to the other nearby felsic granitoid bodies to determine if these signatures are consistent in all the plutonic magmatism. These include the proximal Murray pluton and recently identified Street Township granites in the Grenville Province (Corfu and Easton, 2001). A comparison will help evaluate the genetic relationship between the granitic plutonism and its relationship with the ca. 2.45 Ga mafic MIE.

Granitoid Comparison

The three intrusions primarily classify as granite to monzogranite with the only textural difference being that the Creighton pluton has porphyritic phases. Despite the proximity of the intrusions, high-precision U-Pb geochronology has shown that the Creighton pluton may be approximately 50 m.y. younger than the Murray pluton and Street Township granites (Krogh et al., 1996; Corfu and Easton, 2001; this study). This relatively short temporal gap may explain both similarities and differences in characteristics of the granitoids.

All the plutonic intrusions have roughly the same geochemical features (Table 8.1). Trends on Harker diagrams are roughly the same and the rare-earth element patterns

	Creighton pluton		Murray pluton	Street Township
	Type 1	Type 2		
SiO_2	72.59	68.47	73.81	69.16
Al_2O_3	13.12	13.99	12.43	12.27
MnO	0.04	0.07	0.04	0.10
MgO	0.58	0.93	0.24	0.50
FeO*	2.52	4.91	2.26	5.57
TiO_2	0.31	0.66	0.29	0.54
CaO	1.58	2.59	0.83	2.18
Na_2O	3.05	3.06	3.23	3.68
K_2O	4.94	4.55	5.31	4.09
P_2O_5	0.07	0.16	0.03	0.08
MgO#	28.5	25.7	16.6	13.6
Ba	654	1197	1396	1251
Nb	28.1	34.3	36.7	27.8
Rb	289.7	218.7	198.6	121.1
Sr	103.0	184.8	65.6	146.3
Th	44.1	29.1	28.3	18.6
Y	78.3	101.8	103.6	78.6
Zr	231.8	363.1	469.5	522.9
La	72.87	105.02	95.98	72.4
Ce	165.16	231.03	215.36	216.0
Eu	1.09	2.28	2.17	2.69
Gd	8.80	14.03	14.95	14.01
Yb	6.91	7.61	9.80	8.39
$(La/Yb)_n$	7.69	10.08	6.88	6.51
$(Gd/Yb)_n$	1.06	1.36	1.22	1.43

Table 8.1: Comparison of average geochemistry from Creighton pluton Type 1 (n=18) and Type 2 (n=8), Murray pluton (n=6) (Chai and Eckstrand, 1994; this study) and Street Township granites (n=8) (Easton, 1998).

(LREE enrichment, negative Eu anomaly, flat HREE) are nearly identical, with only the Creighton pluton having slightly more negative Eu anomalies (Figure 8.1a). Primitive mantle normalized spidergrams (Sun and McDonough, 1989) also illustrate the overall resemblance in elemental patterns with strong relative depletions in Nb, P and Ti (Figure 8.1b). However, upon closer inspection it becomes evident that there are some clear chemical differences in the granitoids. Some elements (e.g. Ba, Ca, Rb, K) can be mobilized during low grade metamorphism and the differences show that the intrusions may have been affected to variable degrees but others may reflect on the geodynamic environment of emplacement.

In a geochemical comparison of all the intrusions, the most obvious difference is the SiO_2 concentration. The Creighton pluton has a much wider range in silica content overall, as well as within each specific granitoid type. The Street Township granites possess higher FeO* and MnO values at a given SiO_2 content, plot clearly as tholeiitic on an AFM diagram (Irvine and Baragar, 1975) and have the lowest Th values. The Murray pluton contains the lowest CaO content and is also the most potassic granitoid. The Creighton Type 1 samples tend to be more enriched in Rb and Th while having significantly lower Ba values compared to the other intrusives. An interesting characteristic is the Mg# where there is a distinct boundary at a value of 20 (Figure 8.2a). Samples from the Creighton pluton irrespective of rock type (with the exception of MS99-31, the most silicic sample), plot above this cut-off line whereas the Murray pluton and Street Township granites plot below. A comparative diagram of Zr/Th vs. $FeO+MgO+MnO+TiO_2$ combining selected major- and trace-elements illustrates some of

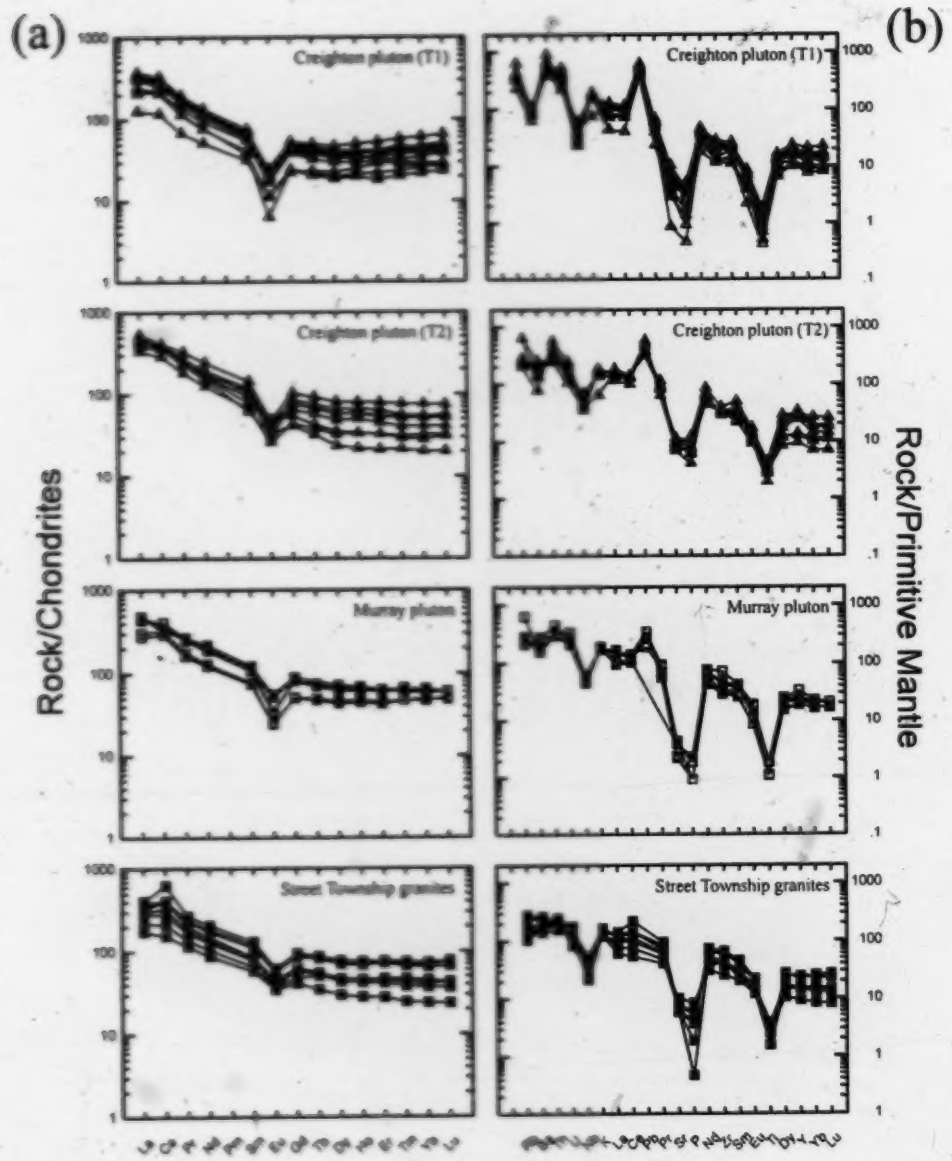

Figure 8.1: Multi-element spidergrams of the Creighton pluton, Murray pluton and Street Township granites. Normalization values from Sun and McDonough (1989). **A)** Chondrite normalized rare-earth element diagram. **B)** Primitive mantle normalized diagram.

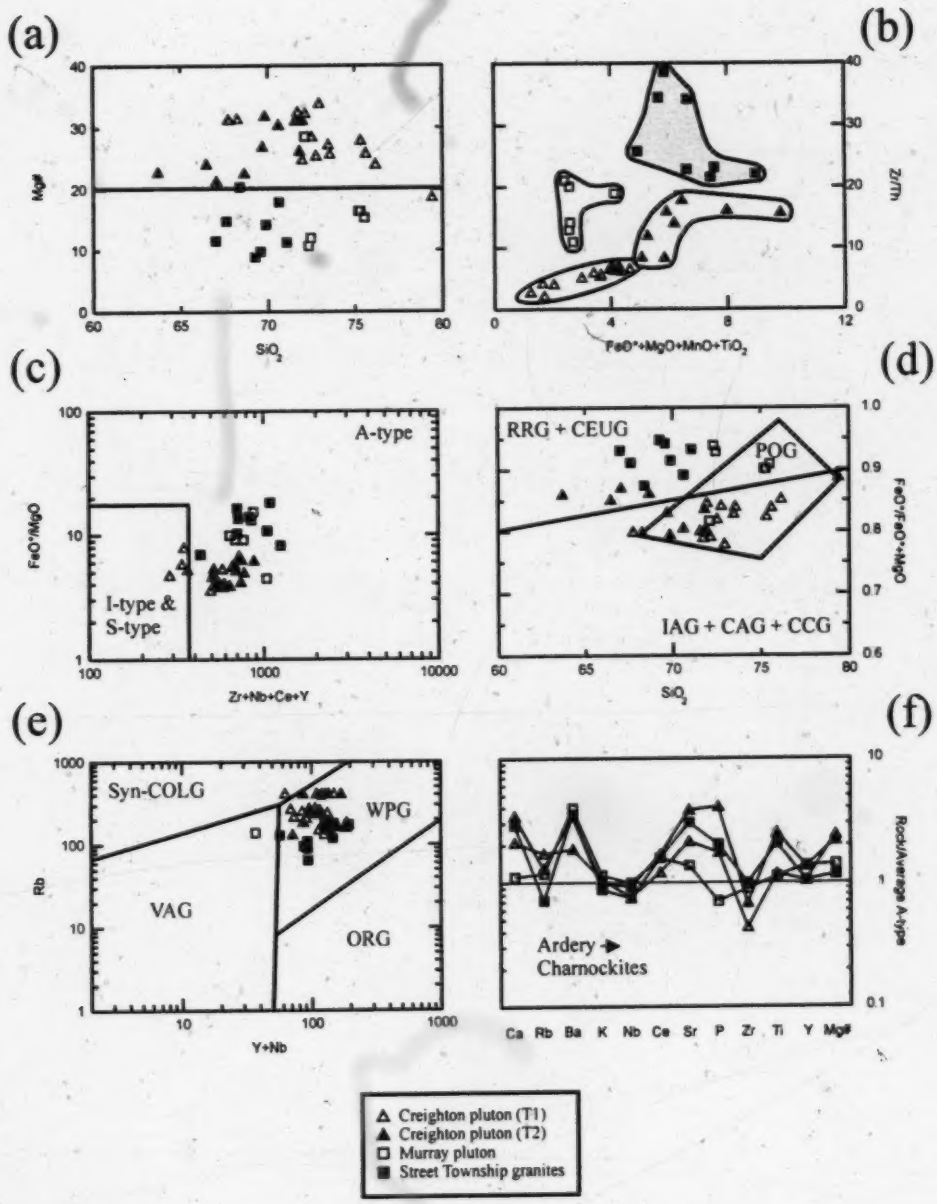
(a)
(b)
(c)
(d)
(e)
(f)
Mg#
SiO2
Zr/Th
FeO*+MgO+MnO+TiO2
A-type
I-type &
S-type
FeO*/MgO
Zr+Nb+Ce+Y
RRG + CEUG
POG
IAG + CAG + CCG
FeO*/FeO*+MgO
Syn-COLG
WPG
VAG
ORG
Rb
Y+Nb
Ardery
Charnockites
Rock/Average A-type
Ca Rb Ba K Nb Ce Sr P Zr Ti Y Mg#
Creighton pluton (T1)
Creighton pluton (T2)
Murray pluton
Street Township granites

Figure 8.2: Comparative geochemical and tectonic discrimination diagrams showing similarities and contrasts between Creighton pluton, Murray pluton and Street Township granites. **(a)** SiO_2 vs. Mg#. Mg# = molar MgO/(MgO+FeO*). **(b)** Multi-element diagram incorporating major and trace elements. **(c)** A-type granite discrimination diagram of Whalen et al., (1987). A-type = anorogenic granite; I-type = intracrustal/igneous derived granite; S-type = supracrustal/sedimentary derived granite. **(d)** SiO_2 vs. FeO*/(FeO*+MgO) diagram of Maniar and Piccoli (1989). IAG = island arc granitoids; CAG = continental arc granitoids; CCG = continental collision granitoids; POG = post-orogenic granitoids; RRG = rift-related granitoids; CEUG = continental epeirogenic uplift granitoids. **(e)** Rb vs. Y + Nb diagrams of Pearce et al., (1984). WPG = within-plate granite; VAG = volcanic arc granite; ORG = ocean ridge granite; syn-COLG = syn-collisional granite. **(f)** Multi-element profile diagram normalized to average A-type granite (Whalen et al., 1987) showing the C-type Ardery Charnockites (Kilpatrick and Ellis, 1992).

the key differences and provides excellent constraints on separating out the granitoid bodies (Figure 8.2b).

No isotopic work has been conducted on the Street Township granites, but one sample from the Murray pluton was analyzed in this study for Rb-Sr, Sm-Nd and common Pb-feldspar to compare to the Creighton pluton. Complete isotopic data for the Murray pluton can be found in Appendix E. The Rb-Sr system appears to have been affected in a similar fashion to the Type 1 granitoids. An initial $^{87}Sr/^{86}Sr$ value of 0.694174 (t = 2477 Ma) was obtained, showing that the Rb-Sr system of the Murray pluton is disturbed. The isotopic ratio is comparable to recalculated values that were previously determined (Fairbairn et al., 1965; Gibbins and McNutt, 1975). The Murray pluton is characterised by Sm/Nd = 0.19, ε_{Nd} (t = 2477 Ma) = -2.04, $f^{Sm/Nd}$ = -0.42, and a depleted mantle model age (Goldstein et al., 1984) of ca. 2.9 Ga. All signatures from the Sm-Nd isotopic system are within the range of values obtained for the Creighton pluton. Common Pb-feldspar values were $^{208}Pb/^{204}Pb$ = 35.812, $^{207}Pb/^{204}Pb$ = 15.454, and $^{206}Pb/^{204}Pb$ = 15.827 and are comparable to values from the Creighton Type 2 granitoids.

Tectonic discrimination diagrams for all the granitic intrusions illustrate the general similarities between the bodies (Figure 8.2). Almost all of the samples plot in the WPG (within-plate granite) field (Pearce et al., 1984) (Figure 8.2e) and are classified as A-type granites (Whalen et al., 1987) (Figure 8.2C). The only difference is on the SiO_2 vs. FeO*/(FeO*+MgO) tectonic diagram (Maniar and Piccoli, 1989). The Street Township granites plot only in the RRG + CEUG (rift-related granitoids + continental epeirogenic uplift granitoids) field but the Creighton and Murray plutons plot in both the RRG + CEUG and POG (post-orogenic granitoids) fields (Figure 8.2d). A multi-

elemental diagram normalized to average A-type granite (Whalen et al., 1987) shows how all three granitoids have similar patterns to the Ardery Charnockites of Kilpatrick and Ellis (1992) (Figure 8.2f). The key difference is the Mg# where A-type granitoids are commonly less than 10 and C-type range from 25 – 40 (Kilpatrick and Ellis, 1992). The Creighton pluton samples average 27.6 whereas the Street Township granites and Murray pluton have averages of 13.6 and 16.6, respectively.

Overall the granites are very similar in mineralogy, geochemistry and isotopic characteristics and appear to have a genetic link despite occurring over a span of 100 m.y. The Street Township granites and the Murray pluton show more rift/anorogenic characteristics from being closely related with the main stages of rifting. The Creighton pluton seems to be an anomalous period of magmatism that occurred subsequent to the main stages of rifting and may explain some of its contrasting geochemical signatures.

Ca. 2.45 Ga magmatism

The ca. 2.45 Ga Matachewan Igneous Events represents a large-scale igneous province whose origins still remain somewhat enigmatic. It is not the purpose here to provide conclusive answers to its genesis but rather to deal with the relationship of the timing of the Creighton pluton with the mafic MIE and how they are linked.

All of the magmatic rocks in the Southern Superior Province that occur between 2.50 and 2.40 Ga exhibit similar geochemical and isotopic characteristics. The rocks include the ca. 2.48 Ga gabbro-anorthosite intrusions (Peck et al, 1995; Prevec, 1993; Vogel et al., 1999), the Hearst-Matachewan dike swarms (Condie et al., 1987; Nelson et

al., 1990; Boily and Ludden, 1991), the Elliot Lake Group and Thessalon volcanics (Jolly et al., 1992; Chai and Eckstrand, 1994; Easton, 1998; this study) and the three granitic intrusions discussed above (Chai and Eckstrand, 1994; Easton, 1998; this study). The MIE-related magmatism outlines well-defined isotopic fields on both ε_{Nd} vs. $f^{Sm/Nd}$ and $^{207}Pb/^{204}Pb$ vs. $^{206}Pb/^{204}Pb$ diagrams (Figure 7.4/7.5). The narrow ranges of ε_{Nd} and $f^{Sm/Nd}$ values suggest that a relatively uniform source reservoir was involved in the genesis of all the magmas. The geochemical signature is defined by enrichment of the LILE (light-ion lithophile elements) and LREE (light rare-earth elements) with relative depletions in Nb, P and Ti and flat HFSE (high field strength elements) (Figure 8.3). This type of pattern is usually attributed to a subduction-related setting.

Although most authors agree on the enriched nature of the MIE magmatism, there is some debate over the mechanism of this enrichment. One possible explanation is that the subduction-like signatures are the result of the metasomatism in the mantle lithosphere of a previously subducted slab (e.g. Boily and Ludden, 1991; Tomlinson, 1996). Another, more recent proposal by Vogel et al., (1998), is that there is a fundamental contrast in the composition and structure of the Archean-Paleoproterozoic mantle from the more modern mantle. The authors support this hypothesis with the evidence that most Archean greenstone volcanic rocks and pre ~2.0 Ga dike swarms possess these subduction-related geochemical signatures and that more modern mantle plume or N-MORB patterns are rare to absent (Condie et al., 1987; Condie, 1994; Vogel et al., 1998). The mantle plume related MIE is proposed to be part of a global rifting event (Heaman, 1997) at ca. 2.45 Ga facilitating the comparison of this hypothesis with other regions of the world (e.g. the Fennoscandian Shield).

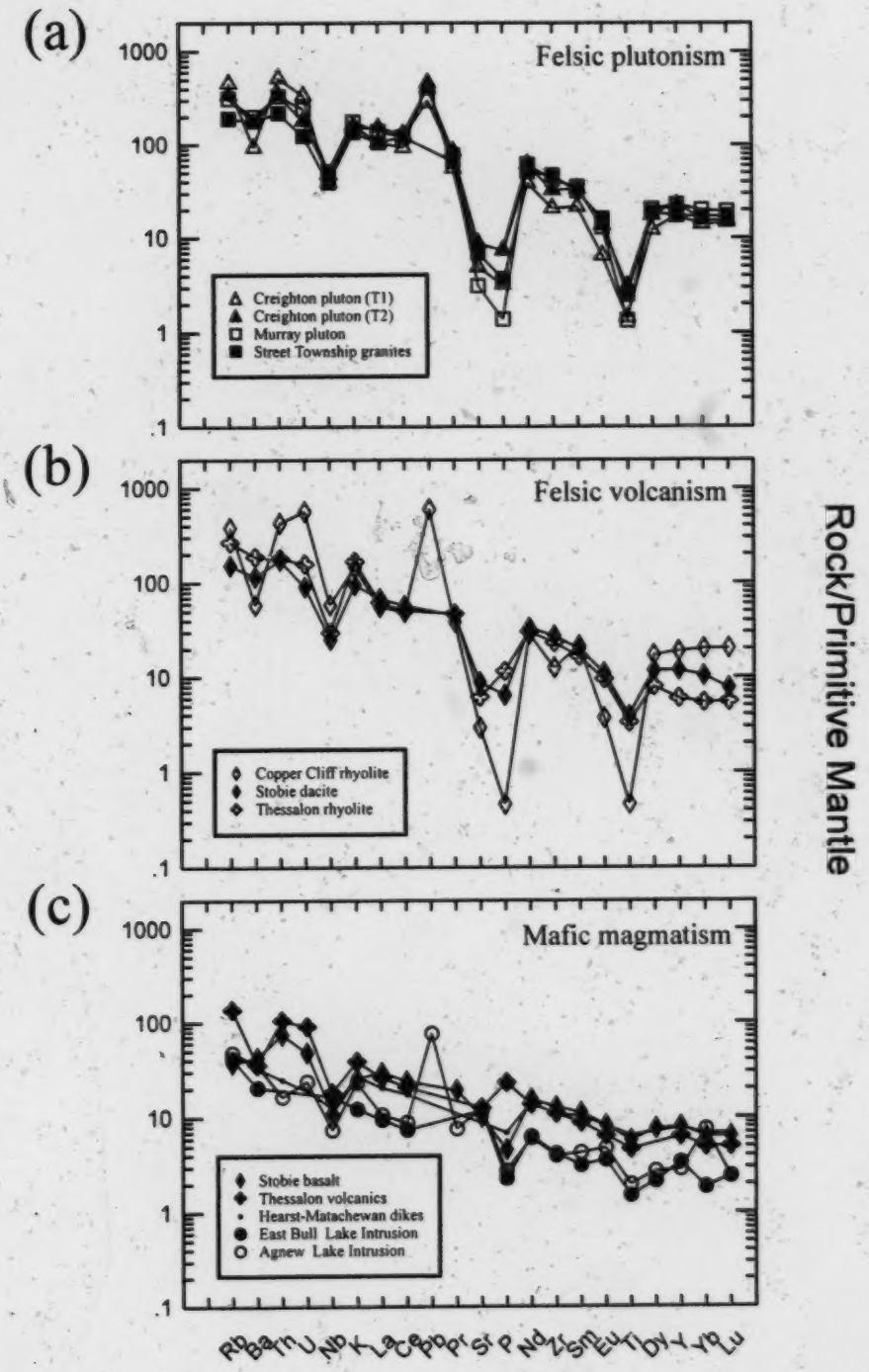
(a)
Felsic plutonism
1000
100
10
1
.1
Creighton pluton (T1)
Creighton pluton (T2)
Murray pluton
Street Township granites
(b)
Felsic volcanism
Copper Cliff rhyolite
Stobie dacite
Thessalon rhyolite
(c)
Mafic magmatism
Stobie basalt
Thessalon volcanics
Hearst-Matachewan dikes
East Bull Lake Intrusion
Agnew Lake Intrusion
Rock/Primitive Mantle

Figure 8.3: Primitive mantle normalized multi-element spidergram of average values for all Paleoproterozoic MIE linked magmatism. Normalization values from Sun and McDonough (1989). **(a)** Felsic plutonism including the Creighton pluton Type 2 (n=8) and Type 1 (n=18) (this study), the Street Township granites (n=8) (Easton, 1998) and the Murray pluton (n=6) (Chai and Eckstrand, 1994; this study). **(b)** Felsic volcanism including the Copper Cliff rhyolite (n=3) (Easton, 1998; this study), the Stobie Dacite (n=4) (Chai and Eckstrand, 1994; Easton, 1998) and the Thessalon rhyolites (n=7) (Jolly et al., 1992; Tomlinson, 1996). **(c)** Mafic magmatism including the Hearst-Matachewan dikes (n=33) (Condie et al., 1987; Nelson et al., 1990; Boily and Ludden, 1991), the Stobie Basalt (n=8) (Easton, 1998), the Thessalon Volcanics (n=9) (Jolly et al., 1992), the East Bull Lake Intrusion (n=21) (James and Born, 1985; Prevec, 1993) and the Agnew Lake Intrusion (n=43) (Prevec, 1993; Vogel et al., 1999).

The three granitic intrusions represent a minor plutonic episode related to the mafic MIE. The Creighton and Murray plutons and the Street Township granites are interpreted to have formed as the result of the melting of mafic-intermediate granulitic crust that was metamorphosed by underplating basalts in a mantle plume driven rift. The discrete differences in the three bodies are explained by the differences in timing and incorporation of variable amounts of a heterogeneous lower crustal material. The significantly younger ages of the Creighton pluton coupled with the kimberlite-borne mafic granulite xenoliths suggests that MIE related magmas may have underplated the crust for an extended period of time and that the duration of the magmatism occurred for over 100 m.y.

CHAPTER 9: CONCLUSIONS

1) The rocks of the Creighton pluton are mainly granite to monzogranite in composition. Texture can be quite variable but overall they possess a simple mineralogy of quartz-plagioclase-potassic feldspar with biotite as the major mafic mineral and trace hornblende and accessory minerals.
2) Mineralogy, geochemistry, U-Pb geochronology and tracer isotopes have identified that the Creighton pluton is actually composed of two separate and distinct intrusions.
3) The 2415 ± 5 Ma Type 1 granitoids compose most of the pluton and are characterized by higher SiO_2 and Th, lower Ba and more radiogenic Pb isotopic ratios relative to the Type 2 granitoids.
4) The 2376.3 ± 2.3 Ma Type 2 granitoids compose a small circular body in the centre of the pluton and are characterized by higher FeO*, MgO, TiO_2, Y, Zr and less radiogenic Pb isotopic ratios relative to the Type 1 granitoids.
5) U-Pb zircon geochronology, Rb-Sr isotopes and common Pb-feldspar isotopes show evidence of open system behaviour due to subsequent geological events.
6) The Creighton pluton is interpreted to be the result of C-type (charnockite) magmatism. It formed from the melting of granulitic crust caused by the underplating of basaltic magmas. The granite is likely the result of the mixing of two sources at depth: 1) a mafic granulitic material and 2) older pre-existing (granulitic?) lower crust.

7) Despite a temporal gap of >40 m.y., geochemistry and isotopes show that the Creighton pluton is genetically linked to the Murray pluton and Street Township granites and the mafic Matachewan Igneous Events (MIE).

8) Based on the age of the Creighton pluton and the kimberlite-borne mafic granulite xenoliths near Kirkland Lake, it is interpreted that MIE related magmas ponded at the base of the crust for over 100 m.y. This would mean that that MIE magmatism spans from ca. 2490 – 2380 Ma, nearly 50 m.y. more than previous interpretations.

REFERENCES

Ames, D.E., Watkinson, D.H., and Parrish, R.R., (1998). Dating of a regional hydrothermal system induced by the 1850 Ma Sudbury impact event. Geology, v. 26, no. 5, p. 447-450.

Ashwal, L.D. and Wooden, J.L., (1989). River Valley pluton, Ontario: a late Archean/Early Proterozoic anorthositic intrusion in the Grenville Province. Geochimica et Cosmochimica Acta, v. 53, p.633-641.

Bennett, G., Dressler, B.O., and Robertson, J.A., (1991). The Huronian Supergroup and Associated Intrusive Rocks; in Ontario Geological Survey Special Volume 4, p. 549-591.

Boily, M., and Ludden, J.N., (1991). Trace-element and Nd isotopic variations in Early Proterozoic dyke swarms emplaced in the vicinity of the Kapuskasing structural zone: enriched mantle or assimilation and fractional crystallisation (AFC) process? Canadian Journal of Earth Sciences, v. 28, p. 26-36.

Card, K.D., (1968). Geology of Denison-Waters area, Ontario. Ontario Department of Mines, Geological Report 60, 63p.

Card, K.D., (1978). Geology of the Sudbury-Manitoulin area, Ontario. Ontario Geological Survey Report, 238 p.

Card, K.D., Gupta, V.K., McGrath, P.H. and Grant, F.S. (1984). The Sudbury Structure: its regional geological and geophysical setting. In: Pye, E.G., Naldrett, A.J. and Giblin, P.E. (Eds.). The Geology and Ore Deposits of the Sudbury Structure. Ontario Geological Survey, Special Volume 1, p. 25-43.

Chai, G. and Eckstrand, R., (1994). Rare-earth element characteristics and origin of the Sudbury Igneous Complex, Ontario, Canada. Chemical Geology, v. 113, p. 221-244.

Chappell, B.W., and White, A.J.R., (1992). I- and S-type granites in the Lachan Fold Belt. Transactions of the Royal Society of Edinburgh: Earth Sciences, v. 83, p. 1-26.

Chappell, B. W., and White, A. J. R. (1974): Two contrasting granite types. Pacific Geology, 8, p 173-174.

Chubb, P.T., Vogel, D.C., Peck, D.C, James, R.S., and Keays, R.R., (1994). Occurences of pseudotahylyte at the East Bull Lake and Shakespeare-Dunlop intrusions, Ontario, Canada. Canadian Journal of Earth Sciences, v. 31, p. 1744-48.

Condie, K.C., Bobrow, D.J., and Card, K.D., (1987). Geochemistry of Precambrian mafic dykes from the Southern Superior Province; in Mafic Dyke swarms, Editors: Halls, H.C. and Fahrig, W.F., Geological Association of Canada Special Paper 34, p. 95-108.

Condie, K.C., (1994). Greenstones through time. *In* Archaean crustal evolution. *Edited by* K.C. Condie. Elseview, Amsterdam, p. 85-120.

Corfu, F., and Easton, R.M., (2000). U-Pb evidence for polymetamorphic history of Huronian rocks underlying the Grenville Front Tectonic Zone east of Sudbury Ontario. Chemical Geology, v. 172, p. 149-171.

Corfu, F., and Lightfoot, P.C., (1996). U-Pb geochronology of the Sublayer Environment, Sudbury Igneous Complex, Ontario. Economic Geology, v. 91, p. 1263-1269.

Cowan, G.A., and Adler, H.H., (1976). The variability of the natural abundance of ^{235}U. Geochimica et Cosmochimica Acta, v. 40, p. 1478-1490.

Creaser, R.A. and Gray, C.M. (1992). Preserved initial 87Sr/86Sr in apatite from altered felsic igneous rocks: A case study from the middle Proterozoic of South Australia. Geochimica et Cosmochimica Acta, v. 56, p. 2789-2795.

Creaser, R.A., Erdmer, P., Stevens, R.A. and Grant, S.L. (1997). Tectonic affinity of Nisutlin and Anvil assemblage strata from Teslin tectonic zone, northern Canadian Cordillera: constraints from neodymium isotope and geochemical evidence. Tectonics, v. 16, p. 107-121.

Cumming, G.L. and Krstic, D. (1987). Geochronology at the Namew Lake Ni-Cu deposit, Flin Flon area, Manitoba, Canada: a Pb/Pb study of whole rocks and ore minerals. Canadian Journal of Earth Sciences, v. 28, p. 1328-1339.

de la Roche, H., Leterrier, J., Grand Claude, P., Marchal, M. (1980). A classification of volcanic and plutonic rocks using R1-R2 diagrams and major element analyses – its relationships with current nomenclature. Chemical Geology, v. 29, p. 183-210.

DePaolo, D.J., (1981). Trace element and isotopic effects of combined wallrock assimilation and fractional crystallization. Earth and Planetary Science Letters, v. 53, p. 189-202.

Dickin, A.P. (1998). Pb isotope mapping of differentially uplifted Archean basement: a case study from the Grenville Province, Ontario. Precambrian Research, v. 91, p. 445-454.

Dietz, R.S., (1964). Sudbury structure as an astrobleme. Journal of Geology, v. 12, p. 412-434.

Dressler, B.O., Baker, C.L., and Blackwell, B. eds. (1992). Ontario Geological Survey Miscellaneous Paper 160, Summary of field work and other activities, 1992.

Dutch, S.I., (1976). The Creighton Pluton, Ontario, and its significance to the geologic history of the Sudbury Region. Unpublished PhD thesis, Columbia University, 125 pages.

Dutch, S.I., (1979). The Creighton pluton, Ontario; and unusual example of a forcefully emplaced intrusion. Canadian Journal of Earth Science, v. 16, p. 333-349.

Easton, R.M., (1998). New observations related to the mineral potential of the Southern Province and the Grenville Front Tectonic Zone east of Sudbury. Ontario Geological Survey, Open File Report 5976, 28 p.

Fairbairn, H.W., Hurley, P.M., and Pinson, W.H., (1965) Reexamination of Rb-Sr whole-rock ages at Sudbury, Ontario. Proceedings of the Geological Association of Canada, v. 16, p. 707-714.

Fedo, C.M., Young, G.M., Nesbitt, H.W., and Hanchar, J.M., (1997). Potassic and sodic metasomatism in the Southern Province of the Canadian Shield: evidence from the Paleoproterozoic Serpent Formation, Huronian Supergroup, Canada. Precambrian Research, v. 84, p. 17-36.

Frarey, M.J., Loveridge, W.D., and Sullivan, R.W., (1982). A U-Pb zircon age for the Creighton Granite, Ontario; in Rb-Sr and U-Pb Isotopic Age Studies, Report 5, in Current Research, Part C, Geological Survey of Canada, Paper 81-1C, p. 129-132.

Gariepy, C., and Allegre, C.J., (1985). The lead isotopic geochemistry and geochronology of late-kinematic intrusives from the Abitibi greenstone belt, and the implications for late Archean crustal evolution. Geochimica et Cosmochimica Acta, v. 49, p. 2371-2383.

Gibbins, W.A., and McNutt, R.H., (1975). Rubidium-Strontium Mineral Ages and Polymetamorphism at Sudbury, Ontario. Canadian Journal of Earth Science, v. 12, p. 1990-2003.

Goldstein, S.L., O'Nions, R.K., and Hamilton, R.J., (1984). A Sm-Nd isotopic study of atmospheric dusts and particulates from major river systems. Earth and Planetary Sciences Letters, v. 70, p. 221-236.

Grieve, R.A.F., Stoffler, D., and Deutsch, A., (1991). The Sudbury Structure: Controversial or misundertood. Journal of Geophysics Research, v. 96, p. 22753-22764.

Halls, H.C., (1991). The Matachewan dyke swarm, Canada: an early Proterozoic magnetic field reversal. Earth and Planetary Sciences Letters, v. 105, p. 279-292.

Halls, H.C. and Bates, M.P. (1990). The evolution of the 2.45 Ga Matachewan Dyke swarm, Canada; in Mafic Dykes and Emplacment Mechanisms, Editors: Parker, Rickwood and Tucker, p. 237-249.

Halls, H.C. and Palmer, H.C. (1990). The tectonic relationship of two Early Proterozoic dyke swarms to the Kapuskasing Structural Zone: a paleomagnetic and petrographic study. Canadian Journal of Earth Sciences, v. 27, p. 87-103.

Heaman, L.M., (1997). Global mafic magmatism at 2.45 Ga: Remnants of an ancient large igneous province? Geology, v. 25, p. 299-302.

Heather, K.B., and van Breeman, O., (1994). An interim report of geological, structural, and geochronological investigations of granitoid rocks in the vicinity of the Swayze greenstone belt, southern Superior Province, Ontario. Geological Survey of Canada Current Research 1994-C, p. 259-268.

Housh, T. and Bowring, S.A. (1991). Lead isotopic heterogeneities within alkali feldspars: implications for the determination of initial lead isotopic compositions. Geochimica et Cosmochimica Acta, v. 55, p. 2309-2316.

Irvine, T.N. and Baragar, W.R.A. (1971). A guide to the chemical classification of the common volcanic rocks. Canadian Journal of Earth Sciences, v. 8, p. 523-548.

Jaffrey, A.H., Flynn, K.F., Glendenin, L.F., Bentley, W.C. and Essling, A.M., (1971). Precision measurements of half-lives and specific activities of ^{235}U and ^{238}U. Physics Review, v. 4, p. 1889-1906

Jolly, W.T., Dickin, A.P., and Wu, T.W., 1992. Geochemical stratigraphy of the Huronian continental volcanics at Thessalon, Ontario: contributions of two-stage crustal fusion. Contributions to Mineralogy and Petrology, 110: 411-428.

Kilpatrick J.A., and Ellis, D.J., (1992). C-type magmas: igneous charnockites and their extrusive equivalents. Transactions of the Royal Society of Edinburgh: Earth Sciences, v. 83, p. 155-164.

Krogh, T.E. (1994). Precise U-Pb ages for Grenvillian and pre-Grenvillian thrusting of Proterozoic and Archean metamorphic assemblages in the Grenville Front tectonic zone, Canada. Tectonics, v. 13, p. 963-982.

Krogh, T.E., Davis, D.W., and Corfu, F., (1984). Precise U-Pb zircon and baddeleyite ages for the Sudbury area; in The Geology and Ore Deposits of the Sudbury Structure, Editors: Pue, E.G., Naldrett, A.J., and Giblin, P.E., Ontario Geological Survey, Special Volume 1, p. 431-446.

Krogh, T.E., Corfu, F., Davis, D.W., Dunning, G.R., Heaman, L.M., Kamo, S.L., Machado, N., Greenough, J.D. and Nakamura, E., (1987). Precise U-Pb isotopic ages of diabase dykes and mafic to ultramafic rocks using trace amounts of baddeleyite and zircon. In: Halls, H.C., Fahrig, W.F (Eds.). Mafic Dyke Swarms. Geological Association of Canada, Special Paper 34, p. 147-152.

Krogh, T.E., Kamo, S.L., and Bohor, B.F., (1996). Shock metamorphosed zircons with correlated U-Pb discordance and melt rocks with concordant protolith ages indicate an impact origin for the Sudbury structure, in Earth Processes: Reading the Isotopic Code, Editors: Hart, S., and Basu, A., American Geophysical Union, Geophysical Monograph 95, p. 343-353.

Krogh, T.E., McNutt, R.H., and Davis, G.L., (1982). Two high precision U-Pb zircon ages for the Sudbury Nickel Irruptive. Canadian Journal of Earth Science, v. 19, p. 723-728.

Lanphere, M.A., Wasserburg, G.J.F., Albee, A.L. and Tilton, G.R. (1964). Redistribution of strontium and rubidium isotopes during metamorphism, World Beater Complex, Panamint Range, California. In: Isotopic and cosmic chemistry, North-Holland Publishing Co., Amsterdam, Netherlands, p. 269-320.

Lewis, C.R., (1951). The Age Relationship of the Murray Granite and "Sudbury Norite". Canadian Mining Journal, May p. 55-62, June p. 70-75.

Ludwig, K.R. (1998). Isoplot/Ex, a geochronological toolkit for Microsoft Excel, Version 1.00b. Berkeley, California, Berkeley Geochronology Center Special Publication 1.

Lugmair, G.W. and Galer, G.L. (1992). Age and isotopic relationships among the angrites Lewis Cliff 86010 and Angra dos Reis. Geochimica et Cosmochimica, v. 56, p. 1673-1694.

Maniar, P. D., and Piccoli, P. M (1989): Tectonic discrimination of granitoids. Geological Society of America Bulletin, 101, p. 635-643.

Meldrum, A., Abdel-Rahman, A.-F.M., Martin, R.F., and Wodicka, N., (1997). The nature, age and petrogenesis of the Cartier Batholith, northern flank of the Sudbury Structure, Ontario, Canada. Precambrian Research, v. 82, p. 265-285.

Moser, D.E. and Heaman, L.M., (1997). Proterozoic zircon growth in Archean lower crustal xenoliths, southern Superior craton – a consequence of Matachewan ocean opening. Contributions to Mineralogy and Petrology, v. 128, p. 164-175.

Muir, T.L., (1984). The Sudbury Structure: considerations and models for an endogenic origin. The Geology and Ore Deposits of the Sudbury Structure, Pye, E.G., Naldrett, A.J., Giblin, P.E. (Eds.). Ontario Geological Survey, Special Volume 1, p. 533-569.

Naldrett, A.J., (1984). Summary, Discussion, and Synthesis. The Geology and Ore Deposits of the Sudbury Structure, Pye, E.G., Naldrett, A.J., Giblin, P.E. (Eds.). Ontario Geological Survey, Special Volume 1, p. 533-569.

Nelson, D.O., Morrison, D.A., and Phinney, W.C., (1990). Open-system evolution versus source control in basaltic magmas: Matachewan-Hearst dike swarm, Superior Province, Canada. Canadian Journal of Earth Science, v. 27, p. 767-783.

Pearce, J.A. (1983). Role of the sub-continental lithosphere in magma genesis at active continental margins. In: Hawkesworth, C.J. and Norry, M.J. (Eds.). Continental basalts and mantle xenoliths. Shiva, Nantwich, p. 230-249.

Pearce, J.A., Harris, N.B.W., and Tindle, A.G., (1984). Trace Element Discrimination Diagrams for the Tectonic Interpretation of Granitic Rocks. Journal of Petrology, v. 25, p. 956-983.

Peck, D.C., James, R.S., Chubb, P.T., Prevec, S.A., and Keays, R.R., (1995). Geology, Metallogeny and Petrogenesis of the East Bull Lake Intrusion, Ontario. Ontario Geological Survey, Open File Report 5923, 117 p.

Popelar, J., (1972). Gravity interpretation of the Sudbury area. Geological Association of Canada, Special Paper 10, p. 103-115.

Prevec, S.A., (1993). An isotopic, geochemical and petrographic investigation of the genesis of Early Proterozoic mafic intrusions and associated volcanism near Sudbury, Ontario. Unpublished Ph.D. thesis, 223 pages.

Prevec, S.A., James, R.S., Keays, R.R., and Vogel, D.C., (1995). Constraints of the genesis of Huronian magmatism in the Sudbury area from radiogenic isotopic and geochemical evidence. Canadian Mineralogist, v. ?, p. 930-932.

Rilller, U., Schwerdtner, W.M., Halls, H.C. and Card, K.D., (1999). Transpressive tectonism in the eastern Penokean orogen, Canada: Consequences for Proterozoic crustal kinematics and continental fragmentation. Precambrian Research, v. 93, p. 51-70.

Robertson, J.A., (1970). Geology of the Spragge area, District of Algoma. Ontario Department of Mines, Geological Report Number 76, 109p.

Roscoe, S.M., Theriault, R.J. and Prasad, N. (1992). Circa 1.7 Ga Rb-Sr re-setting in two Huronian Paleosols, Elliot Lake, Ontario and Ville Marie, Quebec. In: Radiogenic age and isotopic studies, Geological Survey of Canada paper, p. 119-124.

Roscoe, S.M. and Card, K.D., (1993). The reappearance of the Huronian in Wyoming: rifting and drifting of ancient continents. Canadian Journal of Earth Science, v. 30, p. 2475-2480.

Schandl, E.S., Gorton, M.P., and Davis, D.W. (1994). Albitization at 1700 ± 2 Ma in the Subury-Wanapitei Lake area, Ontario: implications for deep-seated alkalic magmatism in the Southern province. Canadian Journal of Earth Sciences, v. 31, p. 597-607.

Smith, P.E., Farquhar, R.M., and Halls, H.C., (1992). U-Th-Pb isotope study of mafic dykes in the Superior Province, Ontario, Canada: uniformity of initial Pb isotope ratios of the Hearst dykes. Chemical Geology, v. 94, p. 261-280.

Stacey, J.S. and Kramers, J.D. (1975). Approximation of terrestrial lead isotope evolution by a two-stage model. Earth and Planetary Science Letters, v. 26, p. 207-221.

Stern, R.A., Percival. J.A. and Mortensen, J.K. (1994). Geochemical evolution of the Minto block: a 2.7 Ga continental magmatic arc built on the Superior proto-craton. Precambrian Research, v. 65, p. 115-153.

Stockwell, C.H., (1982). Proposals for time classification and correlation of Precambrian rocks and events in Canada and adjacent areas of the Canadian Shield; Geological Survey of Canada, Paper 80-19, Part 1: A time classification of Precambrian rocks and events, 135 pages.

Streckeisen, A. (1976): To each plutonic rock its proper name. Earth Science Reviews, 12, p 1-33.

Streckeisen, A., and LeMaitre, R.W., (1979). A Chemical Approximation to the modal QAPF Classification of the Igneous Rocks. Neues Jahrbuch Miner. Abh., v. 136, p. 169-206.

Sun, S.S. and McDonuough, W.F. (1989). Chemical and isotopic systematics of oceanic basalts: implications for mantle composition and processes. In: Saunders, A.D., Norry, M.J. (Eds.). Magmatism in the Ocean Basins. Blackwell Scientific Publications, Oxford, UK, p. 313-345.

Todt, W., Cliff, R.A., Hanser, A., and Hofmann, P., (1996). Evaluation of a ^{202}Pb-^{205}Pb double spike for high-precision lead isotope analysis. Earth Processes: Reading the isotopic code, Geophysical Monograph, v. 95, p. 429-439.

Tomlinson, K.Y., (1996). The geochemistry and tectonic setting of early Precambrian greenstone belts, northern Ontario, Canada. Unpublished PhD thesis, University of Portsmouth, 267 pages.

Vogel, D.C., Keays, R.R., James, R.S., and Reeves, S.J., (1999). The geochemistry and petrogenesis of the Agnew Intrusion, Canada: a product of S-undersaturated, high-Al and low-Ti tholeiitic magmas. Journal of Petrology, v. 40, p. 423-450.

Vogel, D.C., James, R.S., and Keays, R.R., (1998). The early tectono-magmatic evolution of the Southern Province: implications from the Agnew Intrusion, central Ontario, Canada. Canadian Journal of Earth Sciences, v. 35, p. 854-870.

Whalen, J.B., Currie, K.L., and Chappell, B.W., (1987). A-type granites: geochemical characteristics, discrimination and petrogenesis. Contributions to Mineralogy and Petrology, v. 95, p. 407-419.

Yamashita, K., Creaser, R.A., Stemler, J.U., and Zimaro, T.W. (1999). Geochemical and Nd-Pb isotopic systematics of late Archean granitoids, southwestern Slave Province, Canada: constraints for granitoid origin and crustal isotopic structure. Canadian Journal of Earth Sciences, v. 36, p. 1131-1147.

Young, G.M., Long, D.G.F., Fedo, C.M., and Nesbitt, H.W, (2001). Paleoproterozoic Huronian basin: product of a Wilson cycle punctuated by glaciations and a meteorite impact. Sedimentary Geology, v. 141-142, p. 233-254.

Appendix A

Sample Locations

Sample	Rock Type	Longitude (N)	Latitude (W)
Creighton pluton			
LH98-63	Type 1	46° 25' 55"	081° 10' 57"
MS98-1	Breccia	46° 26' 37"	081° 11' 29"
MS98-2	Breccia	46° 26' 37"	081° 11' 29"
MS98-3	Type 1	46° 26' 48"	081° 08' 59"
MS99-13	Type 2	46° 27' 17"	081° 09' 47"
MS99-14	Enclave	46° 27' 17"	081° 09' 47"
MS99-15	Type 2	46° 27' 21"	081° 10' 04"
MS99-16	Type 2	46° 27' 17"	081° 10' 57"
MS99-17	Type 1	46° 25' 17"	081° 10' 57"
MS99-18	Type 2	46° 26' 56"	081° 11' 39"
MS99-19	Dike	46° 26' 56"	081° 11' 39"
MS99-31	Type 1	46° 26' 06"	081° 17' 04"
MS99-32	Type 1	46° 26' 03"	081° 16' 43"
MS99-33	Type 1	46° 25' 47"	081° 15' 47"
MS99-34	Type 1	46° 26' 02"	081° 15' 04"
MS99-35	Breccia	46° 26' 01"	081° 14' 59"
MS99-36	Type 1	46° 26' 11"	081° 14' 39"
MS99-37	Type 1	46° 26' 14"	081° 13' 21"
MS99-38	Type 1	46° 25' 51"	081° 13' 43"
MS99-39	Type 2	46° 25' 11"	081° 18' 25"
MS99-40	Type 1	46° 25' 52"	081° 17' 30"
MS99-41	Type 1	46° 25' 50"	081° 18' 45"
MS99-42	Type 1	46° 28' 57"	081° 04' 18"
MS99-43	Type 2	46° 27' 09"	081° 11' 52"
MS99-44	Breccia	46° 27' 15"	081° 11' 06"
MS99-45	Type 1	46° 28' 15"	081° 10' 41"
MS99-46	Type 1	46° 29' 05"	081° 05' 16"
MS99-47	Type 1	46° 28' 28"	081° 05' 41"

Appendix A

Sample Locations

Sample	Rock Type	Longitude (N)	Latitude (W)
Creighton pluton			
MS99-48	Type 1	46° 28' 09"	081° 07' 24"
MS99-49	Type 1	46° 27' 24"	081° 08' 05"
MS99-50	Type 2	46° 28' 25"	081° 09' 34"
MS99-51	Type 2	46° 29' 07"	081° 09' 11"
MS99-57	Enclave	46° 27' 21"	081° 10' 04"
Murray pluton			
MS98-4	Granite	46° 30' 48"	081° 02' 34"
MS99-20	Granite	46° 30' 56"	081° 03' 09"
MS99-54	Granite	46° 31' 10"	081° 02' 23"
MS99-55	Granite	46° 31' 55"	081° 01' 48"
MS99-56	Granite	46° 32' 39"	081° 00' 16"
Copper Cliff rhyolite			
MS99-52	Rhyolite	46° 25' 41"	081° 08' 40"
MS99-53	Rhyolite	46° 30' 08"	081° 02' 05"

Appendix B

Creighton pluton: Major, trace and rare-earth element data

Sample	LH98-63	MS98-2	MS98-3	MS99-13	MS99-14	MS99-15	MS99-16	MS99-17
Rock Type	Type 1	Breccia	Type 1	Type 2	Type 1	Type 2	Type 2	Type 1
SiO_2	71.49	66.68	71.24	70.02	63.26	66.77	67.99	73.13
Al_2O_3	13.14	13.18	13.20	13.53	14.29	13.56	13.80	12.93
MnO	0.06	0.09	0.05	0.06	0.14	0.10	0.06	0.03
MgO	0.77	1.85	0.77	0.89	2.19	0.93	0.75	0.50
CaO	1.87	3.58	1.94	2.13	2.93	2.66	2.45	1.40
Na_2O	2.94	2.93	3.11	3.06	3.71	3.15	2.54	2.93
K_2O	5.34	4.15	4.92	4.86	2.96	4.50	5.45	5.24
P_2O_5	0.09	0.11	0.09	0.09	0.15	0.23	0.13	0.06
TiO_2	0.38	0.56	0.39	0.42	0.65	0.77	0.66	0.29
Fe_2O_3	3.41	5.87	3.40	4.10	9.50	6.92	5.22	2.90
LOI	0.40	0.77	0.35	0.65	0.74	0.56	0.68	0.76
TOTAL	99.89	99.77	99.46	99.81	100.52	100.15	99.73	100.17
Ba	672	533	598	896	312	1193	1487	625
Ga	17	17	18	20.52	28.58	22.20	20.37	19.21
Hf	7.9	6.9	7.6	8.46	7.98	8.22	8.75	6.97
Nb	25	24	26	38.49	39.85	38.41	30.49	30.40
Pb	29	51	36	35.42	30.41	26.95	26.17	28.18
Rb	266	267	249	>400.00	>400.00	160.08	142.66	>400.00
Sc	6.4	12.8	6.1	9.0	13.8	14.7	10.6	7.3
Sr	78	112	79	144.1	138.1	237.6	196.6	129.2
Ta	3.5	2.97	3.7	2.18	1.37	1.98	1.66	2.89
Th	43	34	41	38.08	29.90	21.21	25.72	43.21
U	8	7.9	8	3.88	7.87	4.66	3.36	10.96
Y	71	63	72	131.13	106.69	122.52	109.74	105.59
Zn	47	95	54	76	184	109	60	31
Zr	284	241	269	316.74	310.71	339.80	357.74	247.79
La	83	68	79	116.19	78.54	90.49	100.30	79.67
Ce	161	132	151	>250.00	184.96	221.68	242.62	193.90
Pr	17	14	16	25.71	18.95	22.20	22.30	16.93
Nd	60	51	58	90.06	70.32	84.10	78.02	56.34
Sm	11	9.5	11	15.84	14.83	16.97	14.58	10.00
Eu	1.2	1.28	1.17	1.77	1.61	2.77	2.37	1.02
Gd	9.9	8.8	9.8	15.64	14.70	15.63	13.38	9.56
Tb	1.6	1.47	1.69	2.54	2.26	2.60	2.17	1.54
Dy	10.2	9.21	10.4	14.64	12.51	14.86	12.29	9.37
Ho	2.24	2.04	2.29	3.39	2.83	3.28	2.86	2.32
Er	6.6	5.7	6.76	9.12	7.88	8.89	7.45	6.34
Tm	1.18	1.1	1.24	1.38	1.17	1.31	1.04	1.05
Yb	7.21	6.4	7.62	9.08	7.53	8.79	7.01	7.21
Lu	1.09	1.01	1.16	1.46	1.24	1.32	1.04	1.24

Appendix B

Creighton pluton: Major, trace and rare-earth element data

Sample	MS99-18	MS99-19	MS99-31	MS99-32	MS99-33	MS99-34	MS99-35	MS99-36
Rock Type	Type 2	Dike	Type 1	Type 1	Type 1	Type 1	Breccia	Type 1
SiO_2	69.29	74.71	79.58	71.48	71.62	71.52	65.15	71.66
Al_2O_3	13.54	12.97	11.08	13.58	13.74	13.42	12.92	13.89
MnO	0.06	0.02	0.01	0.05	0.05	0.05	0.09	0.04
MgO	0.89	0.22	0.13	0.81	0.78	0.79	1.78	0.76
CaO	2.36	1.00	0.58	1.83	1.93	2.04	5.07	2.46
Na_2O	2.55	2.78	2.66	2.92	3.33	3.00	3.80	4.58
K_2O	5.14	6.19	4.93	5.15	4.93	4.79	1.85	2.23
P_2O_5	0.14	0.03	0.01	0.09	0.09	0.09	0.16	0.09
TiO_2	0.58	0.10	0.09	0.38	0.38	0.39	0.92	0.40
Fe_2O_3	4.89	1.29	1.14	3.37	3.42	3.52	7.03	3.23
LOI	0.67	0.38	0.49	0.71	0.59	0.62	1.91	0.68
TOTAL	100.11	99.69	100.70	100.37	97.53	100.23	100.68	100.02
Ba	1321	685	65	720	701	681	190	437
Ga	19.71	16.69	16.06	19.29	19.48	19.22	20.90	18.35
Hf	7.85	3.55	4.66	7.24	6.68	6.41	5.50	6.63
Nb	34.86	17.52	19.46	30.38	31.00	30.66	27.85	29.53
Pb	22.29	38.44	31.06	26.26	31.33	31.11	12.05	36.87
Rb	180.12	201.76	>400.00	>400.00	234.89	>400.00	167.00	146.56
Sc	13.0	4.2	2.6	8.4	8.4	8.5	19.5	8.5
Sr	175.6	98.3	18.2	123.5	154.7	138.7	260.7	219.3
Ta	1.80	2.47	2.10	2.44	2.55	2.50	2.03	2.48
Th	20.83	33.18	55.96	38.96	40.05	42.56	27.64	40.64
U	3.78	11.93	8.43	5.46	7.84	7.85	6.67	9.38
Y	152.79	48.54	49.67	90.37	101.86	98.13	67.18	84.84
Zn	71	26	22	50	48	56	62	47
Zr	329.46	116.38	143.37	274.49	264.93	254.68	209.01	247.85
La	106.56	38.70	49.40	74.92	80.03	88.51	61.93	80.21
Ce	>250.00	91.42	134.91	185.88	198.50	203.88	139.82	182.63
Pr	24.72	7.00	10.89	15.53	17.14	18.74	13.08	16.80
Nd	90.48	22.43	35.93	51.37	58.82	63.03	44.74	57.46
Sm	18.14	4.89	6.34	9.38	10.40	11.67	8.24	10.28
Eu	2.19	0.63	0.37	1.03	1.22	1.32	1.71	1.15
Gd	17.65	4.38	5.03	8.10	10.07	10.81	8.13	9.79
Tb	2.83	0.74	0.78	1.42	1.70	1.76	1.31	1.56
Dy	16.77	5.03	4.81	8.84	10.05	10.55	7.88	9.70
Ho	3.78	1.17	1.14	1.99	2.37	2.41	1.88	2.17
Er	10.63	3.37	3.04	5.80	6.96	6.62	5.58	6.69
Tm	1.43	0.55	0.52	0.96	1.08	1.14	0.85	1.04
Yb	9.37	3.93	3.75	6.76	7.47	7.62	5.52	7.14
Lu	1.32	0.68	0.60	1.02	1.20	1.23	0.88	1.07

Appendix B

Creighton pluton: Major, trace and rare-earth element data

Sample	MS99-37	MS99-38	MS99-39	MS99-40	MS99-41	MS99-42	MS99-43	MS99-44
Rock Type	Type 1	Type 1	Type 2	Type 1	Type 1	Type 1	Type 2	Breccia
SiO_2	72.32	70.20	69.36	76.37	72.23	72.02	71.72	61.69
Al_2O_3	13.71	13.40	13.80	12.76	13.46	13.30	13.80	13.18
MnO	0.05	0.05	0.05	0.02	0.04	0.07	0.05	0.13
MgO	0.75	0.75	0.95	0.23	0.64	0.65	0.85	2.76
CaO	1.89	1.91	2.08	0.74	1.79	1.90	2.57	4.63
Na_2O	3.02	2.91	3.27	2.68	3.08	3.13	3.35	2.71
K_2O	4.92	5.07	4.98	5.82	4.63	4.57	1.93	3.37
P_2O_5	0.09	0.09	0.16	0.03	0.11	0.09	0.13	0.09
TiO_2	0.38	0.37	0.58	0.15	0.39	0.40	0.64	0.63
Fe_2O_3	3.34	3.33	4.10	1.48	3.23	3.97	4.83	7.70
LOI	0.63	0.95	0.65	0.72	1.04	0.71	0.74	2.79
TOTAL	101.10	99.03	99.98	101.00	100.64	100.81	100.61	99.68
Ba	723	702	978	541	767	696	545	366
Ga	20.10	19.56	19.36	16.37	17.95	20.15	21.58	18.68
Hf	6.73	7.17	9.23	4.71	6.64	9.46	9.97	4.24
Nb	30.99	29.52	24.88	17.18	21.95	42.76	29.02	28.03
Pb	37.31	25.39	40.62	32.27	28.92	44.06	31.45	31.24
Rb	>400.00	>400.00	181.23	>400.00	201.88	>400.00	128.73	>400.00
Sc	8.2	8.2	9.2	3.5	7.3	8.0	5.8	20.2
Sr	92.8	105.4	160.8	60.8	136.9	84.0	191.2	138.7
Ta	3.07	2.37	1.83	1.39	2.22	4.61	1.72	1.84
Th	40.01	41.52	31.19	76.14	38.19	50.29	47.31	26.20
U	5.49	7.15	4.40	6.07	6.04	6.94	5.22	7.36
Y	78.88	78.66	61.58	45.46	69.52	106.65	42.64	55.81
Zn	55	49	65	24	45	80	80	123
Zr	251.65	269.75	370.18	148.11	243.16	320.11	389.50	152.04
La	84.04	81.80	79.36	54.81	76.25	81.62	112.45	77.10
Ce	178.20	177.95	177.21	127.23	170.60	186.81	229.19	139.17
Pr	17.74	17.39	17.39	11.16	16.34	17.94	22.37	13.57
Nd	59.72	57.10	59.10	36.68	54.49	61.26	71.09	45.00
Sm	10.79	10.49	10.24	5.91	9.66	11.25	9.45	7.56
Eu	1.13	1.21	1.52	0.67	1.36	1.45	1.94	1.17
Gd	9.94	9.72	8.97	5.01	9.10	11.00	8.54	7.49
Tb	1.62	1.57	1.44	0.84	1.45	1.89	1.21	1.19
Dy	9.81	9.99	8.34	5.12	8.63	12.06	6.03	7.42
Ho	2.33	2.33	1.90	1.23	1.91	2.89	1.24	1.71
Er	7.00	6.73	5.41	3.68	5.49	8.82	3.51	5.17
Tm	1.13	1.08	0.80	0.60	0.83	1.48	0.55	0.81
Yb	8.11	8.02	5.47	4.43	5.97	10.42	3.44	5.43
Lu	1.24	1.16	0.83	0.74	0.99	1.67	0.51	0.84

Appendix B

Creighton pluton: Major, trace and rare-earth element data

Sample	MS99-45	MS99-46	MS99-47	MS99-48	MS99-49	MS99-50	MS99-51	MS99-57
Rock Type	Type 1	Type 1	Type 1	Type 1	Type 1	Type 2	Type 2	Enclave
SiO_2	75.11	73.22	72.70	75.18	71.91	63.09	65.74	65.69
Al_2O_3	12.59	13.93	12.79	13.28	13.13	14.21	14.88	14.08
MnO	0.02	0.04	0.05	0.02	0.04	0.12	0.07	0.12
MgO	0.30	0.61	0.56	0.27	0.51	1.23	0.85	1.91
CaO	0.84	1.59	1.58	0.92	1.40	3.56	2.74	2.80
Na_2O	2.88	3.01	2.85	3.07	3.05	3.20	3.22	4.21
K_2O	5.66	5.31	5.01	5.54	5.35	4.09	5.19	2.37
P_2O_5	0.04	0.04	0.07	0.02	0.07	0.26	0.17	0.15
TiO_2	0.18	0.22	0.31	0.11	0.34	0.92	0.64	0.61
Fe_2O_3	1.72	2.40	3.03	1.40	3.03	8.38	5.41	7.85
LOI	0.79	0.62	0.63	0.65	0.67	0.71	0.87	0.77
TOTAL	100.13	100.99	99.58	100.46	99.50	99.77	99.78	100.56
Ba	562	762	639	613	689	1377	1777	238
Ga	17.07	17.80	18.69	17.74	18.22	23.88	20.69	25.18
Hf	4.77	6.08	6.80	4.44	6.99	11.06	9.26	7.50
Nb	16.37	30.65	30.35	36.58	26.97	49.47	29.00	39.34
Pb	25.53	40.37	42.52	26.18	34.26	23.37	25.51	32.94
Rb	209.73	>400.00	247.03	245.74	270.04	156.96	>400.00	>400.00
Sc	3.7	6.1	6.5	2.9	6.7	19.0	13.0	12.6
Sr	70.1	84.9	99.0	75.5	104.0	163.5	209.1	132.2
Ta	2.29	3.13	3.65	1.91	2.87	3.24	1.52	1.67
Th	41.10	40.69	43.43	32.48	44.10	28.20	20.35	30.03
U	6.06	4.64	7.33	6.42	6.61	2.93	2.15	3.05
Y	57.20	84.46	87.43	48.44	80.08	136.84	57.23	111.81
Zn	27	46	58	30	41	90	78	146
Zr	158.62	200.39	235.20	130.73	228.36	439.99	361.16	300.52
La	58.91	80.98	72.03	29.94	76.51	126.68	108.16	81.91
Ce	132.44	177.54	158.38	72.01	179.96	>250.00	227.54	187.62
Pr	13.10	16.22	15.16	6.50	16.38	31.22	22.60	18.67
Nd	44.55	53.09	50.61	24.17	56.57	113.92	76.95	69.23
Sm	8.53	9.67	9.27	4.91	10.03	21.98	12.02	14.34
Eu	0.99	1.15	1.35	0.65	1.19	2.81	2.86	1.47
Gd	8.06	8.90	9.45	4.66	9.41	21.18	11.25	13.30
Tb	1.23	1.49	1.52	0.88	1.54	3.47	1.61	2.21
Dy	7.72	9.37	9.44	5.85	9.59	20.61	9.02	13.10
Ho	1.69	2.19	2.20	1.43	2.24	4.55	1.92	3.00
Er	5.08	6.60	7.09	4.83	6.86	13.08	5.43	8.27
Tm	0.72	1.09	1.12	0.78	1.11	1.95	0.75	1.29
Yb	4.60	7.69	8.13	5.00	7.31	12.88	4.82	7.80
Lu	0.68	1.16	1.31	0.75	1.15	1.89	0.79	1.24

Appendix B

Murray pluton & Copper Cliff rhyolite: Major, trace and rare-earth element data

Sample	MS98-4	MS99-20	MS99-54	MS99-55	MS99-56	MS99-52	MS99-53	
Rock Type	MG	MG	MG	MG	MG	CCR	CCR	
								wt(%)
SiO_2	75.32	71.81	74.36	74.85	75.11	83.04	75.54	
Al_2O_3	11.88	12.95	12.21	12.30	12.30	8.40	13.80	
MnO	0.04	0.05	0.03	0.03	0.03	0.02	0.02	
MgO	0.15	0.26	0.23	0.21	0.24	0.13	0.20	
CaO	0.78	1.33	0.55	0.57	0.83	1.75	1.52	
Na_2O	3.26	3.31	3.25	3.21	3.28	1.41	2.54	
K_2O	5.45	5.17	5.66	5.36	5.25	3.26	4.43	
P_2O_5	0.02	0.04	0.02	0.02	0.02	0.01	0.01	
TiO_2	0.25	0.39	0.23	0.23	0.24	0.08	0.08	
Fe_2O_3	2.52	3.82	2.35	2.33	2.46	1.24	1.38	
LOI	0.23	0.48	0.51	0.61	0.61	0.54	0.92	
TOTAL	99.90	99.61	99.40	99.72	100.37	99.88	100.44	
								ppm
Ba	1264	1934	1088	1091	1096	243	82	
Ga	19	20.85	19.77	20.03	20.21	22.95	43.55	
Hf	14.2	12.92	11.02	9.31	9.20	3.53	5.96	
Nb	33	32.07	35.17	38.90	43.78	33.99	59.80	
Pb	24	24.23	20.33	24.05	13.15	21.29	63.88	
Rb	163	133.29	>400.00	181.44	173.75	116.38	>400.00	
Sc	2.8	5.5	4.2	3.9	4.4	2.5	2.6	
Sr	46	80.3	50.0	45.8	91.2	83.8	53.3	
Ta	3.4	2.01	2.51	2.46	2.68	2.98	5.01	
Th	26	24.91	25.97	25.86	29.31	29.91	42.47	
U	4.3	5.15	4.57	4.87	7.06	9.39	14.44	
Y	101	93.65	84.45	87.73	150.98	86.33	137.36	
Zn	75	83	94	97	37	19	73	
Zr	522	472.50	367.63	333.65	321.14	86.50	123.30	
La	114	106.67	72.82	65.10	103.27	37.92	27.53	
Ce	218	>250.00	197.57	178.61	>250.00	90.48	74.46	
Pr	25	25.48	17.07	15.39	23.89	11.11	9.68	
Nd	95	93.57	60.59	57.47	87.62	41.66	38.97	
Sm	18	16.60	11.96	11.35	16.69	10.37	11.97	
Eu	2	3.00	1.45	1.41	1.93	0.61	0.45	
Gd	16.8	17.11	10.35	10.48	16.65	11.26	15.24	
Tb	2.78	2.62	1.78	1.86	2.62	1.91	2.99	
Dy	16.5	15.78	11.02	11.78	16.68	12.31	19.90	
Ho	3.7	3.48	2.53	2.71	3.91	2.96	4.78	
Er	9.89	10.32	7.04	7.47	10.35	7.89	13.29	
Tm	1.71	1.54	1.20	1.20	1.61	1.31	2.11	
Yb	10.29	9.93	8.54	7.99	10.95	9.02	14.62	
Lu	1.52	1.54	1.23	1.32	1.54	1.34	2.17	

Appendix C

Mineral Separation Chart

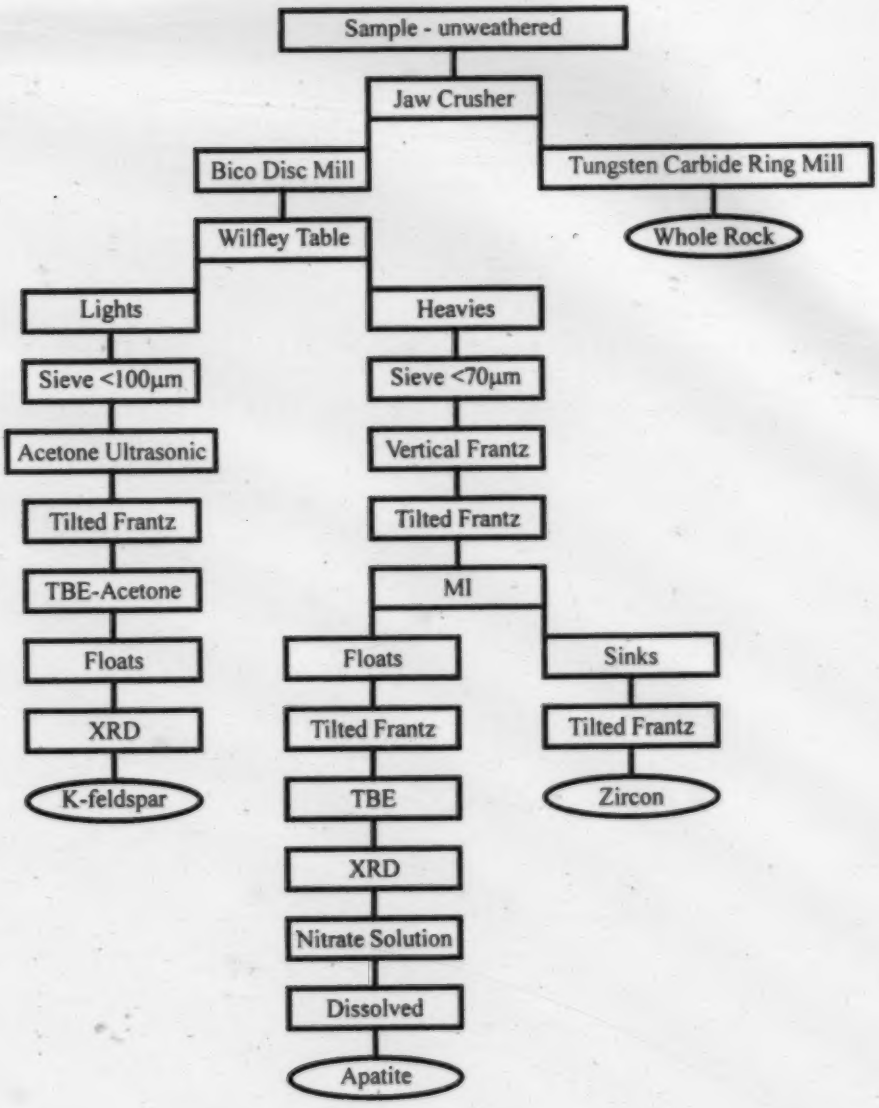

Appendix D

Analytical Techniques: U-Pb Isotope Geochemistry

All U-Pb isotopic work was completed at the Radiogenic Isotope Facility in the Department of Earth and Atmospheric Sciences at the University of Alberta.

Mostly unweathered samples were crushed using a Jaw crusher then powdered with a Bico disk mill. Heavy minerals were separated out using a Wilfley table and then sieved to <70μm. Material was then further separated using a vertical Frantz isodynamic magnetic separator and Methylene iodide (MI). The "sinks" were passed through another Frantz isodynamic magnetic separator at a higher current and side tilt. Zircons were selected for analysis by handpicking under a microscope. Some fractions were subjected to air abrasion (Krogh, 1982) in order to remove cracked and irregular surfaces that may cause discordance.

Grains were cleaned in two steps. The first was a warm HNO_3 bath and then rinsed in millipore water and placed in an ultrasonic bath for 30 seconds. The zircon grains were then rinsed twice with both millipore water and acetone. The grains were transferred to a tin foil "boat", carefully weighed and placed in a pre-cleaned teflon bomb. Bombs were rinsed prior to addition of the acid cleaning. Step 1: 15 drops of 48% HF and 2 drops of 7N HNO_3; Step 2: 30 drops of 6N HCL; Step 3: 15 drops of 48% HF and 2 drops of 7N HNO_3; and Step 4: 15 drops of 48% HF and 2 drops of 7N HNO_3. After each step the bombs were sealed and placed in an oven at 210° for two days.

Each bomb with zircon grains had 30 drops 48% HF and 2 drops HNO_3 added to it along with the appropriate quantity of mixed ^{205}Pb - ^{235}U spike. Spike was calculated using the formula: sample weight x Pb (ppm) x $^{207}Pb/^{206}Pb$ = Pb(ng)/2 = spike (ng). Bombs were then sealed and loaded into a metal carousel and placed in the oven at 210° for 5 days to dissolve the grains. The sample solution was then evaporated on a hot plate. 8 drops of 3.1N HCl was then added to convert the residue to a chloride solute with the bombs then being sealed and heated in the oven at 210° for 24 hours.

Micro columns containing an anion exchange resin were used to chemically separate Pb and U. Note: some zircon fractions analyzed were small enough not to warrant column chemistry. Columns were cleaned three times each by alternating 6.2N HCl and millipore water. Columns were equilibrated using 3.1N HCl with the sample being loaded in the same solution. Columns were additionally rinsed with more 3.1N HCL to remove any Zr and Hf from the columns. Pb was eluted using 6.2N HCl and U with millipore water, both into a pre-cleaned PMP beaker. 2 drops of phosphoric acid was added to the

separates prior to drying. Separates were then loaded onto a rhenium filament with a H_3PO_4/SiGel mixture (phosphoric acid and silica gel).

Isotopic ratios of U and Pb were analyzed on a VG 354 or Sector 54 thermal ionization mass spectrometer using a single collector Daly photomultiplier detector. All Pb data obtained was corrected by a factor of 0.13%/amu (VG 354) or 0.056%/amu (Sector 54). All U data obtained was corrected by a factor of 0.15%/amu (VG 3540 or 0.024%/amu (Sector 54). Isotopic ratios were corrected for mass discrimination based on repeated analyses of the NIST SRM981 Pb and U500 standards. Mass discrimination corrections for the VG 354 were 0.09%/amu (Pb) and 0.16%/amu (U). Mass discrimination corrections for the Sector 54 were 0.15%/amu (Pb) and 0.14%/amu (U). Laboratory procedural blanks were measured by repeated analyses at 2 pg ± 50% for Pb and 0.5 pg ± 20 for U. Decay constants used were $\lambda(^{235}U) = 1.55125 \times 10^{-10}$ a^{-1} and $\lambda(^{238}U) = 9.8485 \times 10^{-10}$ a^{-1} and an atomic ratio of $^{238}U/^{235}U = 137.88$ as recommended by Steiger and Jager (1977) (Jaffrey et al., 1971; Cowan and Adler, 1976). Data were calculated using an in-house software program and linear regression age calculations were performed using ISOPLOT/Ex (Ludwig, 1998)

Appendix E

Analytical Techniques: Rb-Sr, Sm-Nd and common Pb-feldspar Isotope Geochemistry

All Rb-Sr, Sm-Nd and common Pb-feldspar isotopic dilution and analysis were completed at the Radiogenic Isotope Facility in the Department of Earth and Atmospheric Sciences at the University of Alberta.

Rb-Sr and Sm-Nd

Representative whole-rock samples (1-2 kg) were collected in the field for analysis. All weathered faces were removed and samples were crushed using a Jaw crusher. The rock chips were then reduced to ~35 microns with a tungsten-carbide ring mill. Sample powders were weighed into pre-cleaned PFA teflon vials and then spiked by weighed tracer solutions of ^{84}Sr-^{87}Rb and ^{150}Nd-^{149}Sm. The samples were then dissolved by adding vapour distilled 24N HF and 16N HNO_3 solution at a sample/spike ratio of 5:2. The vials were sealed and heated on the hot plate at 150°C for one week. After evaporating to dryness, 10 ml of 6N HCl was added to the fluoride residue to convert the samples to chlorides. Samples were then heated on the hot plate at 100°C for 24 hours. The teflon vials were removed, evaporated to dryness and then dissolved in a loading solution of 3 ml of 0.75N HCl prior to column chemistry. Samples were centrifuged at 5000 rpm for 10 minutes prior to loading in columns.

Rb, Sr and REE were separated using Bio-Rad AG50W-X8 cation-exchange resin (200-400 mesh, H+ form) in Savillex custom Teflon PFA columns (6.4 mm, IB stem, 30 ml reservoir, 11.5 cm 6N HCL equilibrated resin). Separation procedure took place as follows: 6 x 0.50 ml of 0.75 HCl, 3 x 1 ml of 1.5N HCl, 11 ml of 1.5N HCl, collect 5 ml of 1.5N HCl (Rb collected), 4 ml of 1.5N HCl, 5 ml of 2.5N HCl, collect 6 ml of 2.5N HCl (Sr collected), 13 ml of 2N HCL, 2.5 ml of 6N HCl and collect 4 ml of 6N HCl (REE collected).

The Rb and Sr separates were re-dissolved in approximately 1.5 ml of a mixed oxalic and HCl solution and passed through a second set of the same columns to further purify the samples. Both were loaded with 0.25 ml oxalic-HCl mix and used elution solution of 1.5N HCl and 2.5N HCl for Rb and Sr, respectively. In both cases, 5 ml of the elution solution were collected. Sm and Nd were further separated using columns containing BioBeads SX-8 Di-(2-ethylhexyl phospate) coasted 200-400 mesh resin. Samples were loaded with 0.25 ml of 0.025N HCl. Separation procedure took place as follows: 3 x 0.25 ml of 0.025N HCl, 2 x 0.5 ml of 0.025N HCl, 4 – 4.5 ml of 0.25N HCl, collect 3 ml of 0.25N HCl (Nd collected), 0 – 1.0 ml of 0.25N HCl, 1.0 ml of 0.60N HCl and collect 1.0

– 1.5 ml 0.60N HCl (Sm collected). Column blanks are <400 pg for Nd, Sm and Sr and <100 pg for Rb.

Samples were converted to nitrates before loading and analysis. Rb and Sr were loaded onto single rhenium filament beads using a millipore-phosphoric acid and Ta gel mix. Sm and Nd were loaded onto double rhenium filament beads using nitric acid. Sm and Rb were measured on a Micromass 30 thermal ionization mass spectrometer whereas Sr and Nd were measured on a VG 354 thermal ionization mass spectrometer. Measured ratios were normalized to $^{86}Sr/^{88}Sr = 0.1194$ and $^{146}Nd/^{144}Nd = 0.7219$. Repeated analysis of standards produced results of $^{87}Sr/^{86}Sr = 0.7102716 \pm 7$ for the NBS 987 Sr standard (n = 47). The Shin Etsu Nd standard (equivalent to La Jolla) produced repeated analyses of $^{143}Nd/^{144}Nd = 0.512097 \pm 4$ (n = 39).

Common Pb-feldspar

Whole rock samples were crushed using the Jaw crusher and powdered with the Bico disc mill before being separated on the Wilfley table. A "lights" separate was collected then sieved to collect grains <100μm. The grains were then washed in an acetone ultrasonic bath and passed through a tilted Frantz isodynamic magnetic separator. The floats were then collected from a TBE-acetone ($\rho = 2.605$) heavy liquid mixture. The grains were then checked for purity using XRD (x-ray diffraction) and under the microscope. Approximately 300 mg of pure potassium feldspar was then measured out for the leaching procedure.

The mineral grains were subjected to a series of heated leaches over successive nights. The first four are from Cumming and Krstic (1987): 2 ml of 2N HCl, 6 ml of 6N HCl, 3 ml of 16N HNO_3 and 3 ml of 16N HNO_3 + 1 drop of 48% HF. Leach solution from leaches 1 and 4 were saved for isotopic chemistry and analyses. Leach #5 (Housh and Bowring, 1991) was 3 ml of 5% HF and 8N HNO_3 in an 8:1 mix. This solution was then placed on a hotplate for 20 minutes and repeated 4 additional times. The leached residue was then dissolved in 4 – 5 ml of 24N HF and a few drops of 16N HNO_3 by heating overnight on the hotplate. Residues were dried then had 1 – 3 ml of 6N HCl added and heated on the hotplate for 12 hours. The residues were again evaporated and then dissolved in 0.5N HBr solution.

Pb was extracted in Bio-Rad AG1-X8 anion resin (200 – 400 mesh, Cl^- form) columns. Column chemistry is modified after Lugmair and Galer (1992) with the procedure as follows: 0.25 ml of 0.5N HBr, 0.5 ml of 0.5N HBr, 0.5 ml of 0.5N HBr, 0.75 ml of a 0.2N HBr – 0.5N HNO_3 mix, 0.25 ml of a 0.03N HBr – 0.5N HNO_3 mix and collect 1 ml of the previous HBr-HNO_3 mix (collect Pb).

Total blank for the entire chemical procedure was <500 pg, thus no blank corrections were applied. The samples were on a single rhenium filament bead with a phosphoric acid-silica gel mix. Isotopic determinations were made by a VG 354 thermal ionization

mass spectrometer in single collector mode. Measured Pb isotopic ratios were corrected for mass discrimination based on values obtained for NBS (n = 4) and normalized to the value reported by Todt et al., (1996).

Murray pluton: Rb-Sr, Sm-Nd and common Pb-feldspar isotopic data

Sample	Age (Ma)	$^{87}Rb/^{86}Sr$	$^{87}Sr/^{86}Sr \pm 2\sigma$ err (@ 0 Ma)	$^{87}Sr/^{86}Sr_i$ (@ T Ma)
MS98-4	2477	10.97	1.086799 ± 15	0.69417

Sample	Age (Ma)	$^{147}Sm/^{144}Nd$	$^{143}Nd/^{144}Nd$ ± 2s err (@ 0 Ma)	ε_{Nd} (@ 0 Ma)	ε_{Nd} (@ T Ma)	$f^{Sm/Nd}$	T_{DM}[1] (Ma)
MS98-4	2477	0.1142	0.511186 ± 27	-28.30	-2.04	-0.42	2864

Sample	Separate Type[2]	$^{208}Pb/^{204}Pb$	$^{207}Pb/^{204}Pb$	$^{206}Pb/^{204}Pb$
MS98-4	R	35.812	15.454	15.827

^{87}Rb decay constant = 1.42×10^{-11} a^{-1}

[1] T_{DM} calculated using the mantle evolution model of Goldstein et al., 1984

Present day CHUR parameters are $^{147}Sm/^{144}Nd = 0.1967$, $^{143}Nd/^{144}Nd = 0.512658$

Depleted Mantle parameters are $^{147}Sm/^{144}Nd = 0.2186$, $^{143}Nd/^{144}Nd = 0.51316$

^{147}Sm decay constant = 6.54×10^{-12} a^{-1}

Pb isotopic ratios were corrected for mass discrimination based on values obtained for NBS-981 (n = 4) and normalized to the value reported by Todt, et al., (1996).

[2] Separate type legend

R = Residue

Appendix G

MAFIC DIKE

Dr. Larry M Heaman's Theme Song

(With apologies to 3 Doors Down's *Kryptonite)*

I took my hammer to the dike to find emplacement time
I left my errorchrons, open systems way behind
I watched my grad students and trained precise lab crew
U-Pb, there's nothing I can't do, yeah

I washed Teflon bombs, 'braded grains and picked a few
After all I knew lead had to be something to do with U
I really don't mind some lead loss now and then
As long as it's concordant at the end

If I'm discordant then will you still call me Big Heaman
If I've got common lead, will you get down to picograms
I'll regress two-four-five with zircon, baddeleyite
Mafic Dike

You rift terranes, you break the peaks but still I think plume mantle deep
You took for granted the date from Hearst-Matachewan
You picked bad rocks, outcrops misread if not for me, Archean instead
I joined the remnants up with the ages that I found

If I'm discordant then will you still call me Big Heaman
If I've got common lead, will you get down to picograms
I'll regress two-four-five with zircon, baddeleyite
Mafic Dike

If I'm discordant then will you still call me Big Heaman
If I've got common lead, will you get down to picograms
I'll regress two-four-five with zircon, baddeleyite
Mafic Dike

Yeah!

Concordant fractions and you can call me Big Heaman
My errors are low and lead blanks under picogram
My world is two-four-five with zircon, baddeleyite
Mafic Dike